Mahdi Guermazi

In-Vitro Biological Tissue State Monitoring based on Impedance Spectroscopy

Scientific Reports on Measurement and Sensor Technology

Volume 3

Prof. Dr.-Ing. Olfa Kanoun (Editor)

Mahdi Guermazi

In-Vitro Biological Tissue State Monitoring based on Impedance Spectroscopy

TECHNISCHE UNIVERSITÄT
CHEMNITZ

Universitätsverlag Chemnitz
2016

Impressum

Bibliografische Information der Deutschen Nationalbibliothek

Die Deutsche Nationalbibliothek verzeichnet diese Publikation in der Deutschen Nationalbibliografie; detaillierte bibliografische Angaben sind im Internet über http://dnb.d-nb.de abrufbar.

Titelgrafik: Chemnitz School of Metrology
Satz/Layout: Mahdi Guermazi

Technische Universität Chemnitz/Universitätsbibliothek
Universitätsverlag Chemnitz
09107 Chemnitz
http://www.tu-chemnitz.de/ub/univerlag

Herstellung und Auslieferung
readbox unipress
Am Hawerkamp 31
48155 Münster

readbox unipress ist eine Marke der
readbox publishing GmbH
Ruhrallee 9
44139 Dortmund
http://unipress.readbox.net

ISSN 2509-5102 print - ISSN 2509-5110 online

ISBN 978-3-96100-003-6

http://nbn-resolving.de/urn:nbn:de:bsz:ch1-qucosa-206710

In-Vitro Biological Tissue State Monitoring based on Impedance Spectroscopy

DISSERTATION

zur Erlangung des akademischen Grades

DOKTOR-INGENIEUR

(Dr.-Ing.)

vorgelegt

der Fakultät für Elektrotechnik und Informationstechnik

der Technischen Universität Chemnitz

von Msc. Mahdi Guermazi

geboren am 19.07.1979 in Sousse, Tunesien

Einreichung, Chemnitz den 24. 02. 2016

Verteidigung, Chemnitz den 19.05.2016

Promotionskommission

Vorsitzender	Prof. Dr.-Ing. T. Bauschert	TU Chemnitz
Betreuerin/Gutachterin	Prof. Dr.-Ing. O. Kanoun	TU Chemnitz
Gutachter	Prof. Dr.-Ing. N. Derbel	Universität Sfax, Tunesien
Weitere Mitglieder	Prof. Dr.-Ing. J. Himmel	HS Ruhr West
	Dr.-Ing. A.-J. Hempel	TU Chemnitz

Bibliographic Information

Guermazi, Mahdi
In-Vitro Biological Tissue State Monitoring based on Impedance Spectroscopy

Technische Universität Chemnitz
Fakultät für Elektrotechnik und Informationstechnik

Dissertation, 2016 – 155 Seiten, 90 Abbildungen, 21 Tabellen, 124 Literaturstellen

Keywords:
In-vitro measurement, muscles tissue measurement, bio-impedance, meat monitoring, model parameters, Fricke-Cole-Cole model, electrode design, meat diagnosis, feature extraction, neural network, fuzzy logic, meat classification

Abstract

The relationship between post-mortem state and changes of biological tissue impedance has been investigated to serve as a basis for developing an in-vitro measurement method for monitoring the freshness of meat. The main challenges thereby are the reproducible measurement of the impedance of biological tissues and the classification method of their type and state.

In order to realize reproducible tissue bio-impedance measurements, a suitable sensor taking into account the anisotropy of the biological tissue has been developed. It consists of cylindrical penetrating multi electrodes realizing good contacts between electrodes and the tissue. Experimental measurements have been carried out with different tissues and for a long period of time in order to monitor the state degradation with time. Measured results have been evaluated by means of the modified Fricke-Cole-Cole model. Results are reproducible and correspond to the expected behavior due to aging. An appropriate method for feature extraction and classification has been proposed using model parameters as features as input for classification using neural networks and fuzzy logic.

A Multilayer Perceptron neural network (MLP) has been proposed for muscle type computing and the age computing and respectively freshness state of the meat. The designed neural network is able to generalize and to correctly classify new testing data with a high performance index of recognition.

It reaches successful results of test equal to 100% for 972 created inputs for each muscle. An investigation of the influence of noise on the classification algorithm shows, that the MLP neural network has the ability to correctly classify the noisy testing inputs especially when the parameter noise is less than 0.6%. The success of classification is 100% for the muscles Longissimus Dorsi (LD) of beef, Semi-Membraneous (SM) of beef and Longissimus Dorsi (LD) of veal and 92.3% for the muscle Rectus Abdominis (RA) of veal.

Zero-order Sugeno fuzzy logic provides a successful alternative for easy classification. Using the Gaussian membership functions for the muscle type classification and trapezoidal member function for the classifiers related to the freshness classification, fuzzy logic realized an easy method of classification and generalizes correctly the inputs to the corresponding classes with a high level of recognition equal to 100% for meat type classification and with high accuracy for freshness computing equal to 84.62% for the muscle LD beef, 92.31 % for the muscle RA beef, 100 % for the muscle SM veal and 61.54% for the muscle LD veal.

Zusammenfassung

Auf der Basis von Impedanzspektroskopie wurde ein neuartiges in-vitro-Messverfahren zur Überwachung der Frische von biologischem Gewebe entwickelt. Die wichtigsten Herausforderungen stellen dabei die Reproduzierbarkeit der Impedanzmessung und die Klassifizierung der Gewebeart sowie dessen Zustands dar. Für die Reproduzierbarkeit von Impedanzmessungen an biologischen Geweben, wurde ein zylindrischer Multielektrodensensor realisiert, der die 2D-Anisotropie des Gewebes berücksichtigt und einen guten Kontakt zum Gewebe realisiert. Experimentelle Untersuchungen wurden an verschiedenen Geweben über einen längeren Zeitraum durchgeführt und mittels eines modifizierten Fricke-Cole-Cole-Modells analysiert. Die Ergebnisse sind reproduzierbar und entsprechen dem physikalisch-basierten erwarteten Verhalten. Als Merkmale für die Klassifikation wurden die Modellparameter genutzt.

Für die Klassifikation nach Muskeltyp und den zugehörigen Alterungszustand mit neuronalen Netzen wurde ein mehrschichtiges Perzeptron Neuronales Netz (MLP) vorgeschlagen. Dieses Neuronale Netz ist in der Lage ist zu verallgemeinern und bei neuen Testdaten eine hohe Erkennungsrate zu realisieren. Für die 972 untersuchten Testfälle unterschiedlicher Gewebearten wurden dabei 100 % Erkennungsquote erreicht. Eine Untersuchung des Einflusses von Rauschen auf das Neuronale Netz zeigt, dass es die Fähigkeit besitzt Daten, für die das Parameter-Rauschen kleiner als 0,6 % ist, besonders gut zu klassifizieren. Die Klassifizierung erreicht dabei für die Muskel Longissimus Dorsi (LD) und Semi-Membraneous (SM) vom Rind und den Longissimus Dorsi (LD) vom Kalb 100%. Für den Rectus Abdominis (RA) vom Kalb wird eine korrekte Klassifizierung in 92,3% der Fälle erreicht.

Null-ordnung Sugeno Fuzzy-Logik führt auch zu einer leistungsfähigen Alternative für die Klassifizierung. Unter Anwendung der Gaußschen Zugehörigkeitsfunktionen für die Gewebe- und trapezförmige Zugehörigkeitsfunktion für die

Zustandserkennung erreicht die Fuzzylogik ein gutes Generalisierungsvermögen und damit eine gute Klassifizierung der entsprechenden Daten. Die Fuzzylogik erreicht eine Gewebeartklassifikation mit 100% Erkennungsquote. Für die Zustandserkennung bei Rindfleisch wird für den LD eine korrekte Klassifizierung mit einer Quote von 84,62 % und für den RA liegt dieser Wert bei 92,31 %. Bei Kalbfleisch liegen die Werte für den SM bei 100 % und für den LD bei 61,54 %.

Acknowledgement

I would like to express my gratitude to my supervisor, Prof. Dr Olfa Kanoun for providing me the chance to be a member of the Chair for Measurement and Sensor Technology at Technische Universität Chemnitz. I kindly appreciate her encouragements and suggestions for this research work and the preparation of this thesis, for her continuous assistances, helps and supports.

I would like to thank Prof. Dr. Nabil Derbel my supervisor at Ecole Nationale d'Ingénieurs de Sfax (ENIS) for his support and big help throughout the PhD duration.

I also would like to thank the Deutscher Akademischer Austausch Dienst (DAAD) for the financial support and the opportunity to make my PhD in cooperation between Germany and Tunisia.

I like to express special thanks to all my colleagues at the chair for Measurement and Sensor Technology for their help considering experimental measurement set-ups and their valuable advice and encouragements. I shared excellent moments with you, I will have it in my memory forever. I also would like to thank all the professors and colleagues of the CEM Lab (Control Energy Management Laboratory).

I wish to address my appreciation to my parents, my wife, my brothers, my wife parents and brothers, to my family and friends for their continuous support and love during my whole education and my life at all.

Chemnitz, the 24th of February 2016

Mahdi Guermazi

Contents

List of Figures

List of Tables

Glossary

$A(\omega)$	Complex admittance
a_d	Radius of the dipole
a_i	Input of the NN MLP
a_j	Output of the hidden layer in the NN MLP
a_k	Input of the layer output in the NN MLP
a_s	Radius of the sphere
A_t	Coefficient transformation matrix in PCA method
BF	Muscle biceps fermoris
C	Capacitance
C_m	Capacitive element in Fricke model
CP	Counter propagation neural network
CP1	Characteristic point 1
CP2	Characteristic point 2
CP3	Characteristic point 3
CPE	Constant phase element
C_s	Cell membrane capacitance (Damez et al.)
D	Displacement field
D(a, b)	Euclidian distance between points a and b
DFD	Dark, firm, and dry hams
DO	Desired output
e	Elementary charge
E	Electric field
E'_1	Electric field of layer 1
E'_2	Electric field of layer 2
e_k	Error between the desired output and the output
F	Principal components in the PCA method
F_c	Characteristic frequency
F_{new}	New data set in PCA method
I(t)	Current signal
J_1	Current density 1
J_2	Current density 2
k	Boltzmann constant
K_a	Constant of the CPE depending on the frequency
LD	Muscle longisimus dorsi
LVQ	Learning vector quantization network
m	Counter ion mobility.
MF	Membership functions
MLP	Neural network multilayer perceptron

MP	Model parameters
N	Muscle neck
NN	Neural network
N_r	Normalized data
ø	Phase angle
O	Original data
P	Polarization density.
PCA	Principal component analysis
PCs	Principal components
p_s	Volume fraction of spheres
PSE	Pale, Soft, Exudative hams
R_0	Resistance part at zero frequency in Cole-Cole model
R_∞	Resistance at infinite frequency in Cole-Cole model
RA	Muscle rectus abdominis
R_e	Resistive element in Fricke model
RFN	Reddish, firm and non-exudative
R_i	Resistive element in Fricke model.
R_p	Resistance of ECF (Damez et al.)
R_s	Resistances of ICF (Damez et al.)
RSE	Reddish, soft and exudative
S	The n.p diagonal matrix in PCA method
s_j	Input of the hidden layer in the NN MLP
SM	Muscle semi-membraneous
SOFM	Self-organizing feature maps
SVD	Singular value decomposition in PCA method
T	Temperature
U	n.n left singular valued vector matrix of X in PCA
U(t)	Amplitude of the signal
U_p	Meat in closed boxes
V	p.p right singular valued matrix of X in PCA
V_P	Meat exposed directly to the air of the fridge
W	Weight of the winner neuron
W_{ji}	Output of the network weights (MLP)
W_{kj}	Hidden layer weights of the output layer (MLP)
X_d	Data set in PCA method
$\underline{Z}$	Complex impedance
Z_{CPE}	Complex impedance of CPE
α	Dispersion parameter with a value between 0 and 1
α dispersion	Dispersion at low frequencies
β dispersion	Dispersion at radio frequencies

γ dispersion	Dispersion at high frequency
δ_j	Error of the hidden units in the NN MLP
δ_k	Error of the output units in the NN MLP
$\varepsilon(t)$	Gradient step at iteration t
ε_0	Vacuum permittivity
ε'_1	Relative permittivity of material 1
ε'_2	Relative permittivity of material 2
η	Viscosity
λ	Eigenvalue in PCA method
μ	Membership function value or equation
σ'_1	Conductivity in material 1
σ'_2	Conductivity in material 2.
σ_i	Singular values of the matrix X in PCA method
τ	Characteristic time constant
ω_m''	Radial frequency in the pick of CP_2

1. Introduction

One of the most important challenges in meat industry is to obtain reliable and fast information on meat quality and freshness throughout the production process in order to provide guaranteed product quality and high safety for consumers.

EU policies protect the needs of consumers and encourage the production of safe, nutritious and affordable meats. Meat industry consists of several stakeholders like control agencies of meat, import-export companies and meat quality research laboratories. Different meat scandals throughout the last decades have shown the importance of meat quality assessment during production, transportation and storage, as well, exposure to inadequate temperature leads to the meat deterioration.

Furthermore, corruption by printing wrong labels on old meat is often reported. Also there is commonly practiced corruption that consists of the mixing of different meat prices and by selling other meat or muscle whose price is cheaper than that desired by the consumer.

1.1 Motivation

For meat state monitoring fully automatic, easy to use systems are necessary in order to replace laboratory procedures which consist in general of taking meat probes and analyzing them under microscopes and using special expensive equipment. These procedures are time-consuming and generate big costs, so that they cannot be applied for a large number of probes without increasing the costs significantly.

With online measurement devices, an online monitoring throughout the meat production process can be realized taking into account a large number of probes and in an easy practicable way. The more features are measured by this way; the better it is for both industries and consumers. Such a device should have low-cost and measure decisive parameters. The aim thereby is not to completely replace laboratory methods, but to widen the measurements to a large number of muscles and to recognize anomalies, which can be subjected to further detailed investigations.

Meat quality is manifold and cannot be measured easily like a simple measurement quantity. It includes different aspects related to microbial attacks, existence of certain substances and hormones and structure changes of the muscle during maturation processes. Especially for beef, maturation of the meat is necessary before it is consumed in order to get it tender.

In order to fulfill these requirements, electrical measurement methods, such as bio-impedance, come into reach because of the easy principle and the possibility for low costs realization.

1.2 Structure of muscles and biological tissues

Meat muscle is a structured tissue corresponding to an aggregation of cells in about 60% of fluid. Two thirds of fresh meat fluid is inside the cell (intracellular) and one third is inside the cell (extracellular) (Figure 1).

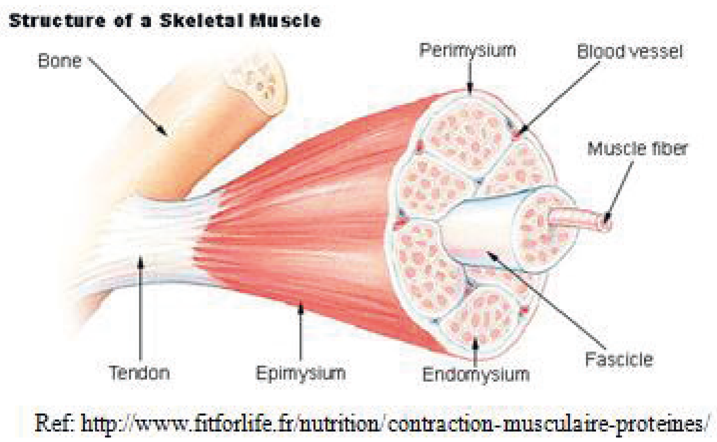

Figure 1 Biological tissue structure

The biological tissue is changing with post-mortem time following its physical characteristics. Maturation state of meat influences its fibers structure and conductivity and leads to observable changes of its complex impedance. Conductivity measurements are of a high interest because they provide good information for meat characterization about its structure and aging. The complex impedance includes the complex conductivity and the permittivity and gives therefore more information about the state of the tissue and the cell membranes than classical capacitive or resistive measurements.

Both intracellular and extracellular fluids are electrolytes containing free ions able to transport electrical charge that permits to consider that the meat can be approximated to be an electrolyte. Electrolytes are conducting liquids and have as carrier's free charges positive ions (cations) and negative ions (anions). In any liquid being electrically neutral, the number of positive charges carried by all of the cations is equal to the number of negative charges carried by all anions. In the absence of external electric current the ions are driven in a disordered agitation. During the passage of electric current, ions are animated in a double overall movement: The positive ions move in the conventional direction of the current and negative ions move in opposite directions (Figure 2).

Two current carrying electrodes in an electrolyte are the source and sink of electrons: From electrons of the metal, to ions or uncharged species of the electrolyte. Living tissue is electrically and macroscopically predominantly an electrolytic conductor. Tissue DC currents are therefore, ionic currents in contrast to the electronic current in metals. The total ionic conductivity of a solution depends on the concentration, the activity, the charge and the mobility of all free ions in the solution. Most important ions contributing to the ionic current in biological tissue are K^+, Na^+ and Ca_2^+ [1].

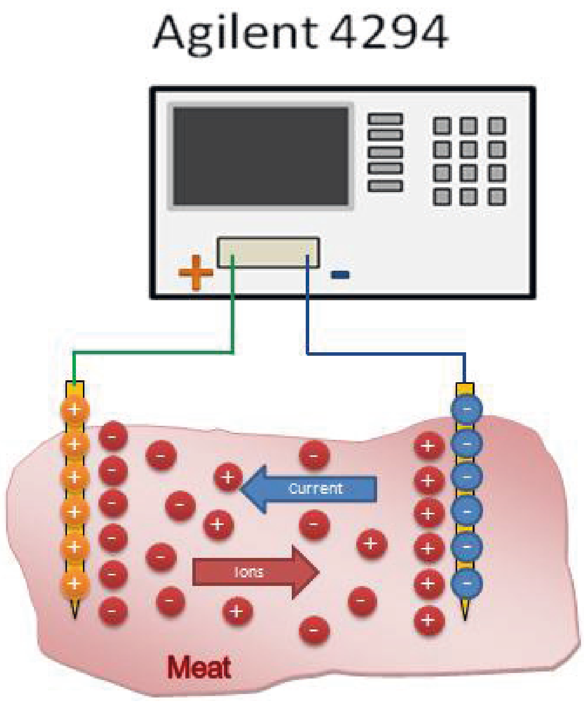

Figure 2. Ionic current and double layer effects

1.3 Impedance spectroscopy

Impedance spectroscopy represents a suitable measurement method which can serve as a basis for development of in-vitro measurement system for assessing the freshness of meat. The maturation state of meat leads to observable changes of its complex impedance [2].

For in-vitro measurements, the excitation signal, expressed as a function of time, can be a voltage or a current, because there are no current limitations like safety requirements in in-vivo measurements.

Impedance spectroscopy measurements are often analyzed by using an equivalent circuit model. The objective is to find a model whose impedance fits to the measured data. The type of components in the model and their interconnections controls the shape of the impedance spectrum.

1.4 Meat diagnosis

Diagnosis is in general the identification of the existence, the nature and the causes of a certain phenomenon. The first objective for diagnosis is to find suitable features that can be used for meat classification. The goal consists thereby of simplifying the amount of resources required to describe a large set of database or constructing combinations of variables to still describing data mining with sufficient accuracies. Analytical approaches have been proposed for the use in the rapid and quantitative monitoring of meat spoilage. These include intelligent methodologies dealing with data and problems that need a high performance of analysis and one of the most important methods are neural network [3, 4, 5] and Fuzzy logic.

1.5 Structure of the thesis

In this thesis, we propose to use the bio-impedance spectroscopy as system identification technique to develop a new diagnostic method for biological tissues. The dissertation is structured in six chapters including the first chapter; the introduction. An explanation about the structure of the different proposals and objectives is shown in Figure 3. These chapters are: state of the art, experimental investigation, modeling and feature analysis, data mining and classification of tissue and state and conclusion.

In chapter 2, we present the state of the art of bio-impedance measurements for tissue monitoring in order to analyze different methods developed for biological tissue analysis, especially experimental techniques, the modeling and feature extraction from impedance spectrum. The state of the art of data mining for tissue classification is also presented. Different methods of feature extraction are investigated especially mathematical methods, such as principal component analysis (PCA). Different techniques of classification are also presented especially using neural networks and fuzzy logic.

In chapter 3, experimental investigation are described including the measurement setup, the meat preparation before measurement and the design of a suitable electrode structure In order to reach reproducible and consistent measurements in spite of anisotropy effects.

In chapter 4, appropriate methods to analyze the measured spectra of meat are investigated and tested. These methods are decisive and are therefore, validated by the correlation between methods of analysis and biological fundamentals.

In chapter 5, feature extraction is investigated in order to get accurate diagnosis by finding the suitable method of classification to reach a high classification probability during learning and test phases.

In Chapter 6, the conclusion and perspectives of the work are presented.

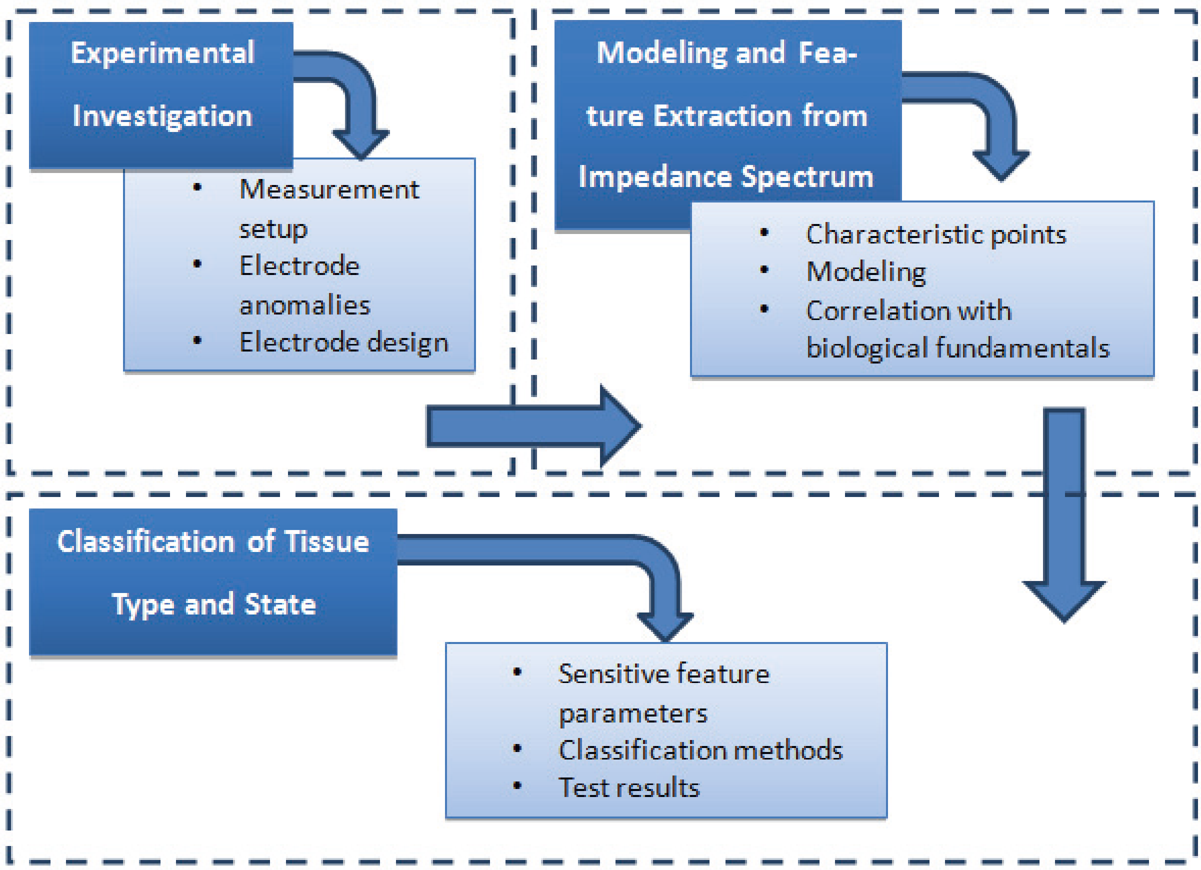

Figure 3. Dissertation overview

2. State of the art

2.1 Introduction

In the first part of this chapter, we present the state of the art of measurements based on impedance spectroscopy and show the advantages of the method and the physical phenomena in the frequency range [40 Hz-110 MHz] that permits the monitoring of the biological tissue state.

The second part of the state of the art consists of the presentation of data mining methods for the determination of the suitable feature and the work related to classification methods, neural networks and fuzzy logic.

2.2 Experimental measurement based on impedance spectroscopy

2.2.1 Impedance spectroscopy measurement method for biological tissue

Impedance spectroscopy is an established method for the measurement of material properties in corrosion research, material interfaces, characterization of chemical processes and recently also in life sciences as biology and medical diagnosis [6].

It is a promising method which allows getting a lot of information like reported in [7]. It offers more information over the frequency dependence with a relative simple measurement procedure based on the measurement of a transfer function at excitations of the device under test. Another important advantage of impedance spectroscopy is the possibility to realize measurement systems with low costs and short measurement times as reported in [8] compared to other measurement methods. It allows the separation of different dispersion types. It provides more measurement data at the same value of the measured quantity, while being non-invasive.

Several laboratory methods can be principally adopted for measurements of biological tissues, such as meat and special muscles. They need in most cases a complicated measurement setup and lead to high costs [2]. Therefore, they cannot be adopted very often and are generally not accessible for end users. Different authors, for example Wulf & Page [9], reported about limitations due to the difficulty finding suitable signal processing methods which are able to extract a lot of information.

Pliquett has reported in [10], that bio-impedance measurement is a simple and nondestructive way for the characterization of agricultural products, for quality assessment and for process control, that allows the design of a robust equipment suitable for process engineering. The recommendation for measurement is that it is necessary to optimize the frequency range for each application. A sophisticated data processing is needed for retrieving parameters, directly correlating with quality or process parameters and makes impedance measurements practically useful without need of highly trained technicians.

Several studies have been conducted on bio-impedance [11, 12, 13]. The first research involving measurements on meat using complex impedance spectroscopy was published by Callow in the 1930s [14], who explained that the electrical impedance of muscle decreases rapidly during the pre-rigor period and that electrical properties of meat change with time of storage until 14 days after slaughter [15-16]. Several studies have been carried out on the postmortem evolution of electrical meat properties. Damez et al. conducted several investigations for the measurement and characterization of meat [17-18-19] especially anisotropy sensing and dielectric behavior of meat during maturation that reflects major changes occurring in meat structure and tenderization. Altman et al. [20, 21] have made the comparison between impedance spectroscopy with the resistance for the computing of lamb carcass composition.

2.2.2 Probes and procedure used in bio-impedance measurement

Experimental procedure is very important for in-vitro bio-impedance measurement in order to get reproducible and valuable measurements. For that, the electrode configuration is a decisive factor, because meat has an anisotropic structure and the electrode contact is very important. Different probes are used for in-vitro bio-impedance measurements such as needle electrodes and non-penetrating circular electrodes. Penetrating electrodes are excessively used for different bio-impedance measurement.

Ghatass et al. [22] have investigated the beef meat quality. The beef meat sample has been vacuum-packed and stored at 4°C. The measurements are carried out by a LCZ meter Model 4277A, designed for measurements in the frequency range of 10 kHz to 1 MHz by means of two silver plated electrodes with silver chloride coating having a diameter of 20 mm.

Damez et al. [19] have realized a measurement procedure using the impedance analyzer HP 4194A. Beef meat measurements were carried out in 4 times in day 2, 3, 6 and 14 and scanning 80 frequencies ranging from 1 kHz to 1500 kHz. Meat has been vacuum packed and stored at 4°C. The used probe is consisting of 2 stainless steel electrodes with a distance of 5 cm with a diameter of 0.6 mm making it possible to take measurements both longitudinally and transversally to the fiber direction.

Tetra polar electrodes (Figure 4) are often used in bio-impedance field. Impedance measurements are taken by means of a set of four electrodes arranged parallel to each other. The two outers (current or excitation) electrodes provide the input signal (usually a current) to the investigated tissue. This creates an electric potential distribution that is measured by the other two inner (voltage or pickup) electrodes [23].

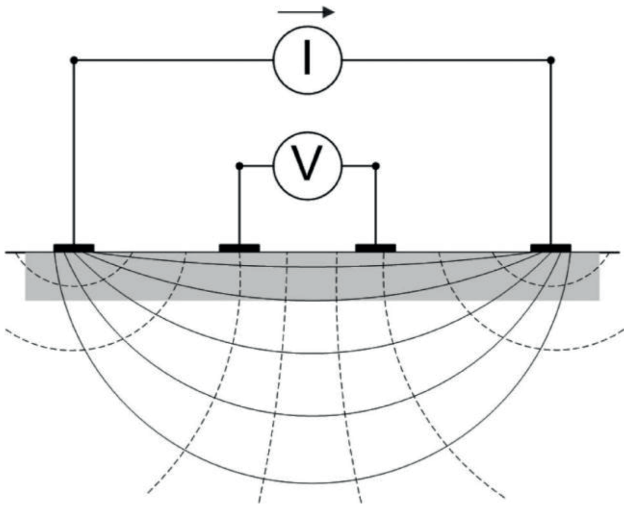

Figure 4. Diagram of tetra polar measurement set-up [24]

Oliver et al. [25] investigated impedance spectroscopy for ham meat quality selection by using four pin electrodes. Investigation is performed with a measurement set-up using the impedance analyzer HP4192A scanning from 8 kHz to 1 MHz.

Negri et al. [26] have reported a new particle swarm optimization method for fitting electrical bio-impedance spectra. Bio-impedance spectrometer is recorded via two electrodes of a tetrapolar probe into bovine liver, heart, topside and back muscle samples. Distance between electrodes is 2.5 mm and diameter of electrode is 1 mm. Injected current is 1 mA at the frequencies range from 0.5 kHz up to 1 MHz (Figure 5).

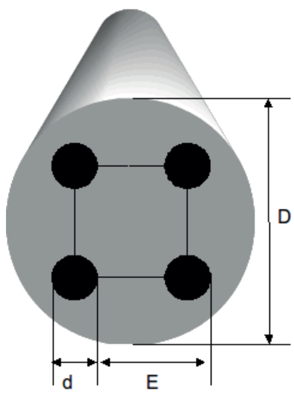

Figure 5. Tetra polar electrode [26]

Lepetit et al. have developed different geometries of electrodes working with or without penetration to muscle [27]. They are like plates electrodes made consisting of two electrodes realized by two rows of five cylindrical bull nosed stainless steel probes with a distance of 20 mm between the two rows of probes and with the same electrical potential on each row. They also have developed bars electrodes made of two parallel, rectangular cross-sectional bars of stainless steel with a distance of 10 mm between the two bars. Other geometries of needles electrodes are made of two rows of nine cylindrical needles and with a distance of 10 mm between the two rows of needles, with the same electrical potential of each row.

It has been reported that needles electrode has shown a big disadvantage considering reproducibility in anisotropic materials. Altmann et al. [28] have used different directions of probe insertion for the computing of intramuscular fat by impedance spectroscopy (Figure 6. Directions of puncture [28]).

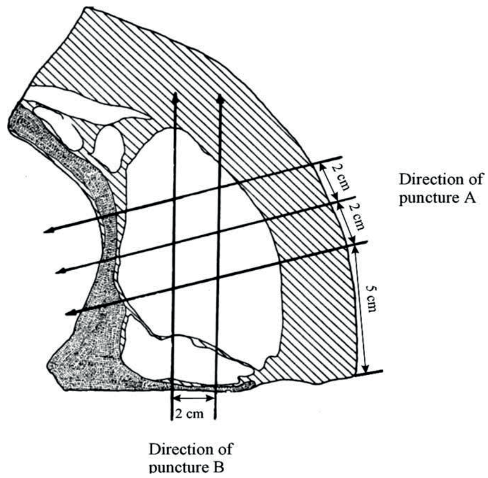

Figure 6. Directions of puncture [28]

The probe is inserted three times with a distance of 5, 7, and 9 cm from dorsal midline. The used penetration depth of the field lines is 0.8 mm for an average with a frequency range between 500 Hz and 100 kHz. They confirm that the increase in penetration depth by increasing the electrode gap would compromise the local resolution. The stroke of the electrode system is 120 mm. It is fully inserted into the muscle prior to the measurement.

Anisotropy dependency is identified by Swatland et.al [29] and Bokadian et al. [30] during meat measurement. They classify three directions for the placement of electrodes for the measurement of electrical properties of meat that are across the fibers and parallel to their long axis, then across the fibers and perpendicular to their long axis and the third is along the fibers and perpendicular to their long axis (Figure 7).

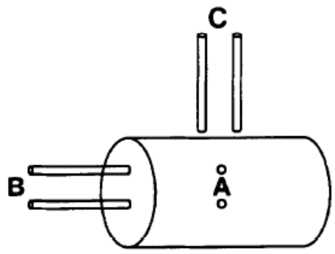

Figure 7. Three orientations of a pair of parallel needles in a muscle sample [29]

To avoid the influence of anisotropy, Damez et al. [18] proposed an tal solution consisting of the measurement longitudinally then transversally to the fiber direction to allow diametrically opposite electrodes successively commutated in order to measure the impedance in a radial direction (

Figure 8).

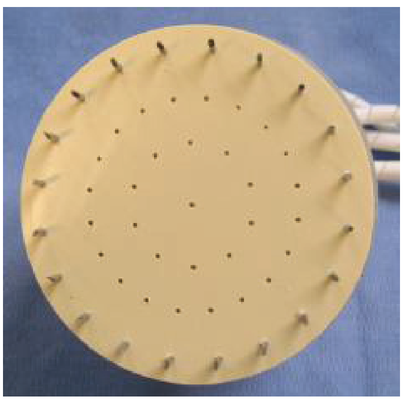

Figure 8. The 8 cm in diameter 20 electrodes probe using the bipolar method [18]

García-Breijo et al. [31] have proposed a solution that consider a cylindrical geometry of the electrodes. It consisting of a hollow needle made of stainless steel that acts as the outer electrode inside which a wire made of steel and it plays the role of inner electrode and with a dielectric material, the epoxy resin between both electrodes (Figure 9). The needle is the same as used in medical applications for carrying out electromyography. It is made of stainless steel and acts as the outer electrode in the system. The inside wire is made of steel and it plays the role of inner electrode. Between both electrodes, there is a dielectric material, namely epoxy resin. The utilized needle has an outer diameter equal to 0.46 mm.

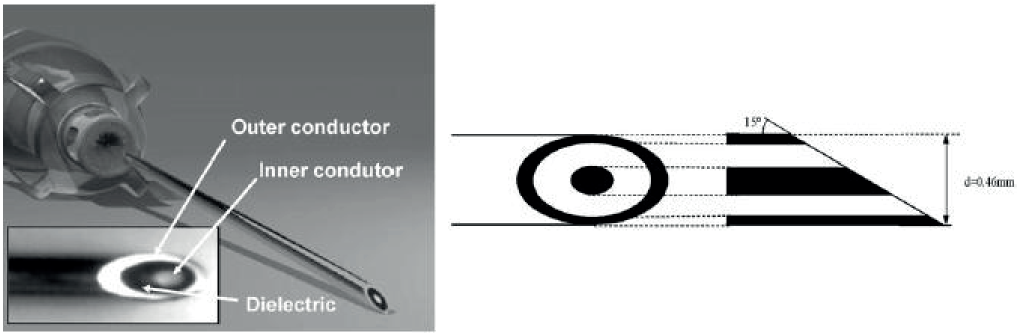

Figure 9. Concentric measuring cell [31]

Non contacting electrodes are also used in bio-impedance measurements. Chevalier and al. have conducted a research on fish measurements [32]. Three probes with different electrodes geometries are concurrently tested. Independently on the used probe, the salt content of samples has been successfully evaluated by linear computing models based on conductance and increment capacitance data. The probe has been made of two concentric platinum electrodes fixed on a non-conducting support. The two concentric electrodes system has been chosen in order to carry out measurements on anisotropic material such as fish muscle. This system measured impedance at two different frequencies 1 MHz and 10 MHz. Conductance and capacitance have been determined from impedance measurement and have been displayed on multisensory control unit.

Mohiri et al. [33] have presented the computing of meat permittivity based on its blood volume, an impedance analyzer (Agilent 4294) connected to a parallel plate dielectric fixture (Agilent 16451B) with a 5 mm guarded electrode used to measure the permittivity of both; the meat and the muscle fibers (Figure 10). A good contact between the electrodes and the samples are carefully made as required in the contacting electrode measurement method. The quantity measured by the impedance analyzer is only the capacitance.

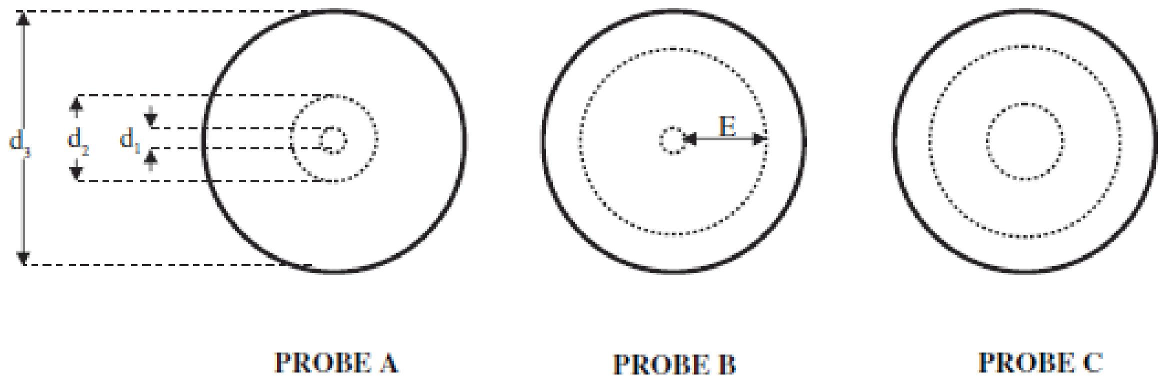

Figure 10. Schematic description of different probes used in the study in [33]

A similar study using the same measurement material, describes the analysis of capacitive variations in the fish, slaughtered and non-slaughtered cow and pig meats [34], where four disc shaped electrodes are used, A, B, C and D that differ from each other in diameter and the method used to measure dielectric properties. Electrode B shall be used to measure the meat capacitance and loss factor. A parallel plate capacitor of platinum-disc shape electrodes is used to measure the capacitance of the meat.

The diameter D of the electrodes and the distance d between them are 2.5 cm and 1 cm, respectively. The meat sample is put between the two plates; with the gap of 1cm. The capacitance C depends on the dielectric permittivity of the meat sample.

Giraldez [35], used the capacitive method with a parallel plate fixture connected to an impedance analyzer. The electrode of the fixture has a 38 mm x 38 mm guarded/guard electrode, has been used and the diameter of the used samples has been chosen equal to 46 mm. The thickness has been determined individually for each meat sample with an accuracy of ±0.01 mm (Figure 11).

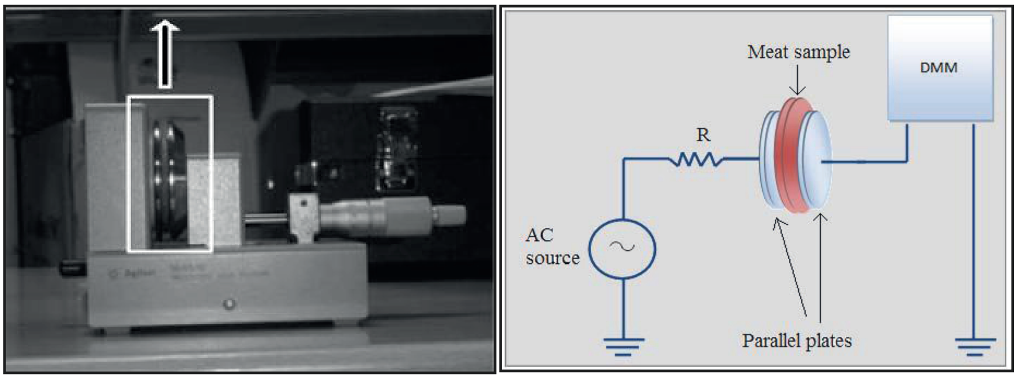

Figure 11. Capacitive Variations Study of Fish, Cow and Pig [35]

The thickness of the samples is in the range 2-4 mm due to the limitations in the slicing system. Preliminary experiments demonstrated that, in this thickness range, the dielectric properties of each loin do not present significant differences. The contacting electrode method (Rigid Metal Electrode) has been used. The method consists of setting the sample between the electrodes, ensuring good contact between the electrodes and the sample.

2.2.3 Critical review of methods based on impedance spectroscopy

The electrode design and the measurement procedure have been investigated by several authors and researchers. Different probes are used for in-vitro bio-impedance measurements especially needle electrodes and non-penetrating circular electrodes. The distance between electrodes and length embedded into the sample were considered. In the following Table 1 we gives a summary about a selection of different geometrical configurations of needles probes from literature including information about measurement procedures, such as the storage temperature and the frequency range.

Table 1. Summary of selected methods for in-vitro bio-impedance measurement

	Ghatass et al.	Damez et al.	Oliver et al.	Negri et al.	Altman et al.
Frequency range	10 kHz - 1MHz	1 kHz -1.5 MHz	8 kHz- 1 MHz	0.5 kHz-1MHz	0.5 kHz-0.1 MHz
Electrode	silver-plated electrodes with a silver chloride	stainless steel	Pin electrodes	-	Stainless steel puncture needles
Number of electrodes	2	2	4	4	4
Length	-	5 mm	-	-	35 mm
Diameter	20 mm	0.6 mm	-	1 mm	0.3 mm
Direction	Parallel	Parallel and perpendicular	-	-	Parallel and perpendicular
Penetration depth	-	> 5 mm	-	-	0.8 mm
Gap between two electrodes	-	5 cm	-	2.5 mm	20 mm
Vacuum packed meat	Yes	Yes	-	-	-
Temperature	4°C	4°C	-	-	-

Needle electrodes insure a very good contact but have a big disadvantage considering reproducibility in anisotropic materials. Biological tissues, particularly meat have an anisotropic structure, so that impedance varies according to whether the current runs parallel or perpendicular to muscle fibers [36]. The conductivity of meat increases in the case of measurement in parallel to the muscle fibers. In this case the current is better conducted by the fibers than in other cases where it is obliged to cross them. Different authors propose the use of tetra polar electrodes, it is clear that this type of electrodes shows the same problematic of reproducibility. We realized several laboratory tests using the two probes that give a high efficiency when the calibration is done to remove of cable and electrodes effects. Non-penetrating circular electrodes, overcome the anisotropy effect in two dimensions. However it has a bad contact to the rough surface of the meat and needs a sufficient force applied to get acceptable results. An investigation will be presented in the next section to confirm the anomalies of the needles penetrating electrodes and the non-penetrating circular electrodes.

Sensitive measurements with high reproducibility represents an important challenge and the use of a cylindrical geometry present a necessity to avoid the anisotropy dependency.

The objective would be therefore to develop an electrode that can guarantee reproducible and consistent measurements in spite of these effects. Different theoretical and experimental investigations will be provided for the proposed electrode configuration in order to ensure a reduction of the inadequate electrode contact and the influence of anisotropy at the same time.

Measurement procedure, especially the meat preparation represents also an important step in order to ensure correct measurement. Different experimental preparation of meat will be presented with the proposed solution that permits to avoid the appearance of bacteria and reduces the water loss in meat. The goal is to allow getting information about the meat for long period of time and maintains the same state of the meat as in meat selling sector.

2.3 Physical phenomena and modeling of a biological tissue

2.3.1 Physical phenomena in the frequency range [40 Hz-110 MHz]

Using laboratory measurement setups, a bio-impedance measurement is generally done in the whole frequency range [40 Hz-110 MHz] [37]. The spectrum results show that three areas of dispersion α, β and γ are observed (Figure 12) as described in [38].

Foster and Schwan [39] have modeled these dispersion types for several biological tissues. Grimnes & Martinsen [1] have given a general introduction to bio-impedance measurement about the relevant electrochemical mechanisms, such as ionic conductivity, charge transfer reactions, double layers and diffusion mechanisms.

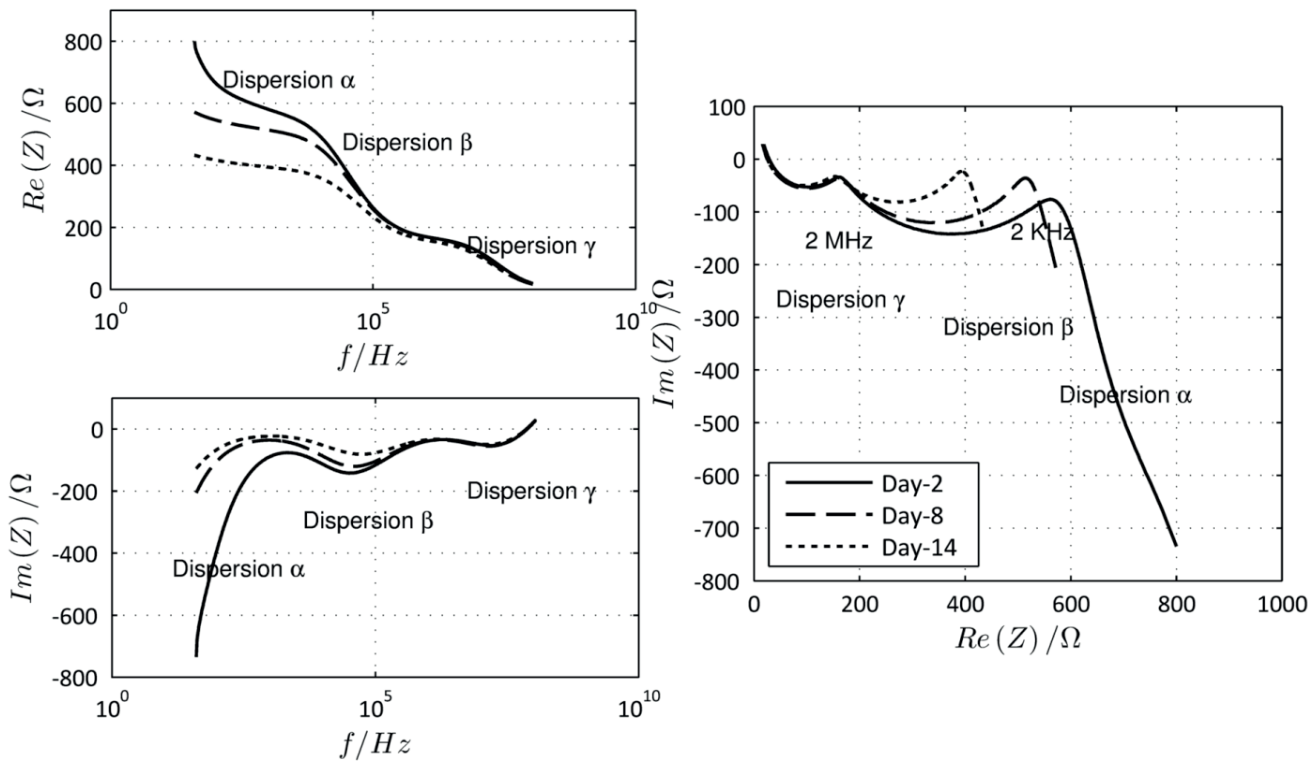

Figure 12. Nyquist plot of the muscle longisimus dorsi (LD) of Beef [40]

At low frequencies the dispersion α is dominant [41]. The current cannot pass through the cells because of its high resistance [42]. It flows outside the biological cells due to the diffusion and lateral movements of the ions along the insulating membrane of the cells (Figure 13).

One of the important phenomena that contributes to the α-dispersion is the counter ion polarization effects described by Schwartz [43]. He has considered the case when an external field is applied on a particle surface; the free counter ions move initially laterally will be polarized and will be slightly displaced relative to the particle. The re-establishment of the original counter ion atmosphere, after the external field is switched off, will be diffusion controlled and the corresponding time constant according to Schwartz theory is given by:

$$\tau = \frac{a_s^{\,2} e}{2\mu kT} \tag{1}$$

Whereas is the radius of the sphere, e is the elementary charge and m is the counter ion mobility. This leads to the α dispersion.

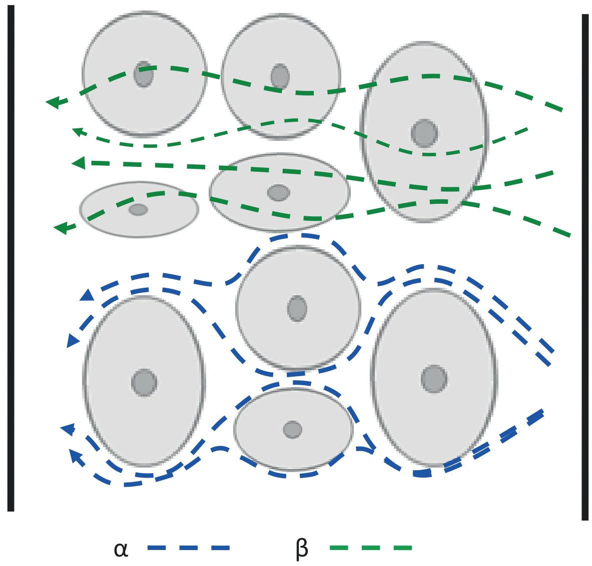

Figure 13. Explanation of physical phenomena in the α and β dispersion

At radio frequencies, β dispersion is observed. It is associated with the dielectric properties of the cell membranes and their interactions with the extra and intracellular electrolytes. One of the phenomena that contribute to the β dispersion is the Maxwell-Wagner effect [44, 45, 1] due to the interfacial relaxation process occurring in systems where the electric current passes at the interface between two different materials [46].

At these frequencies, cells are polarized in response to the electric field. Cellular membranes act as barriers to the flow of ions between the intra and extracellular fluids (Figure 13). To illustrate this phenomenon, we consider a material consisting of two juxtaposed layers of different properties and submitted to an electric field. Initially, if the interface between the two materials is not charged, Poisson low [47] requires that the electric displacement D is constant.

$$\overrightarrow{D} = \varepsilon_1^{'}\overrightarrow{E_1} = \varepsilon_2^{'}\overrightarrow{E_2} \tag{2}$$

Where E'1 is the electric field of layer 1, E'2 is the electric field of layer 2, ε'1 is the relative permittivity of material 1 and ε'2 is the relative permittivity of material 2.

The current densities of the two materials can then be connected by:

$$\frac{\overrightarrow{J_1}}{\overrightarrow{J_2}} = \frac{\sigma_1^{'}\overrightarrow{E_1}}{\sigma_2^{'}\overrightarrow{E_2}} = \frac{\sigma_1^{'}\varepsilon_2^{'}}{\sigma_2^{'}\varepsilon_1^{'}} \tag{3}$$

Where J1 is the current density 1, J2 is the current density 2, σ'1 is the conductivity in material 1 and σ’2 is the conductivity in material 2.

If, $\sigma_1^{'}\varepsilon_2^{'} = \sigma_2^{'}\varepsilon_1^{'}$, the interface has zero density of free charges. However, the difference in current densities implies that the interface is actually charged [41]. This imbalance implies an accumulation of charges at the interface between the two layers, resulting in the occurrence of an induced dipole at the interface (interface polarization). Maxwell [48] derived an analytical solution for the conductivity s of a dilute suspension of spherical particles by:

$$\frac{\sigma - \sigma_2}{\sigma + 2\sigma_2} = p_s \frac{(\sigma_1 - \sigma_2)}{\sigma_1 + 2\sigma_2} \tag{4}$$

Another contribution to β dispersion is the relaxation caused by protein and amino acids residues [8, 49], where ps is the volume fraction of spheres.

At microwave frequencies, the γ dispersion is dominating. This dispersion is observed at high frequency due to the permanent dipole relaxation of small molecules as water dipoles. In the presence of an alternating field, the polar molecules such as water molecules or certain proteins are rotated. This rotation is not instantaneous and therefore a relaxation phenomenon is inherent. Debye [50] describes the orientation of the permanent dipoles (such as water molecules) as a purely viscous phenomenon, without force reminders, which can be approached by a first-order system with a time relaxation constant given by [51]:

$$\tau = \frac{4\ \pi\ \eta\ a_d^{3}}{k\ T} \tag{5}$$

With η: Viscosity, ad: the radius of the dipole, k: the Boltzmann constant and T: the temperature.

Dipole size considers a major influence in the lifetime of relaxation. Typically, the orientation of molecules of water (pure water) occurs with relaxation times on the order of a few picoseconds with a frequency close to 20 GHz. For comparison, the polar protein presented in biological tissues is in general much larger than water molecules and relaxation frequencies are then much smaller (a few MHz). Any macromolecules or proteins will produce dispersions at frequencies ranging from the α range through the γ range, depending on the size and charge of the molecules. A summary is shown in (Table 2).

Table 2. Summary of the frequency ranges

Dispersion	Frequency range	Physical phenomena
α	x mHz-x kHz	- Cell membranes are isolating - Cellular membrane acts as barriers to the flow of ions - Current flows extracellular - Diffusion and lateral movement of ions along cell membranes
Β	x kHz- x MHz	- Interfacial relaxation process (Maxwell-Wagner-Effect) between intracellular and extracellular regions - Current flows extracellular and intracellular
Γ	x MHz- x GHz	- Dipole relaxation of small molecules - Current flows extracellular and intracellular

Cell suspensions typically exhibit significant β dispersion in the radio frequency range. This is due to the Maxwell-Wagner effect at the interface between the intra or extracellular solution and the phospholipids membrane. In addition, the water molecules cause a γ dispersion.

For meat monitoring the dispersion β is more suitable than α and γ dispersion because it includes information referring to the behavior of the cell membranes integrity, which changes with aging. The advantage in comparison with α dispersion is that the current spreads in the intracellular and extracellular region.

The γ dispersion information about the biological tissue is available, but it is not specific for aging processes influencing mainly the cell membranes. To summarize, the requirements of muscle tissue's monitoring can be determined from laboratory measurements of impedance spectroscopy. Thereby the working frequency for meat characterization should be in the sector of the dispersion β.

2.3.2 Modeling of biological tissue and feature analysis

The first electrical model used for the characterization of biological tissues has been introduced by Fricke and Morse [52]. The model presented in Figure 14 and the equation 6 serves to approximate also an aggregation of cells. According to several studies in this area, it can be used to characterize biological tissues and consequently meat.

It consists of a resistive element Re representing extracellular fluids in Ω placed in parallel with the capacitive element Cm, representing insulating cell membranes in series with a resistive element Ri representing intracellular fluids.

$$Z_{model} = \frac{1}{\frac{1}{\mathrm{R_e}} + \frac{1}{R_i + \frac{1}{j.c_m.\omega}}} \tag{6}$$

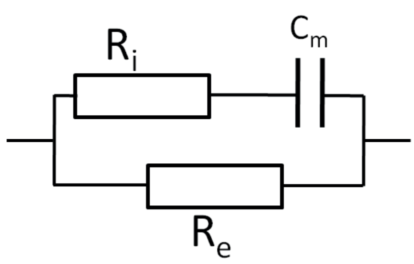

Figure 14. Fricke model

Fricke noticed that the capacitance often varies with the frequency [53]. This is confirmed when it is observed that the Fricke model is not enough accurate to fit experimental results [54, 55, 56]. A depressed semicircle is denoted in the Nyquist-plot of the impedance spectrum.

By studying the dispersion and adsorption on the dielectric, Cole introduced in 1940 [57] the first mathematical expression able to describe the depressed semi-circles by finding the behavior of CPE (Constant Phase Element) when measuring living tissues electrical impedance. The following equation shows a description of the Cole-Cole empirical equation explained and shown in [1] and in [58] (Figure 15).

$$Z^{*} = R_{\infty} + \frac{(R_0 - R_{\infty})}{1 + (i\omega\tau)^{\alpha}} \tag{7}$$

Where R_0 is the resistance part at zero frequency in Ω, R_∞ is the resistance at infinite frequency in Ω, τ represents the characteristic time constant and α is the dispersion parameter with a value between 0 and 1.

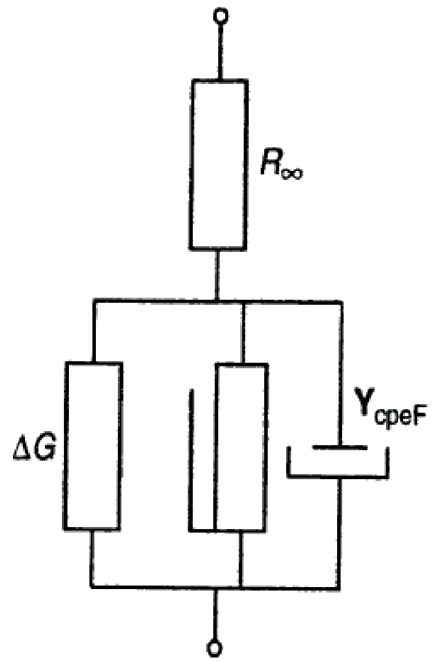

Figure 15. Cole-Cole model [1]

CPE describes a dispersion of the capacity depending on the frequency. The impedance of CPE is described according to equation 8 [1-6-59]. When α is close to 0, the CPE describes a resistance, close to -1 it describes an inductance, close to 1 it describes a capacity and finally, for the value of 0.5, the result is equivalent to the Warburg diffusion impedance.

$$Z_{CPE} = \frac{1}{K_a (j \cdot \omega)^{\alpha}} \tag{8}$$

Cole-Cole model has been extensively used in different investigations for biological tissue characterization [10, 25, 26, 60, 61, 62], Haemmerich et al. [63] have used Cole-Cole model during the measurement of changes in electrical resistivity of swine liver. After occlusion and postmortem, they have described the Cole-Cole circle (Figure 16).

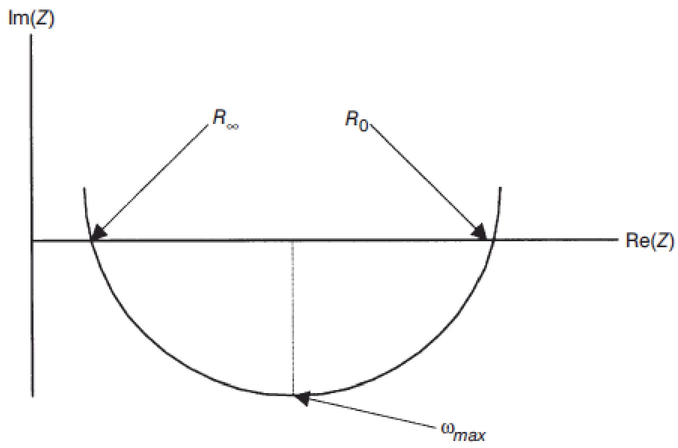

Figure 16. Cole-Cole Circle [63]

The resistivity of swine liver tissue has been measured in vivo, during induced ischemia and post-mortem between 10 Hz and 1 MHz. Haemmerich mentioned that the resistivity decrease is accompanied by a decrease in both the extracellular resistance Re and membrane capacitance Cm. The decrease in Re is in agreement with the increase in the extracellular fluid volume (Figure 17).

Konishi et al. have explained that the use of the Fricke model can ideally explain the biological tissue [64]. They have defined the model parameters R_e, R_i and C_m according to the Cole-Cole equation, following resistances R_0 and R_∞, that corresponds to the impedance at very low and very high frequencies. The model equation is given according to the following equations:

$$R_0 = R_e \tag{9}$$

$$R_i = \frac{R_o R_\infty}{R_0 - R_\infty} \tag{10}$$

$$C_m = \frac{1}{\omega_{\max}\left(R_e + R_i\right)} \tag{11}$$

Where $\omega_{\max}$ is the pulsation which gives the maximum imaginary part of the nyquist plot of impedance (Figure 16).

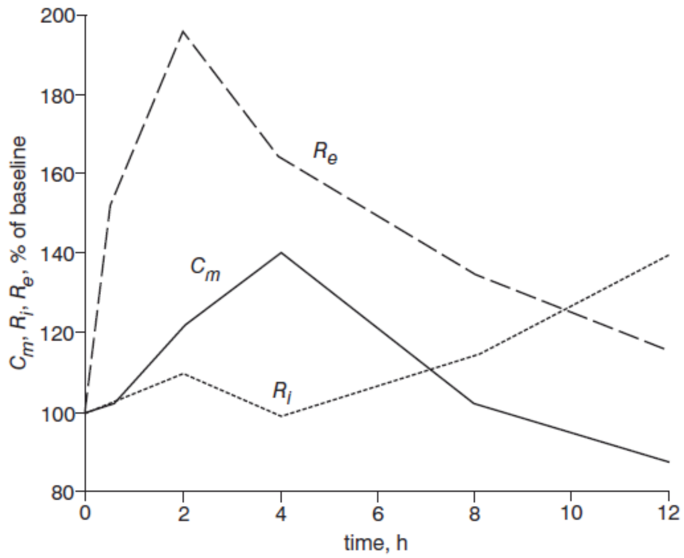

Figure 17. Changes in R_e, R_i and C_m during first 12 h of a tissue sample [63]

For the analysis of parameters over time, Konishi has mentioned that the membrane capacity Cm rises initially and reaches its peak 4 h post-mortem, due to the increase in membrane surface resulting from cell swelling. After post-mortem, resistivity decreases due to several factors. An increase in extracellular fluid, due to loss of membrane integrity post-mortem allows the continuity between intracellular and extracellular fluid compartments. The decrease in R_e is in agreement with the increase of extracellular fluid volume. After that tissue suffers extensively from post-mortem damage and cell membranes begin to break down.

Damez et al. [19] have included a method to combine Cole-Cole and Fricke model for the behavior of the meat as follows:

$$\tau = \left(R_s + R_p\right)\, C_s \tag{12}$$

$$R_0 = R_p \tag{13}$$

$$R_\infty = \frac{R_p R_s}{R_p + R_s} \tag{14}$$

R_0 and R_∞ are the impedance at very low and very high frequency, respectively. τ is the time constant. In this model, R_{p} and R_{s} represent the resistances of ECF and ICF, respectively, while C_{s} is the cell membrane capacitance. The parameters analyses over time of Damez et al. are given in Figure 18.

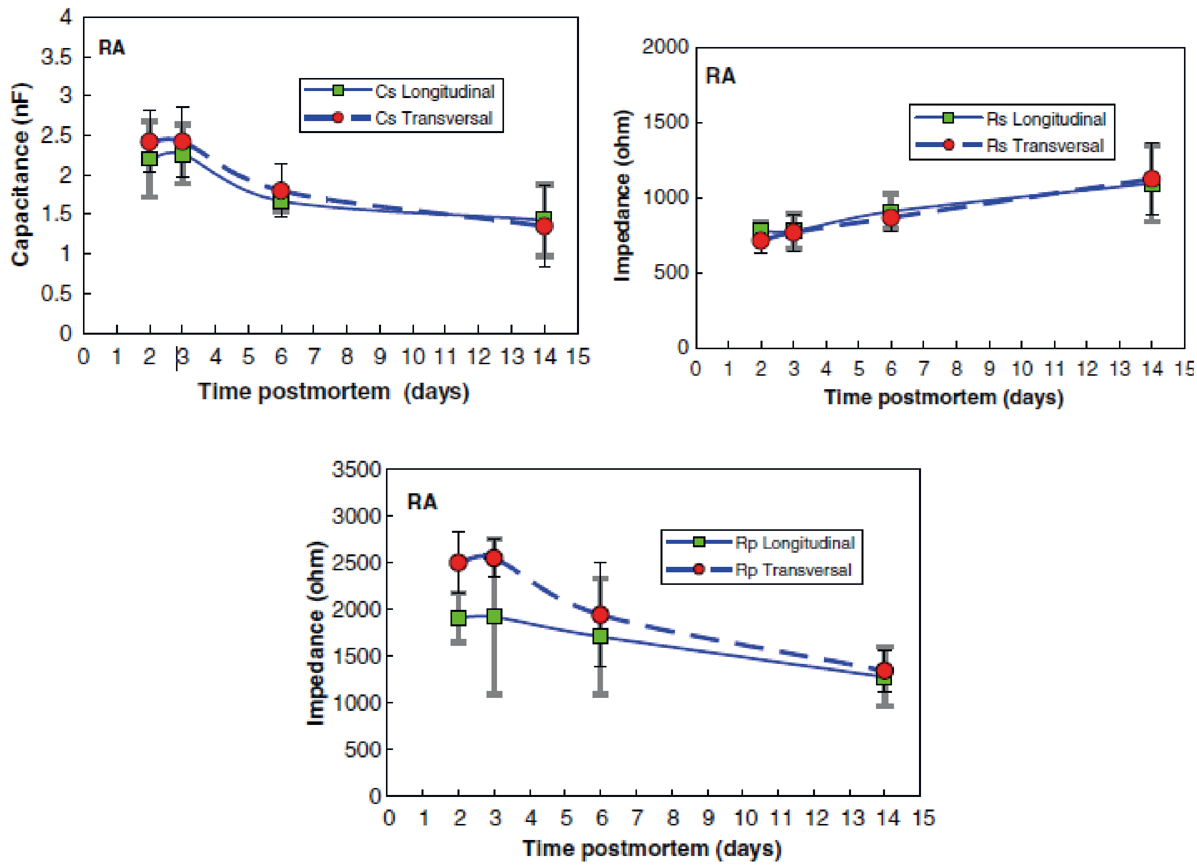

Figure 18. Evolution of model parameters for the muscle (RA) [19]

From the day 2 (D2) to the day 14 (D14), the capacitance C_s decreases according to membranes lysis and oxidation of the phospholipid membrane layers. R_p decreases due to an increase of the flow of free ions and an increase of the volume of extracellular compartments. However, R_s increases because of the increase of concentration in ICF.

Macdonald confirmed that the empirical approach of Cole-Cole mainly serves to parameterize the data without clarifying the underlying mechanisms [65]. He has mentioned that it is more appropriate to use either an isolated CPE properly separated to other parameters C or R [59]. Pliquett also confirmed and mentioned [10] that several attempts to find a physical meaning for the parameters in the Cole-Cole model didn't reach a satisfying result. Ivorra et al. [66] have confirmed that above theories do not easily explain the fact that α evolves with time under certain circumstances. An experiment on cold preservation of rat kidneys shows that the evolution of α is completely independent of the rest of bio-impedance parameters. Ivorra has explained that α follows some sort of induced damage that has nothing to do with the cellular edema.

Martinsen [41] has mentioned that because of their simplicity, the Cole-Cole model have been used extensively in the literature. It should be noted that a circular arc locus is not a proof of any accordance with Fricke's law or the Cole equation.

2.3.3 Critical review

Different investigations demonstrate that impedance spectroscopy is a promising method. The advantage is to get a lot of information and the possibility to realize measurement systems with low costs and with short measurement times. Working frequency range and the analysis of different physical mechanisms occurring in the impedance spectra represent an important challenge for a correct characterization. This will be investigated in this work by experimental measurements, which will be subjected to analysis and comparison with expected values and trends given from physical considerations.

The analysis of measured tissues represents also an important part for meat characterization. Different authors have used the Fricke model or the Cole-Cole model. An appropriate model for the meat should be investigated in order to be validated by the correlation to biological basics.

Modeling of the meat has been linked to membrane modifications, but all these models have not been clearly explained. Although it has been shown that there is no model usable especially for meat characterization until now and that fits with the meat spectrum. A close connection between evolution of the model of the electrical meat impedance and the dependence of model parameters on aging represent an important goal.

2.4 Data mining and tissue classification

Several investigations have been carried out in the field of meat and food diagnosis. We will show some of them in this section that have similar principle of diagnosis methods. An overview is given about different results realized with data mining and classification methods related to the topic of biological tissue monitoring.

2.4.1 Features and classification of biological tissue

Different features of the impedance spectra can be adopted for data mining such as the use of model parameters, the use of characteristic points, the extraction of data at a fixed frequency or the use of the whole measurement results. The most used feature as input for classification is the model parameters. According to the literature, Principal Component Analysis (PCA) has been often used to reduce features to only the necessary inputs [67, 68, 69].

MLP network, multilayer perceptron is the most frequently used neural network in the different application of biological tissue classifications and also in medical applications [70] and is known by its high accuracy [71].

Guerrero et al. [72] have used Cole-Cole model parameters to describe the relationship between sensory properties and electrical parameters of different meat qualities of hams for the muscles SM (Semi-Membranous) and the muscle BF (Biceps femoris). The used parameters are R_0 that correspond to the electrical impedance at lower frequencies, R_{inf} that correspond to the electrical impedance at high frequencies, α that correspond to the shape adjustment parameter and fc that correspond to the characteristic frequency of the region under measurement at which the imaginary part of the electrical impedance is the largest in absolute value. A fifth parameter is introduced: the ratio between R_{inf} and R_0 that corresponds to the parameter proportional to the ratio of extracellular water to total water in meat.

Principal component analysis is used in order to group different hams, and to locate them in the biplot. They are classified in three groups according to the main components, hams having pH45 (define as the pH at 45 min post-mortem) lower than 5.85 were classified as PSE (Pale, Soft, Exudative), hams with pHu (defined as the pH at 24 h post-mortem) higher than 6.0 as DFD (Dark, firm, and dry) and the rest as normal hams. EIS prototype correctly detected 69.2 and 56.0% for SM and BF muscles, respectively of the problem hams in terms of pastiness. Authors have suggested that the electrical parameters evaluated in green hams by the EIS prototype could be useful for predicting pastiness in dry-cured ham.

Also, for the application of bovine tissue classification, Negri et al. [26] have used features for classification composed by the Cole-Cole parameters R_0, R_∞, τ and α. Results show that using the fitted Cole-Cole model parameters instead of the full spectrum as the input of a neural network can enhance its classification rate and significantly reduce its topology when tested with experimental bovine tissue spectra.

The same method has been used by Filho et al. [73] for classification to assess bovine milk quality. They have confirmed the use of the Cole-Cole parameters may have a better classification than the use of the raw acquired spectrum. Using a multilayer perceptron (MLP), the recognition percentage can reach 94.6% to classify adulterated milk samples within the type of impurity added, Water (H_2O) or hydrogen peroxide (H_2O_2). The used MLP is composed by a hidden layer with two neurons, an output layer with three neurons defining each class (milk, milk with H_2O, milk with H_2O_2).

Farell et al. [74] have made the online assessment of food as it cooks performed using an optical reflection method. During cooking a series of chemical reactions lead to a change of colors. These colors changes occur in the visible region of the electromagnetic spectrum. Principle component analysis has been applied to the spectra recorded from the food products, which has allowed the dimensions of the input layer of the interrogating artificial neural network to be reduced from many 10s to typically 3. This results in a high efficiency and a low demand of computation power in the system. The used artificial neural network is a feed forward network with one hidden layer that uses the back propagation algorithm for its training. The classification is obtained using the color scale. Results show that the network give an almost good classification has been observed despite some uncertainties.

Qiao et al. [75] have used the principal component analysis to compress the entire spectral wavelengths (430–1000 nm) into 5, 10 and 20 principal components (PCs). The so called ImSpector collected spectral images in a wavelength range of 400–1000 nm with a spectral resolution of 2.8 nm and a spot radius <9 µm.

Results show that reddish, firm and non-exudative (RFN) and reddish, soft and exudative (RSE) samples have been successfully grouped cluster analysis showed that the RFN and RSE samples were successfully grouped with a total corrected ratio as 75 to 80%. The MLP network yielded the corrected classification as 69% by 5 PCs and 85% by 10 PCs. The transfer function of tansig has been used for the hidden layer and the Purelin one for the output layer. The training algorithm of Bayesian regularization (Trainbr) has been used in order to avoid over fitting.

Winquist et al. [76] have assessed ground beef meat's quality generating good classification result when using an unsupervised training neural network. After reducing the data set from 56 samples to 25 samples using PCA algorithm, authors have classified the meat into three different qualities: Fresh, doubtful and disgusting. A three-layer network has been trained to recognize the storage time and the type of ground meat.

The MLP is consisting of 15 input signals. The input layer consists of 15 neurons corresponding to the 15 elements in the sensor array. The hidden layer consists of seven units. The output layer consists of two units, equal to the number of output variables to be identified and classified. The classification has been found good especially for disgusting state where no misclassification has occurred in the test phase.

Chandraratne et al. [77] have used in their investigation on lamb carcass classification system, texture analysis and artificial neural networks. Features are composed by digital images of lamb chops used to calculate twelve image geometric variables. In addition, a set of ninety texture features has been used to extract the textural information and the texture analysis is based on the co-occurrence matrix method. Principal component analysis (PCA) was used to reduce the dimensionality of feature spaces with six geometric variables and eight co-occurrence texture variables. Three-, four- and five-layer multilayer perceptron (MLP) networks have been performed on the classification process. The classification accuracy from three-layer MLP is 93.1%.

LVQ network (Learning Vector Quantization) presents a successful network for meat and food classification. Janghel et al. [78] have tried to reach a high performance by comparison between different models: Multi-Layer Perceptron (MLP), Radial Basis Function Network (RBF), Learning Vector Quantization (LVQ) and Competitive Learning (CL), to help doctors detecting the presence of the cancer with a high efficiency.

The objective is to develop a diagnosis system using neural network model for breast cancer detection. Using 10 medical features as input data for the neural network models, the comparison results show that the Learning Vector Quantization (LVQ) with an accuracy of 95.82% is the best neural network in detecting breast cancer.

Chuang et al. [79] have developed a method for differentiating a cancerous tissue from adjacent normal tissues and classifying different functional regions in a complex biological tissue using neural networks. As measurement method, they have used the mass spectroscopy imaging aiming to visualize molecules on tissues surfaces. A comparison is carried out between the self-organizing feature maps (SOFM) and the LVQ neural network to identify the tissue and non-tissue regions as a first step, then to identify cancerous human tissues from the normal ones.

LVQ classification neural network has proven its efficiency, the compared data and images show that the computing results obtained by LVQ agree well with classification results. Results show an error rate of less than 23.38% for the identification of cancerous regions and an error rate of less than 9.08% for identification of the adjacent normal regions.

Other neural networks are used in the meat classification and computing, such as radial basis neural networks and counter propagation (CP). Prevolnik et al. [80] used the near infrared spectra to evaluate pork's meat properties. Comparing Back propagation (BP) and counter propagation (CP) for the neural networks with PLS (partial least squares) regression. Error computing has been found to be (2.2–2.5%) for the neural networks.

Balasubramanian et al. [81] have developed models that classified the beef samples into two groups; unspoiled and spoiled based on the microbial population. Maximum total classification accuracies using radial basis function neural networks above 90% obtained for the samples stored at the two temperatures.

After performing PCA to determine the number of principal components that explains 99% or higher variations in the dataset, redundancies have been eliminated and the dimensionalities of a dataset have been reduced. Among the methods used for classification and diagnosis, fuzzy logic is considered as an important technique which deals with uncertainty problems and gives usually good results in various areas.

Fuzzy logic is widely used in medical applications for diagnosis of tuberculosis, cancer, asthma, diabetes, aphasia, malaria, HIV disease, pulmonary embolism, cortical malformations and pancreatic diseases [82]. Researchers have used fuzzy logic to an earlier detection of breast cancer [83, 84]. Results are found to be very useful and helpful for oncologists, radiologists and doctors. Thus, fuzzy logic, as an intelligent system, will be with great help especially when saving the patient's life could be possible.

Balancia et al. [85] have classified cancer within its risk degree. Taking as inputs the age of the patient and the tumor size; a fuzzy logic system has been developed using FuzzyTECH which generates the cancer risk degree. The defuzzified outputs when compared with clinical observations are found to be almost similar. Other researchers [86] used MATLAB toolbox to estimate the risk degree of a breast cancer using the Mamdani fuzzy inference. After choosing the membership functions and aggregation for the 8 input factors, the system has been tested using available patient and healthy people. Optimal performances have reached 87%. Fuzzy logic classifier in estimating the risk of neonatal death has been shown to be useful in a variety of input values by Fernando et al. [87]. Neonatal mortality is defined as the death that occurs up to 28 days of life and it's an important population health indicator.

A Mamdani fuzzy inference developed in MATLAB software has as inputs the birth weight of the newborn baby with four fuzzy sets and the gestational age with three fuzzy sets. When compared with experts' observations, the fuzzy system gave good results with a correlation coefficient of about r=0.96.

Human health management under uncertainties is the underlying issue of Jampour et al. [88] especially when humans are exposed usually to animals and domestic products. When cattle suffer from serious disease, it would be necessary to detect such risk to protect humans from eventual contamination.

Hence, researchers have developed fuzzy logic systems using MATLAB software to diagnose diseases with neurological signs in cattle. After several studies, it has been found that the signs to be considered as fuzzy inputs are: Animal body temperature, salivary secretion, blindness and the hyper reaction to environmental agent to finally determine one of the five disease types: Poly Encephalomalacia (PEM), lactation tetany (LT), Bovine Spongy Encephalopathy (BSE), Rabies, silent form (R), Lead poisoning, acute form (LP).

Jampour et al. have shown that among 20 cases tested, 3 samples suffer a mismatching which is considered as acceptable. Neshat et al. [89] have proved that a fuzzy logic system can be applied as an assistant for improvement of medical diagnosis.

In fact, a fuzzy inference system has been developed to diagnose liver disorders offering then a faster, cheaper, and also more reliable and more accurate results than traditional methods. Using FIS tool in MATLAB, a modeling of a fuzzy system with 7 input data and one output data presenting the liver disorder risk has attained a performance 91%.

Table 3 gives an overview of all studies using MLP network previously presented, table 4 gives an overview of all studies using LVQ network previously presented and table 5 gives an overview of selected previous studies using Fuzzy logic.

Table 3. Summary of selected investigations including MLP network

Filho et al. (2011)	
Main objective	Classification of adulterated bovine milk within the type of impurity
Features	Cole-Cole model parameters
Performance	MLP with a performance of 94.6%
Farrell et al. (2005)	
Main objective	Quality assessment of food
Features	Cole-Cole model parameters
Performance	MLP with a high accuracy equal to 100%
Qiao et al. (2007)	
Main objective	Pork quality and marbling level assessment
Features	Hyper spectral imaging
Performance	MLP network with a performance 65% with 5, 85% with 10 PCs
Winquist et al. (1993)	
Main objective	Beef meat's quality
Features	Feature extracted from the electronic nose
Perforamance	MLP training, almost good classification results especially the disgusting state
Chandraratne et al. (2003)	
Main objective	Lamb carcass classification
Features	Digital images of lamb
Performance	MLP network with an accuracy 93.1%

Table 4. Summary of selected realized work in biological tissue using LVQ

Janghel et al. (2010)	
Main objective	Diagnosis and prediction of breast cancer
Features	Clinical tests reports
Performance	ANN with Multi-Layer Perceptron (MLP), Radial Basis Function Network (RBF), Learning Vector Quantization (LVQ) and Competitive Learning (CL). The LVQ reaches the best performance with 95.82%
Chuang et al. (2012)	
Main objective	Differentiating cancerous tissue from normal tissues and classifying the different functional regions in a complex biological tissue
Features	Mass spectrometry imaging (MSI)
Performance	Comparison between SOFM and LVQ. The results showed an error rate less than 23.38% for the identification of the cancerous regions and an error rate less than 9.08%

Table 5. Summary of selected investigations using fuzzy logic

Prasath et al. (2013) - Saleh et al. (2011) -Latha et al. (2013) - BALANICĂ et al. (2011)	
Objective	Breast cancer detection
Features	Hospitals oncology
Classification	Fuzzy logic, test results are similar with those of doctors' observations
Yılmaz et al. (2011)	
Main objective	Detection of cancer and identification of the cancer type
Features	Data have been obtained from hospitals' information and statistics
Performance	Fuzzy logic ➔ Mamdani inference type with 8 inputs. Performance is 87%
Nascimento and Ortega (2002)	
Main objective	Estimating the risk of neonatal death (death of newborn infants)
Features	Data were obtained from hospitals' information and statistics
Performance	Fuzzy logic ➔ Mamdani inference type: Inputs are the birth weight of the newborn baby with 4 fuzzy sets and the gestational age with three fuzzy sets. Correlation coefficient of about r=0.96 compared with experts' observations
Mahdi and Mohsen Jampour (2011)	
Main objective	Diagnosis of cattle and domestic animals with neurological disease signs
Features	Veterinary observations and results
Performance	Fuzzy logic ➔ four input signs and five output disease type Acceptable classification: among 20 cases only 3 present mismatching
Neshat at al. (2008)	
Main objective	Diagnosis of liver disorders
Features	Data collected by a liver disorder specialist
Performance	Fuzzy logic ➔7 inputs and 1 output: the liver disorder risk. Performance 91%

2.4.2 Theoretical background

In this section we will present the theoretical background related to the most important parts of methods presented in different researches: PCA method, neural network with MLP and LVQ and fuzzy logic methods.

PCA belongs to statistical methods of multivariate analysis [90]. It is a method of transforming the initial data set of high dimensions into a new data set represented by a vector of samples. The goal of this transformation is to concentrate the information and reduce their dimension by considering the data variance. The PCA method is a linear transformation as described in the equation 15 which transfers the original possibly corresponding data set X to a new uncorrelated data set Fnew. The new data set Fnew has the same dimension as the original data set X. At is the coefficient transformation matrix.

$$F_{new} = A_t \times X \tag{15}$$

First few components (columns) of the new data set Fnew contribute the majority of variances and are considered to be the principal components, which can reflect the original data matrix without big information losses. They have smaller dimension and are uncorrelated to each other, which makes the analysis of the data much easier. The input data set Xd is in the form of matrix as shown in equation 16, where p is the number of the parameters and n is the number of the observations.

$$X_d = \begin{pmatrix} x_{11} & x_{12} & \cdots & x_{1p} \\ x_{21} & x_{22} & \cdots & x_{2p} \\ \vdots & \vdots & \vdots & \vdots \\ x_{n1} & x_{n2} & \cdots & x_{np} \end{pmatrix} \tag{16}$$

Artificial Neural Network (ANN) was invented in 1943 by McCulloch and Pitts [91] with the presentation of the formal neuron which is an abstraction of the physiological neuron. In 1949, Hebb [92] presented the learning rules. Currently, several models of networks are still inspired by the Hebb rule. In 1958, Rosenblatt [93] developed the perceptron model. This is a neural network inspired by the visual system. This is the first artificial network able of learning from experience. In the same period, the Adaline (Adaptive LINAR Element) model has been introduced by Widrow and Hoff [94]. This model has been subsequently the base model multilayer networks. In 1969, Minsky and Papert [95] published a review of properties of the perceptron, having a great impact on research in this area. In 1972, Kohonen [96] presented associative memories and offered applications to pattern recognition. In 1982 Hopfield [97] presented a completely looped network, which analysis the dynamics. An artificial neural network is a mathematical model that mimics the architecture and the functionalities of a biological neural network. Neural networks, composed of artificial cell structures (Figure 19), are an approach for addressing the perception problems, memory, classification, learning and reasoning. Neurons are connected by weights which control the behavior of the whole structure. The adaptation of these weights gives neural networks the ability to learn and remember information. Learning artificial neural network is a very important phase for the implementation. It consists to determine or to change the network settings to adopt a desired behavior. It consists to determine the weights of the connections according to the problem at hand.

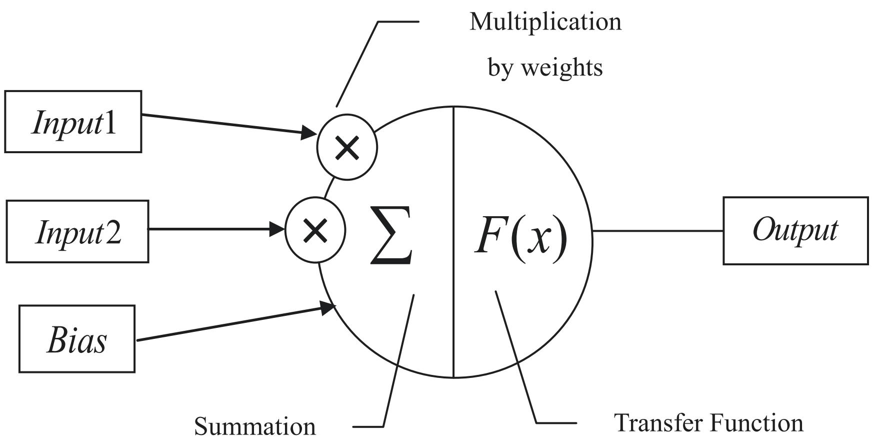

Figure 19. Artificial neuron structure [98]

Neural networks can be classified into three categories [99], supervised training, unsupervised training and hybrid. Table 6 contains a selection of neural networks and their corresponding learning algorithms.

Table 6. Neural network types and their learning algorithms

Paradigm	Learning Rule	Architecture	Learning Algorithm	Task
Supervised	Error-correction	Single or multilayer perceptron	Perceptron learning algorithms Backpropagation Adaline and Madaline	Pattern classification Function approximation Prediction, control
	Boltzmann	Recurrent	Boltzmann learning algorithm	Pattern classification
	Hebbian	Multilayer feed-forward	Linear discriminant analysis	Data analysis Pattern classification
	Competitive	Competitive	Learning vector quantization	Categorization Data compression
		ART network	ARTMap	Pattern classification Categorization
Unsupervised	Error-correction	Multilayer feed-forward	Sammon's projection	Data analysis
	Hebbian	Feed-forward or competitive	Principal component analysis	Data analysis Data compression
		Hopfield network	Associative memory learning	Associative memory
	Competitive	Competitive	Vector quantization	Categorization Data compression
		Kohonen' s SOM	Kohonen' s SOM	Categorization Data analysis
		ART networks	ART1, ART2	Categorization
Hybrid	Error-correction and competitive	RBF network	RBF learning algorithm	Pattern classification Prediction, control Function approximation

In a supervised learning, the training data are pairs of input and desired output values that are traditionally represented in data vectors. The operator should clearly supply the network with the desired targets that shouldn't be chosen randomly by the system. This type of learning is widely used in classification and pattern recognition. The response of the network to the inputs is measured. Weights are modified to reduce the difference between the actual and desired outputs. They are corrected according to the error value. Such a training is also called "learning with a teacher" since a control process knows the correct output answer for the set of selected input vectors. For unsupervised learning, only the inputs are supplied to the network; the output values are generally unknown. The neural network adjusts its own weights so that similar inputs cause similar outputs. The network must itself identify, classify or recognize the incoming inputs without any external assistance or "teacher" which is not the case in this thesis. The hybrid learning combines both supervised training and unsupervised training.

Similar to neural network, the validation of fuzzy logic is carried out using unknown data. In this case, Fuzzy logic is used for classification and clustering.

Fuzzy logic has been first introduced by Zadeh [100]. It is a mathematical technique dealing with imprecise data and problems that have solutions unlike logic. It resembles more to human logic since it works with range values. Unlike classical theory which deals with binary propositions ("false" or "true"), fuzzy logic avoids dealing with categorical systems. A global architecture of fuzzy logic system is shown in Figure 20.

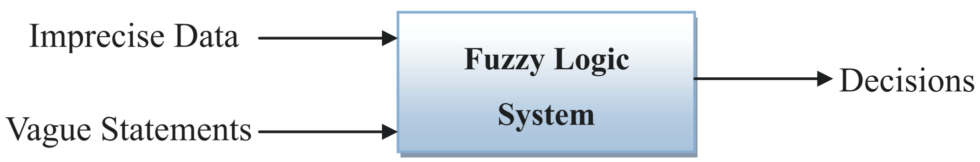

Figure 20. Global architecture of a Fuzzy logic system

The process of fuzzy inference system includes three principal steps [101]:

- Fuzzification of input variables and choice of suitable membership functions
- Construction of fuzzy rules and making decision
- Defuzzification

An explanatory architecture of fuzzy inference process is shown in Figure 21.

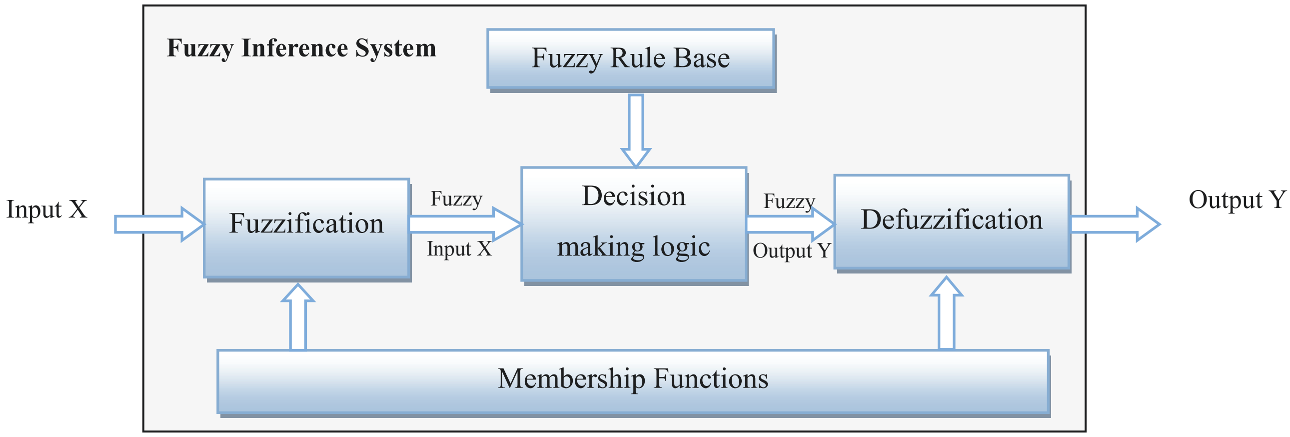

Figure 21. Block structure of a Fuzzy system

In fact, the model's parameteres (received data) undergoes a feature's extraction process (information) which is a preparatory step for our classification method. The resulted data are then fuzzified using membership functions. Afterward, Fuzzy values are analyzed using fuzzy rules to get our fuzzy outputs. After deffuzification, the new data are then compared and classified with similarities to get the desired clusters.

Fuzzification is the conversion of crisp input data into fuzzy values or linguistic variables using membership functions. These fuzzy values reflect the human perspective of the given system. These fuzzifiers are membership functions determined depending on a subjective view of the problem and an individual's perception of the situation. Depending on the desired class and performances, simple functions are used to build membership functions such triangular, trapezoidal and Gaussian ones.

Fuzzy rules, which have the general form of "IF X is A THEN Y is B", are destined to map the fuzzy input X to the fuzzy output Y. In a logical context, X is referred to be a linguistic variable and A is a linguistic value. The 'IF' part of the rule is called antecedent; the 'THEN' part is called consequent. Connection between the rules is achieved using logical operators AND, OR and NOT. AND or min takes always minimum of the functions values. OR (max) takes the maximum of the presented functions.

Defuzzification is the conversion of a fuzzy set quantity to a precise and deterministic set quantity. This step is necessary because in several applications, where the implementation is required, machines could only work with crisp or binary values and not with linguistic variables.

After defuzification, the new data are compared and classified to get desired clusters [102]. Two important types of fuzzy logic systems exist and are much used for diagnosis, Mamdani inference [103, 104] and Takagi-Sugeno inference [105].

Mamdani method is suitable for nonlinear systems, characterized by a fuzzy set consequent in the fuzzy rule that has the form of

$$R: IF \ \ L(x_1 \ is \ A_1, ..., x_k \ is \ A_k) \ \ THEN \ \ (y_1 \ is \ B_1, ..., y_n \ is \ B_n)$$

x_1,.., x_k are the inputs of membership functions, A_1,.., A_k are the fuzzy sets of the antecedent part, y_1,.., y_n are the outputs of the membership functions, B_1, ..., B_n are the fuzzy sets of the consequent part and L is the logical function connecting the propositions.

For Takagi-Sugeno Method (TS)**,** output membership function or more precisely the rule consequent is only linear or constant. If the rule consequent is constant we call the model a zero-order Sugeno model which has the following form:

$$R_0 : IF \ \ L(x_1 \ is \ A_1, ..., x_k \ is \ A_k) \ \ THEN \ \ y = k$$

Where k is a crisply constant defined by the operator.

If the rule consequent is a linear function the Sugeno model is called a first-order Sugeno model with the following expression:

$$R_1 : IF \;\; L(x_1 \; is \; A_1, \ldots, x_k \; is \; A_k) \;\;\; THEN \;\; y = f(x_1, \ldots, x_k)$$

Hence, for a first order Sugeno model we should find some linearity dependence between the outputs and the inputs of the membership functions.

Another difference between Mamdani and Sugeno methods is that all output membership functions of TS method are singleton spikes, and the implication and aggregation methods are fixed and cannot be edited. The implication method is simply multiplication, and the aggregation operator just includes all of the singletons [106].

2.4.3 Critical review of methods used for data mining and classification

The use of information gathered from the measured impedance for different beef muscles in different periods of time represents a critical challenge. According to the literature, Principal Component Analysis (PCA) has been used for data mining. This method will be used in this work in order to verify the consistency of features will be used for the classification. For diagnosis, the classification needs a supervised learning network transforming a set of input signals into a set of output signals, since the targets are already predefined. This transformation is determined by an external adjustment supervised system parameters, the training examples are supplied with their membership class. Its examples are called stimulus input. The network output is called target. A comparative approach is efficient to decide about suitable classifiers.

3. Experimental investigations

3.1 Introduction

This chapter deals with experimental investigations and especially the bio-impedance measurement procedure. Sensitive measurements with high reproducibility represent an important challenge in order to build a solid basis for meat diagnosis. For reproducibility, we need overcome both anisotropy and contacting effects. We aim therefore to develop electrodes with suitable configurations. The electrode configuration is supported by simulations using the Finite Element Method that provides information about the distribution of the electric field in the meat sample.

3.2 Measurement setup

The measurement setup consists of a laboratory impedance analyzer (Agilent 4294 A) [107] connected to a personal computer for data acquisition. The spectrometer generated a signal within a frequency band ranging from 40 Hz to 110 MHz (Figure 22).

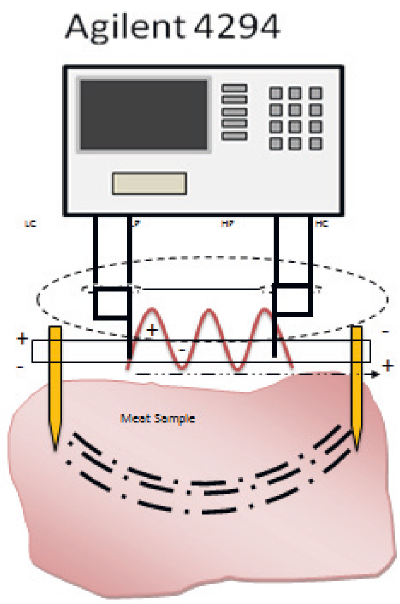

Figure 22. Bio impedance measurement set-up

Electrodes are connected with a sample in series. A calibration of the electrode is programmed in LabVIEW that aims to eliminate influencing effects, especially cable effects, before every measurement. The measurement set-up automation is carried out using the graphical Lab VIEW software. Lab VIEW allows the transfer of results from the impedance analyzer to the computer. It permit also reading them in different physical forms such as the real and the imaginary parts of the impedance and the admittance. Also it enable the presentation in Nyquist and Bode diagrams. The same presentation is done using Matlab software.

Electrochemical impedance is normally measured using a small excitation signal. The experiment (Figure 23) shows that the use of voltage amplitude of 500 mV provides a better signal to noise ratio then 5 mV and then 50 mV. For in vitro measurement, this excitation voltage will be adopted in all our in-vitro bio impedance measurement.

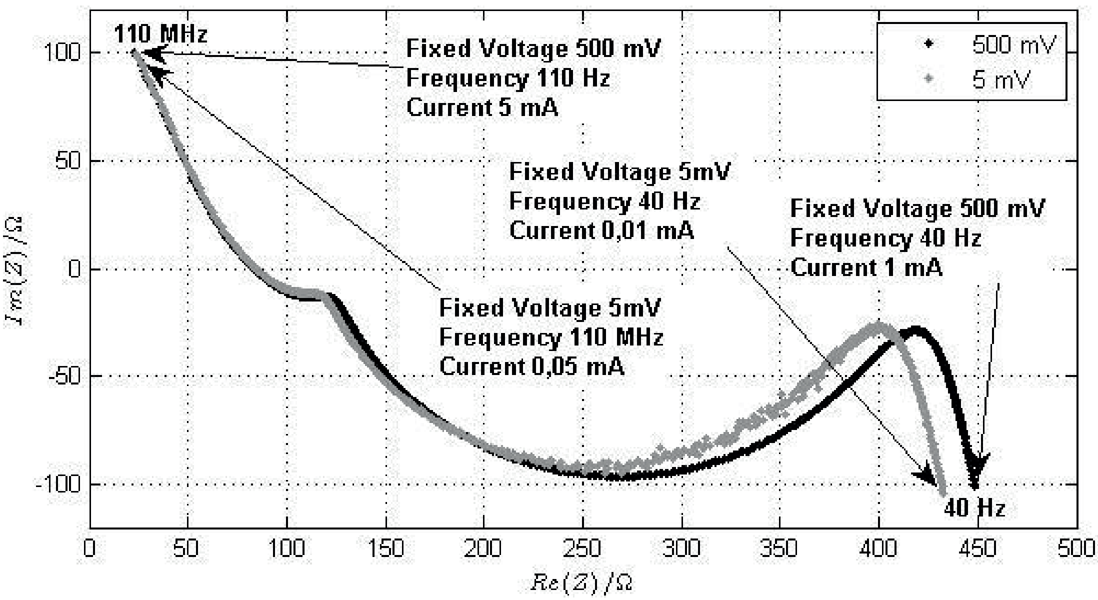

Figure 23. Excitation signal in the frequency range between 40 Hz and 110 MHz

Therefore, we choose the maximum value in the linearity region (500 mV) as a value of the voltage excitation on muscle tissue. When the voltage amplitude is fixed to 500 mV, the current is increasing from 1 mA at low frequency (40 Hz) to 5 mA at high frequency (110 MHz). At 5 mV, the current would be increasing from 0.01 mA (40 Hz) to 0.05 mA at 110 MHz. The extraction of model parameters (Figure 24) is carried out using the evolutionary algorithm described in [108] as well as in [109]. This algorithm realizes global convergence of the corresponding regression, so that the probability to trap into local minima during parameter extraction decreases. Therefore, the parameter extraction is very robust even for models with a higher complexity.

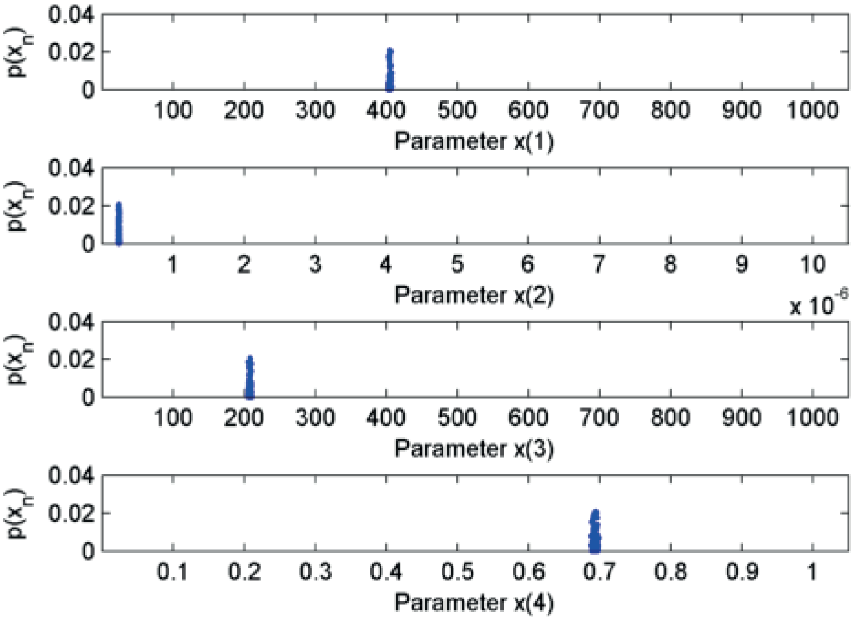

Figure 24. Parameters extraction by evolutionary algorithms

During post-mortem experiments, the appearances of bacteria on the surface of meat and water losses are considered as problematic. Two measurement procedures are proposed to investigate the influence of these two factors during measurements. In the first measurements, meat conserved in closed boxes in the fridge has been investigated. In the second measurements, meat has been maintained without conservation and exposed directly to the air of the fridge. A progressive deterioration of muscles by bacteria that attacks the muscle proteins is denoted during the measurement with conservation of meat in closed boxes. Meat conserved in box went through a very slight decrease of 1.5 g of liquids during four days, this is 1.2 % of the total weight. The first manifestations of this phenomenon are the appearance of a bad odor and changes of the appearance of the meat (Figure 25). Thereafter, when the phenomenon intensifies, the meat develops putrid odor and black area. At this stage, the meat is no more consumable for humans. The main microorganisms responsible for the putrefaction of meat surface are aerobic bacteria. These bacteria are always present on the meat right from the point of slaughter. The growth and the activity of these bacteria are dependent primarily on the temperature. For the measurement of meat without conservation and exposed directly to the air of the fridge, another phenomenon is encountered. The meat becomes dry and a decrease in weight is caused by the loss of liquids from the meat, it becomes drier and leads to a change of color, which turns into dark red, black (Figure 26). The meat exposed to air loosed 11 g in four days, which is 8% of the total weight. As seen in (Figure 27) the liquid loss is shown for the two cases.

Figure 25. Deterioration by bacteria of the meat conserved in boxes after 4 days

Figure 26. Meat dries during measurement in open environment after 4 days

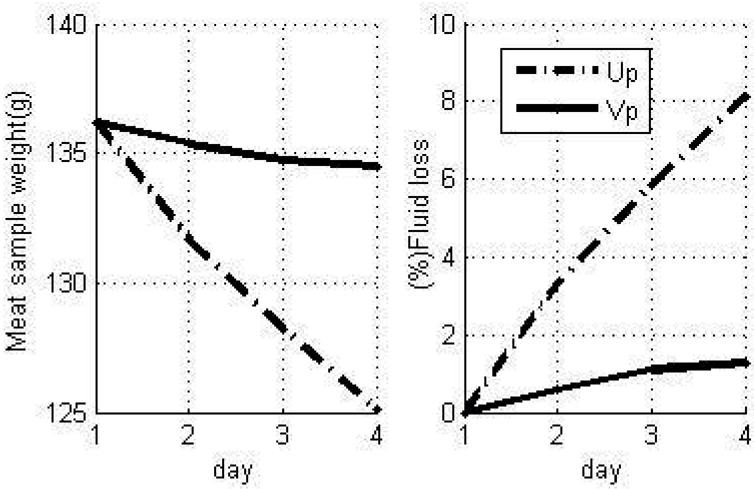

Figure 27. Liquid loss by bad conservation [110]

An experimental procedure is proposed to avoid the appearance of bacteria and to reduce water loss in meat during experiment post-mortem. The solution consists of vacuum packing the meat using a vacuum sealer system and places it in climate chamber in the temperature of 2°C (Figure 28). Meat is vacuum packed to reduce drying effects and influence of bacteria. Maintaining the same meat humidity is not only important to rebuild real storage condition. It is also very important for reproducible measurement since prior investigations have shown that drying of meat leads to a shift of impedance values to higher values and changes considerably the sensitivity to aging. During experiments, meat is stored at a temperature of 2 °C to maintain similar conditions used in meat selling sector and reducing effects of temperature changes on impedance.

Measurements with different muscles have been carried out with time referenced to the time of slaughter. In general, samples with a very low fat content are chosen to avoid electrode contact effects. The post-mortem measurements are carried out during two weeks. This allows getting information about the meat for long period of time and maintains the same state of the meat as in the food chain.

Figure 28. Proposed experimental procedure with packed meat

3.3 Investigations of the influence of anisotropy

Different investigations are carried out for anisotropy and the contacting effects dependency during meat measurement. For the anisotropy dependency, a first experiment is done using needle electrodes (Figure 29) in a beef muscle SM (Semi- Membranous) in 4 directions in relation to the fibers direction: 0° (parallel), 45°, 90° (perpendicular) and 135°. Results (Figure 30) show a big dependence on the direction of the electrodes. This is due to the fact that parallel to the fiber, the current can be better transported than perpendicular to it. Because of difficulties to exactly meet the angles in different experiments, results seem to be nonlinear. Therefore, in order to make an accurate investigation, a second experiment has been carried out.

Figure 29. Investigation of anisotropy with needle electrodes

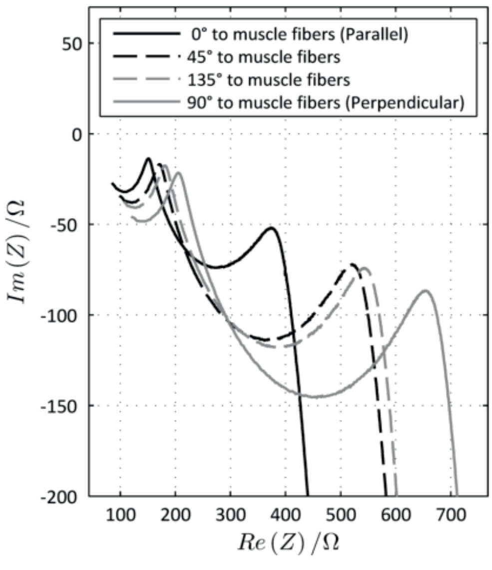

Figure 30. Nyquist plot in 4 positions to fibers direction

In the second measurement, a probe composed by 36 needle electrodes and 18 angles with a step of 10° (Figure 31) has been designed. For example, for an angle of 20° the needle number 16 are chosen. For the angle 160° the needles number 2 are chosen. Experimental results (Figure 32) show an almost linear distribution of the spectrum behavior with the angle. Small deviations are observed between 0° and 180° due to the mechanical stress during the experiment and rest errors. Nevertheless, these changes are very small and therefore negligible. Some research groups suggested to measure in parallel or perpendicular to the direction of fiber direction. This deviation shows that this would be not really possible. On the one hand, it is difficult to exactly detect the direction of the fiber of muscles. On the other hand, small changes of the direction of electrodes lead to significant changes of the impedance spectrum.

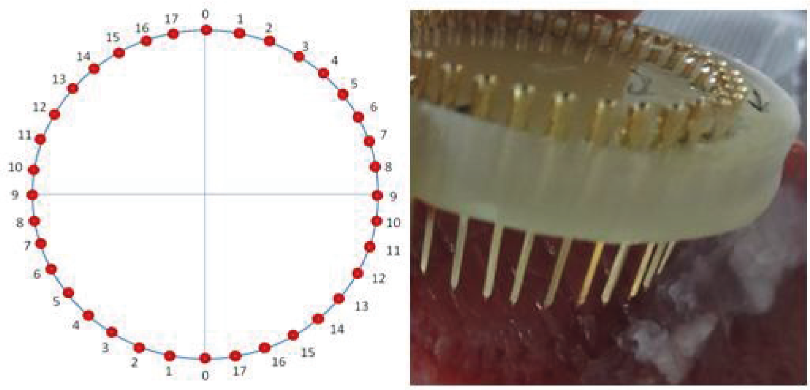

Figure 31. Anisotropy investigation probe

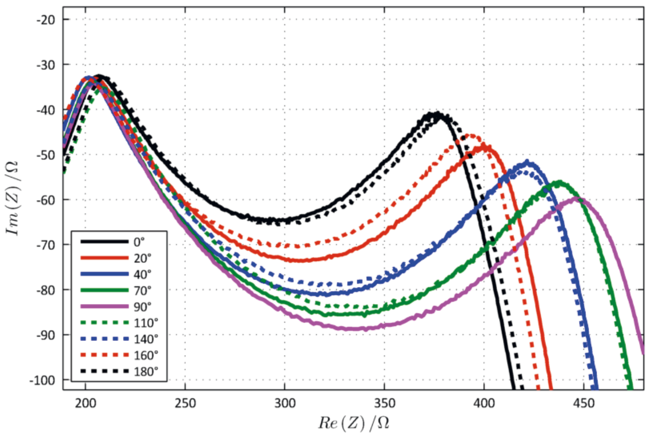

Figure 32. Nyquist plot for different angles to fibers direction

Results of the anisotropy investigations are analyzed deeply by evaluating the characteristic points in the impedance representation of the dispersion β that allow meat characterization [20] especially the characteristic point 1 and 2 (CP1 and CP2) (Figure 33). CP1 corresponds to maximum of the spectrum in the transition region between α and β dispersion and CP2 corresponds to the minimum of the spectrum near the predominant critical frequency of the β dispersion. Characteristic points can be easily determined as maxima and minima of the imaginary part in the corresponding frequency ranges of the impedance as explained in Figure 33.

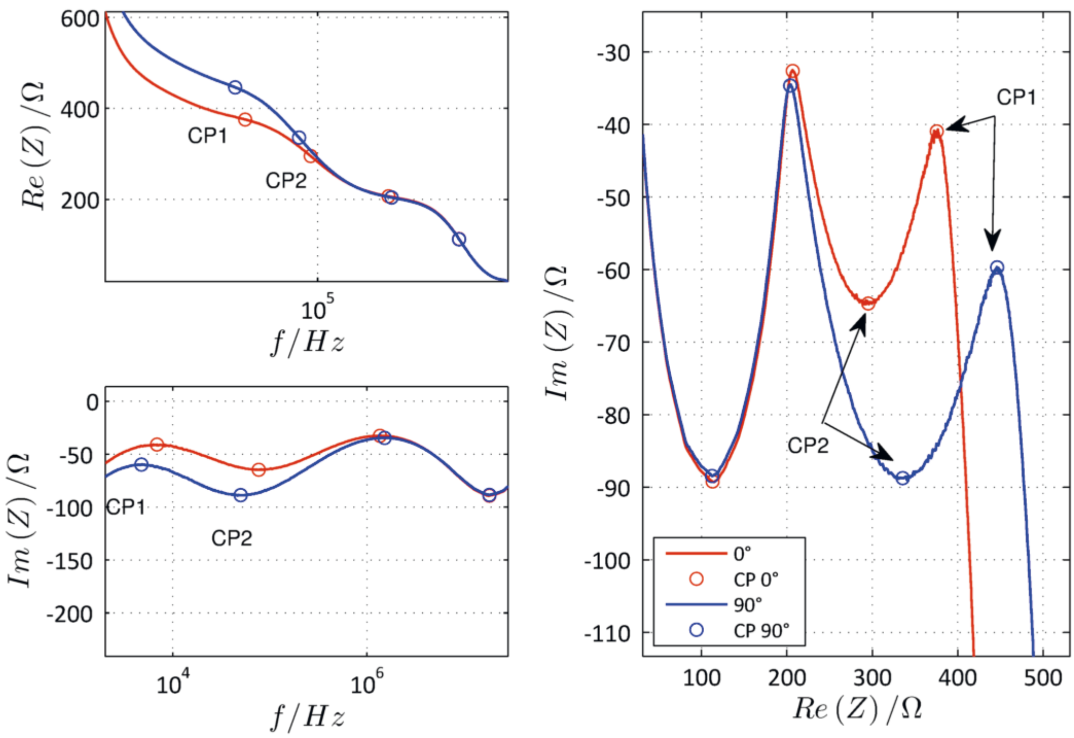

Figure 33. Fiber direction dependency of characteristic points

Figure 34 shows the angular dependency of characteristic points CP1 and CP2. For spectral results in the region of the β dispersion, meat conductivity varies in dependence of the angle. When the angle to fiber is close to 0°, corresponding to electrodes parallel to the muscle fibers, the conductivity increases, in this case the current is better conducted by the fibers than in other cases where it is obliged to cross them.

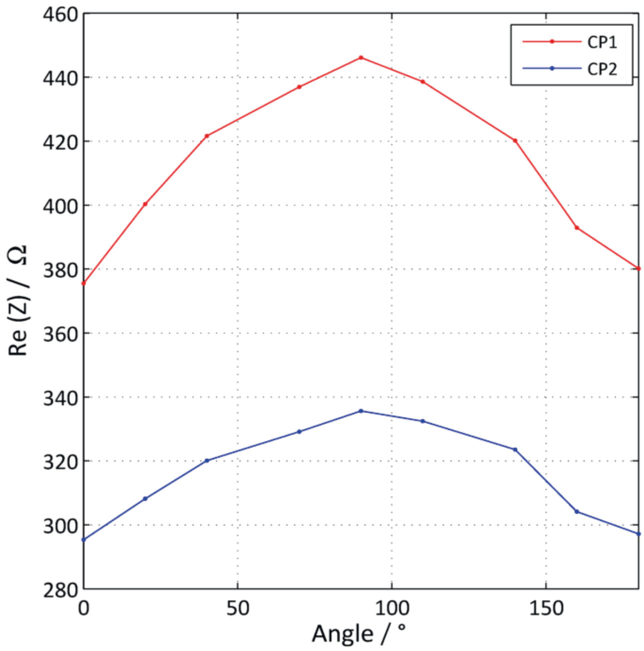

Figure 34. Angle dependency of the considered characteristics points CP1 and CP2

Re (Z) value is minimal at the angles 0° and 180° that correspond to the case parallel to the fiber direction, approximately 380 Ω for the CP1 and 300 for the CP2. Re (Z) increase according to the angle value with approximately 400 Ω for the angle 20° and 160° for the CP1 and approximately 310 Ω for the CP2. The impedance reaches a peak value at the angle close to 90° that corresponds to the position perpendicular to fiber.

The behavior of the critical points of the spectrum in dependence of the angle is better predictable than impedance points at specific frequencies. This means, that critical points CP1 and CP2 are very good features for describing the behavior of the impedance spectrum.

3.4 Influence of contacting effects

In order to demonstrate the influence of contact effect, a measurement of meat is realized using a cylindrical non penetrating electrode with and without applied force (Figure 35). Different beef muscles (N ‘neck’, LD ‘longisimus dorsi’, RA

‘Rectus Abdominis’ and SM ‘Semi Membranous’) are subjected to the experiment. Results show changes of the impedance according to the force applied (around 5 N) on the electrode (Figure 36). This effect becomes more serious if the meat surface is drying, e.g. because of aging.

Figure 35. Cylindrical probe with and without applied force

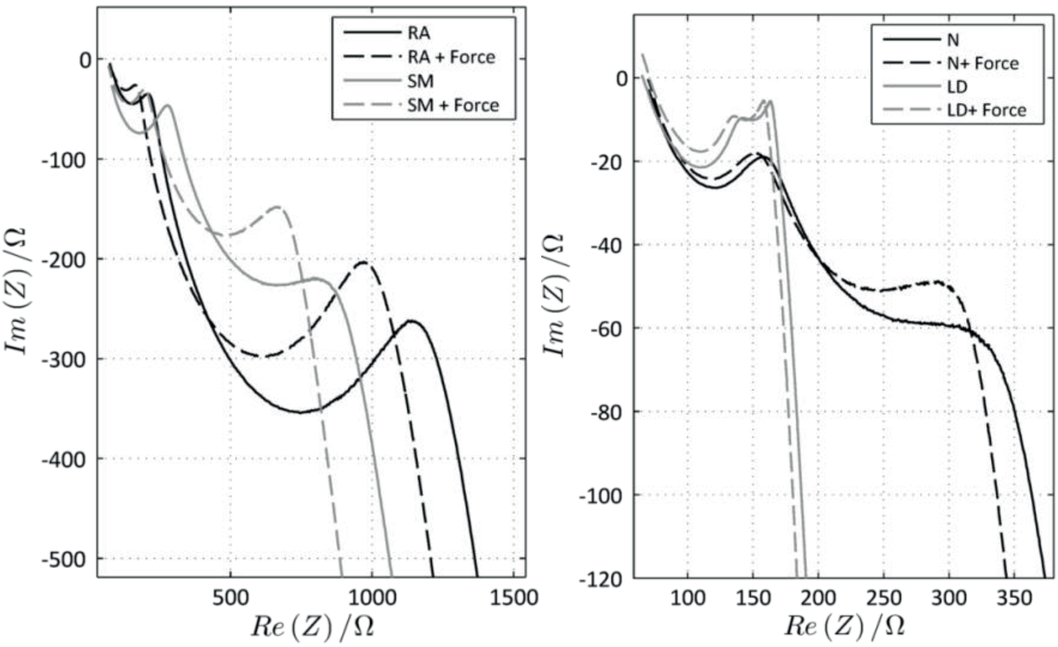

Figure 36. Impedance spectra dependency to an applied force

The investigation confirms existence of a bad contact between electrodes and meat for the non-penetrating probes because of the rough surface of the meat. Acceptable results are only possible when applying sufficient forces (Table 7).

Based on these investigations, we propose electrodes having a cylindrical geometry to eliminate the anisotropy effect in two dimensions and combining cylindrical non penetrating electrode and needle electrodes.

Table 7. Penetrating and non-penetrating electrodes

Needles penetrating electrodes	Cylindrical non penetrating electrodes
	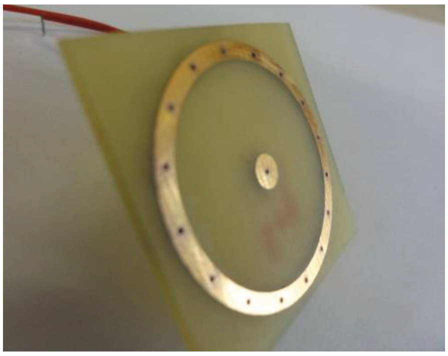
+ very good contact	+ Overcomes the fibers direction dependency
- Fibers direction dependency	- Bad contact to the rough surface - Drying increases resistance

3.5 Electrode design

According to the previous studies, a probe is developed with a cylindrical geometry consisting of 9 steel needle electrodes coated with gold [37, 40] (Figure 37). To ensure a measurement in a big representative volume of meat, we choose that the inner electrode has a distance of 15 mm to the outer electrodes. Electrodes deeply inserted into the sample and located close to each other show the most stable values according to different tests and according to the literature. This proves the importance of needle electrodes that can be inserted in the meat. They do not destroy the meat structure a lot, as a length of only 10 mm is chosen. In order to provide information about the distribution of the electric field in the meat sample, an electrode configuration with nine needles in cylindrical configuration is investigated by Finite Element Methods (Figure 38 and Figure 39).

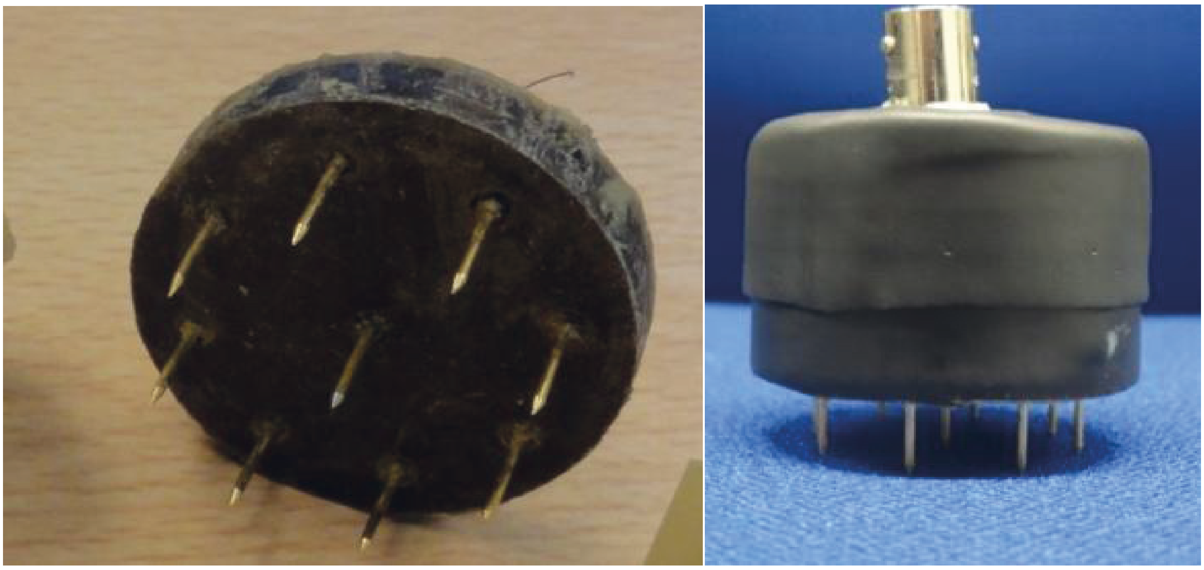

Figure 37. Final design of electrode

The phantom in the simulation is chosen according to the following geometric parameters: Length 80 mm, width 80 mm, height 40 mm. The conductivity has been chosen equal to 0.3 S/m and the relative permittivity has been chosen equal to 100 as mentioned in [111, 112, 113].

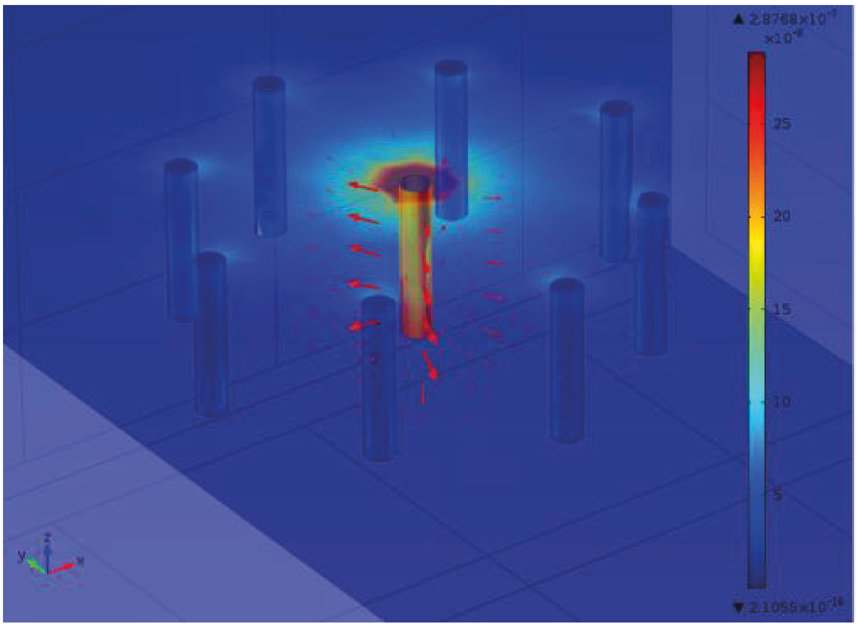

Figure 38. Electric displacement field in 3D

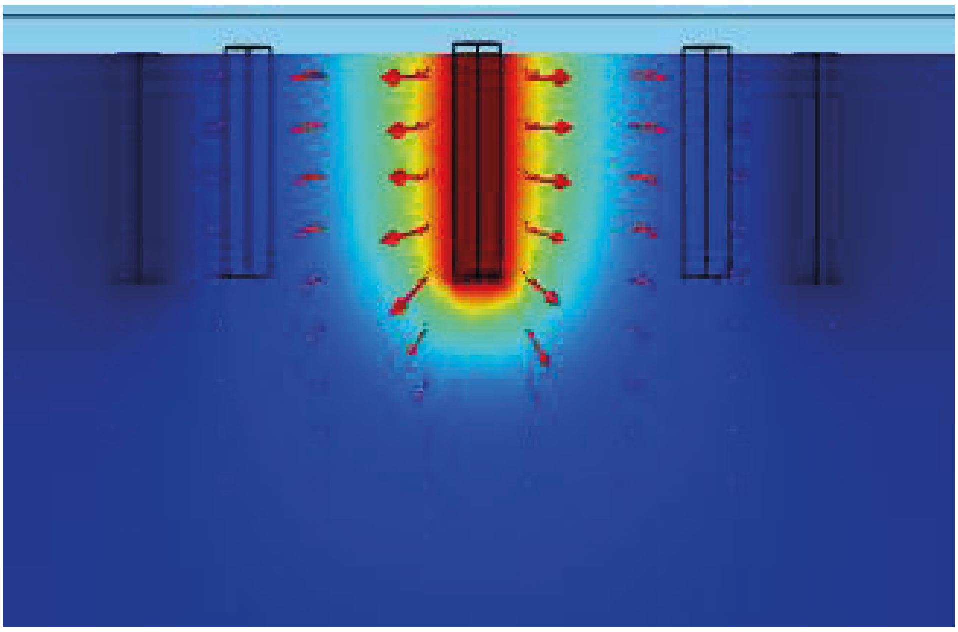

Figure 39. Electric displacement field in YZ view

In presence of an electric field, the phantom is subjected to a displacement of free charges (conduction current) and a movement of charges (displacement current) depending on the electrical conductivity σ and the dielectric permittivity ε respectively. The displacement field corresponds to the following equation, where E is the electric field, ε_0 is the vacuum permittivity and P is the polarization density.

$$D = \varepsilon_0 \cdot E + P \tag{17}$$

The simulation shows that the electric displacement field D varies in the frequency range [10 kHz-10 MHz] between 2.87 10-7 C m^{-2} to 2.1 10-16 C m^{-2} and propagates in the whole volume of the phantom in all possible directions. The choice of 9 electrodes with a diameter of Ø 1 mm and 10 mm depth represents an accurate configuration. The electrode design is tested for different experiments with sufficiently big meat samples. It shows a good reproducibility over time [37] as can be seen in the next chapter.

3.6 Final remarks

The aim of this chapter is to define the measurement procedure for the bio impedance measurement of meat including measurement set-up, excitation signals and probe contacting and probe design. The proposed experimental procedure involve of vacuum packing the meat with a conservation temperature of 2°C during the measurement process ensures avoiding the appearance of bacteria and permits to reduce water loss in meat during experiment post-mortem.

Using the Finite Element Method, a suitable assessment of the volume of the meat sample has been defined. We conclude that the use of electrodes with a circular geometry allows an independency on the anisotropy in two dimensions.

The use of small needles to contact the meat allows a good contact to meat. The final sensor design consists of one central cylindrical electrode and eight surrounding needle electrodes made of gold plated steel (Ø 1 mm).

All these elements, which are decisive for the quality of measurement, have been investigated theoretically and experimentally. Especially the design of the probe, which is critical for the reproducibility, was subject to different theoretical and experimental investigations.

4. Modeling and feature analysis

4.1 Introduction

In this chapter, the evolution of the behavior of beef meat impedance in a long period of time is investigated. The idea is to characterize the relationship between the post-mortem maturation state and the meat impedance change as a basis for developing an in-vitro measurement method for the freshness of meat.

For investigation, we choose the most important muscles that permit to access to visible results even in a long period of time. The three different selected muscle types are Longisimus Dorsi (LD), Rectus Abdominus (RA) and Semi Membranous (SM) (Figure 40).

With these three muscles, we build a database for data mining and classification of tissue type and state. For modeling and feature analysis, we will use two muscles for each animal, the beef and the veal; for the beef (LD-B and RA-B), for the veal (SM-V and LD-V).

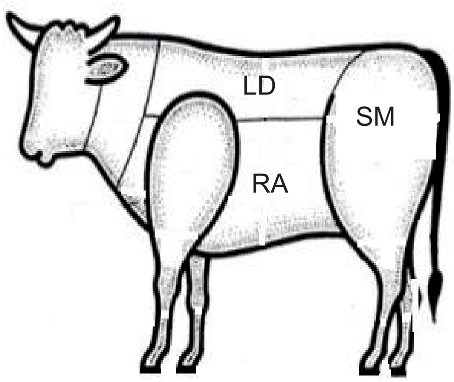

Figure 40. Selected muscles for investigation

In Figure 41, we can clearly see the muscle fibers of beef and veal used for the experiment with a zoom equal to x 1000, the thickness of the muscles fiber are around 80 µm, 70 µm, 60 µm and 45 µm for the muscles LDB, RAB, SMV and LDV, respectively. Muscles fibers of beef are thicker than the muscles fibers of veal. This should be verified by the behavior of the impedance. There is a difference between muscles of the same beef and also muscles of the same veal. This is mainly due to several factors, especially biologic characteristics of each muscle.

Figure 41. Muscles/ Fresh (zoom x 1000)

Measurements have begun in day 2 or 3 after slaughter. Measurements have been carried out for several days in order to characterize the degradation process. The chosen meat samples have a comparable very low fat content and allow therefore a comparison considering the influence of aging.

Meat is vacuum packed and stored at a temperature of 2 °C to be in similar conditions with the conditions in the food chain. The developed circular penetrating probe explained in the last section is used for measurements.

Figure 42 shows typical plots of imaginary part against real part of impedances for different muscles of beef and veal between days 2 or 3 and 14. Results show clearly the three areas of dispersion α, β and γ.

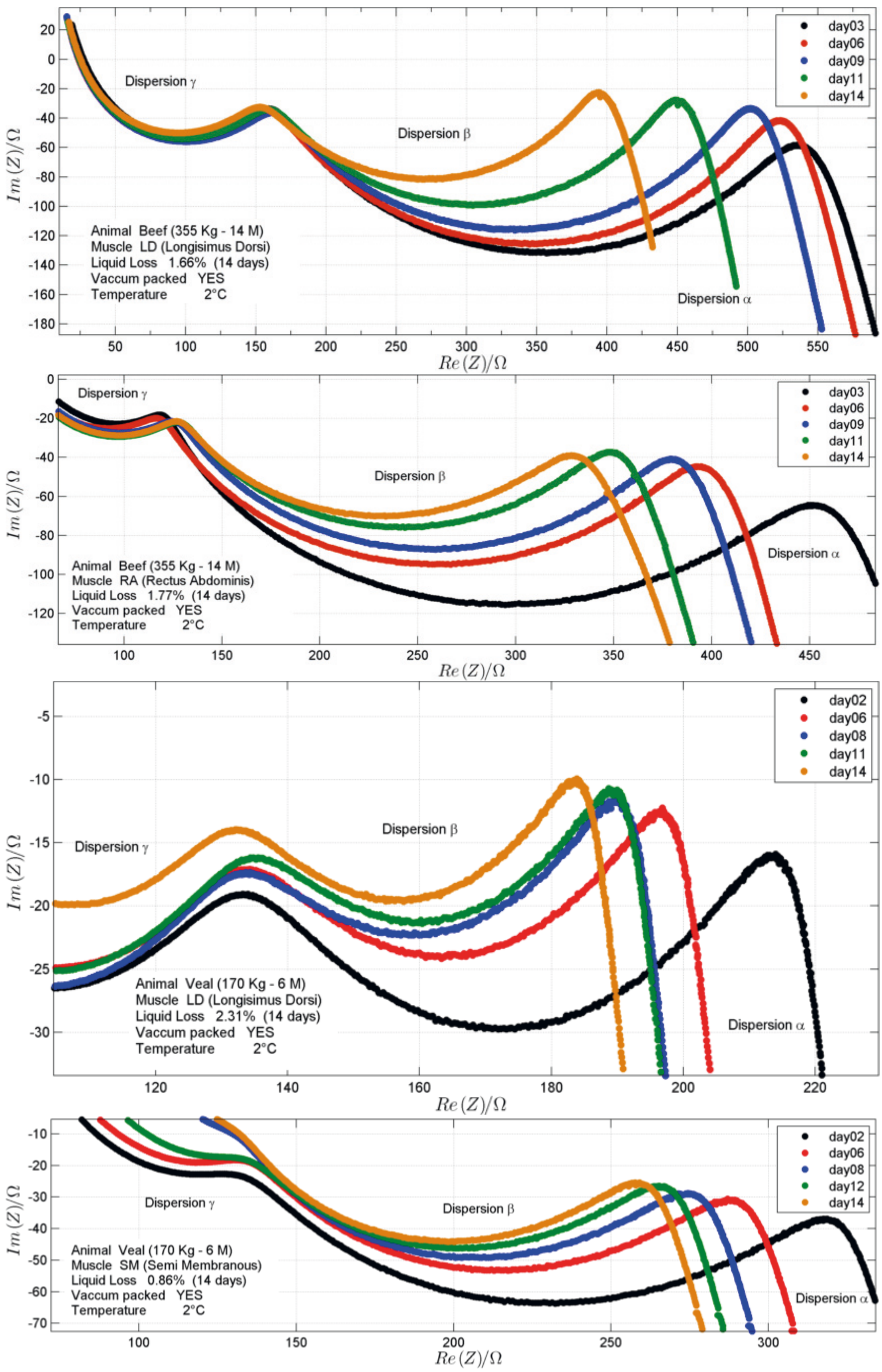

Figure 42. Impedance spectra of the meat muscles of beef and veal

4.2 Characteristic points and their dependency on aging

Different methods can be adopted for data mining such as the use of model parameters, the use of characteristic points, the extraction of data at fixed frequency or the use of the whole measurement results. Different phenomena can be easily recognized and characteristic points of the spectrum can be recognized, even if they change in frequency. Often local maxima and minima of the spectrum in the Nyquist plot are considered as characteristic points. An example of characteristic points analysis in meat measurement is given in the following Figure 43. The first characteristic point CP1 is related to the transfer region between α and β dispersion. The second characteristic point CP2 corresponds to the local minimum imaginary part of the impedance in the semi-circle that corresponds to the dispersion β. The third characteristic point CP3 is related to the transfer region between β and γ dispersion. It can be identified by the local maximum of the imaginary part of the impedance in this transfer sector. The module of the impedance is given for the different muscles over time in Figure 44. Characteristics points CP1 and CP3 have been calculated for different muscles from the measured impedance spectra between days 6 to day 14 (Table 8).

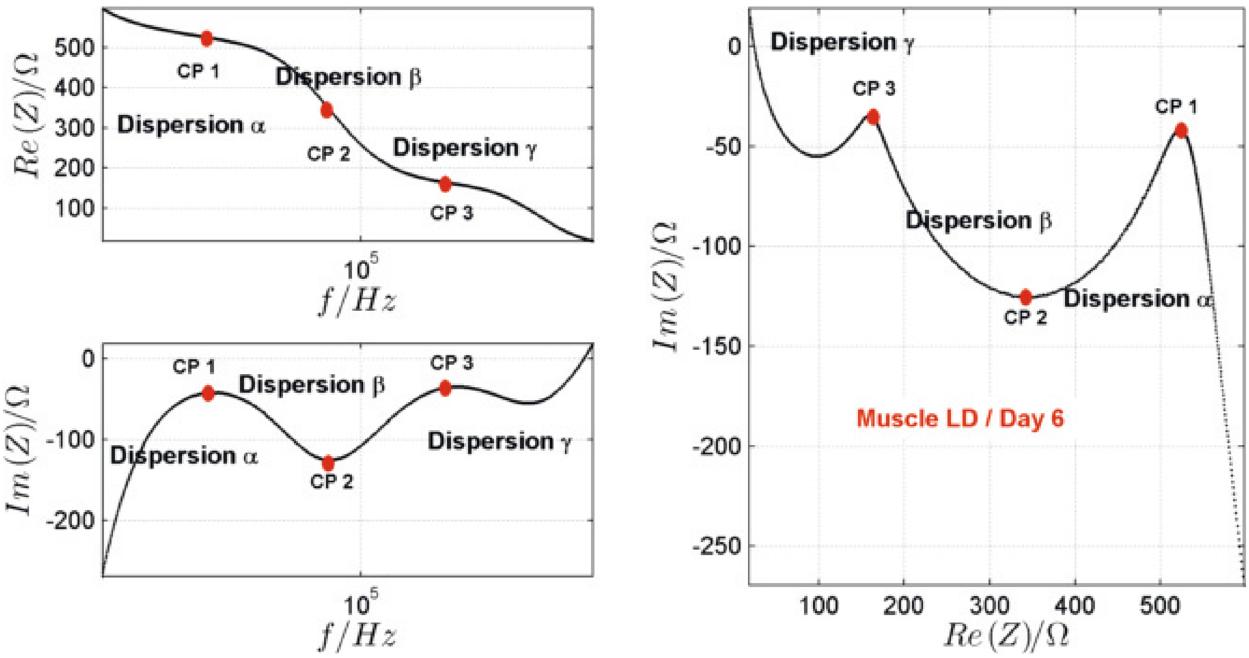

Figure 43. Characteristic points of the muscle LD / day 6

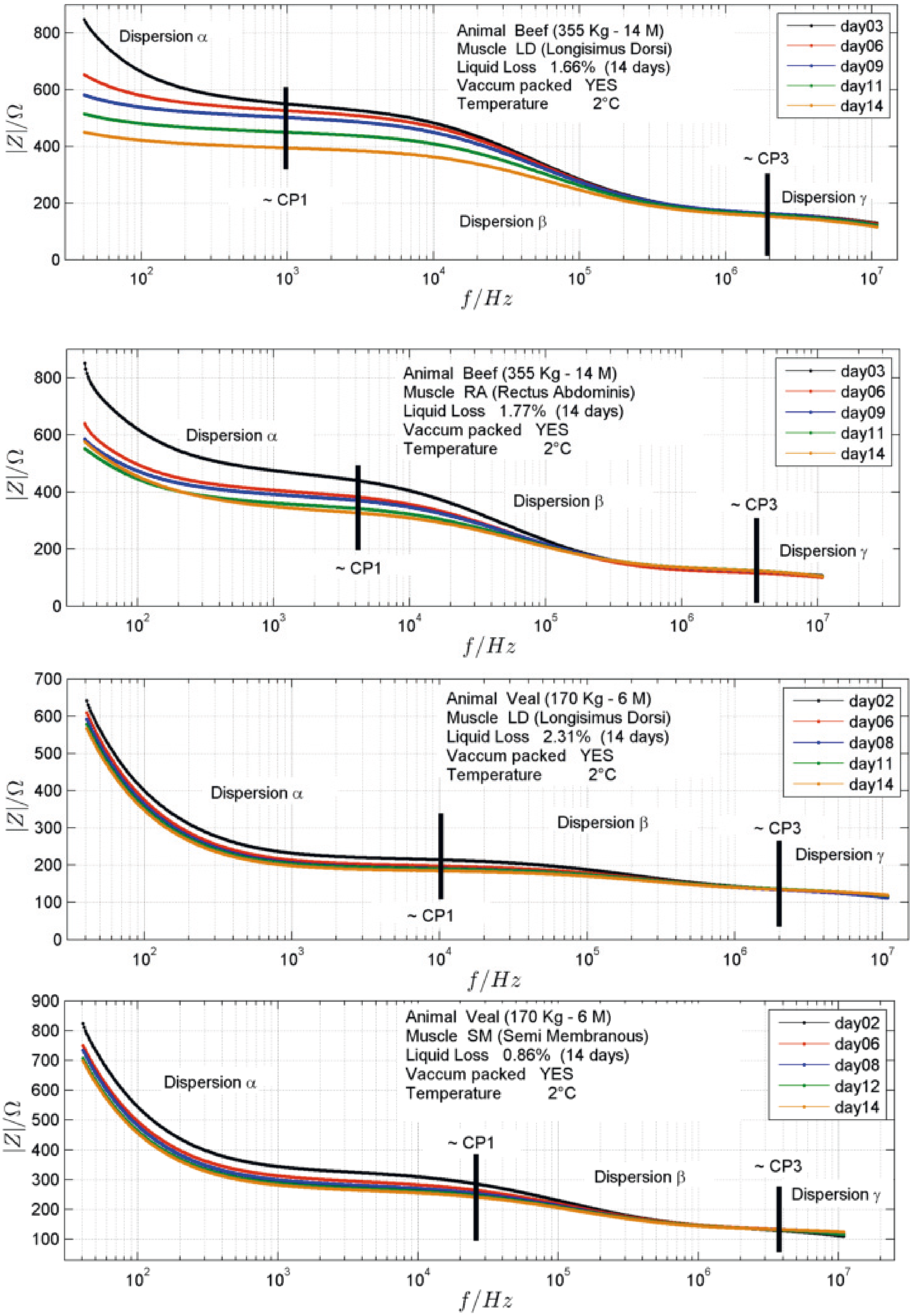

Figure 44. Impedance model of the beef and veal muscles

Table 8. Characteristic points CP1 and CP3

		CP1			CP3		
	Day	Frequency (kHz)	Impedance (Ω)	Impedance modulus (Ω)	Frequency (MHz)	Impedance (Ω)	Impedance modulus (Ω)
LDB	3	1.66	535 - 58.2i	538.70	1.90	160 - 33.8i	163.53
	6	1.10	523 - 41.7i	524.66	1.66	160 - 34.4i	164.57
	9	0.97	501 - 33.4i	502.44	1.63	161 - 36.1i	165.44
	11	0.93	449 - 27.7	450.70	1.60	159 - 34.1i	162.70
	14	0.93	394 - 22.7i	395.42	1.54	152 - 32.5i	156.39
RAB	3	2.23	451 - 64.4i	455.57	3.50	118 - 18.2i	119.39
	6	1.79	394 - 44.6i	397.07	2.75	116 - 19.9i	118.35
	9	1.79	381 - 40.9i	383.46	2.37	125 - 21.5i	126.76
	11	2.59	346 - 37.2i	348.79	2.01	127 - 21.8i	129.58
	14	3.17	328 - 38.9i	330.52	2.04	126 - 21.5i	128.80
SMV	2	5.43	317 - 36.9i	319.14	4.13	126 - 22.6i	128.00
	6	6.30	287 - 30.6i	288.66	4.62	130 - 18.1i	131.55
	8	5.85	275 - 28.8i	276.22	5.46	130 - 10.1i	130.51
	12	6.66	265 - 26.4i	266.58	3.25	132 - 17.7i	133.26
	14	6.42	259 - 25.4i	260.33	1.79	135 - 13i	135.71
LDV	2	11.19	213 - 16i	213.60	2.12	134 - 19i	135.34
	6	12.20	196 - 12.2i	196.37	2.04	134 - 17i	135.07
	8	12.90	189 - 11.4i	189.34	1.76	133 - 17.3i	134.12
	11	15.60	188 - 10.7i	188.30	2.04	134 - 16.1i	134.96
	14	13.20	183 - 99.3i	183.27	2.51	132 - 13.9i	132.73

For the muscle types LDB, RAB, SMV and LDV, the impedance range at low frequencies is respectively changing after several days. The impedance is decreasing over time. This phenomenon is observes in the first characteristic point CP1 for different muscles and it has common observation than values of Z for biological tissues which decreases with frequency.

The beef impedance is much higher than the veal impedance which is in line with the thickness of muscles. Impedance decrease over time is given bellow:

- $\Delta\,|Z|_{\mathrm{LDB\_CP1}} = 143.28\ \Omega$
- $\Delta\,|Z|_{\mathrm{RAB\_CP1}} = 125.05\ \Omega$
- $\Delta\,|Z|_{\mathrm{LDV\_CP1}} = 58.81\ \Omega$
- $\Delta\,|Z|_{\mathrm{SMV\_CP1}} = 30.33\ \Omega$

For the characteristic point CP3, the impedance modulus is almost the same that corresponds to a value smaller than 10 Ω for different muscles.

- $\Delta\,|Z|_{\mathrm{LDB\_CP3}} = 7.14\ \Omega$
- $\Delta\,|Z|_{\mathrm{RAB\_CP3}} = -9.41\ \Omega$
- $\Delta\,|Z|_{\mathrm{LDV\_CP3}} = -7.71\ \Omega$
- $\Delta\,|Z|_{\mathrm{SMV\_CP3}} = 2.61\ \Omega$

Characteristic points are helpful for a good diagnosis of the meat, but the information is not enough sensitive and another method of analysis should be added.

In the next section, we will give another method to analyze the spectra consisting of the physical modeling.

4.3 Modeling of bio-impedance spectra

Modeling represents an important method to analyze the impedance spectrum and therefore to extract suitable features. A depressed semi-circle is denoted in the Nyquist-plot of the impedance spectrum in the β dispersion region of the meat measurement (Figure 42). The depressed semi-circle is due to the distribution in the current density along the solution interface as a result of the surface in homogeneity.

Fricke model is totally related to the behavior of one cell. The biological tissue corresponds to an aggregation of cells containing intracellular and extracellular fluids that submit influences in its structure and subject to a visible change with post-mortem time.

According to the study presented in chapter 2 and in order to consider the CPE-behavior in the spectrum, it is necessary to combine the model of Fricke to the empirical equation of Cole-Cole that consists of replacing the capacitance that corresponds to the insulting cell membrane by a constant phase element that depends on frequency. We propose to extract directly the model parameters from the spectrum [37, 114] and to analyze them according to the theories of Fricke and using the Cole-Cole empirical equation (equation 18) with the same resistive element (R_e) representing extracellular resistance placed in parallel with the resistive element (R_i) representing intracellular resistance in series with the constant phase element (CPE) that corresponds to the insulating cell membranes (Figure 45).

$$Z_{\mathrm{mod}el} = \frac{1}{\frac{1}{R_{ex}} + \frac{1}{\frac{1}{\left(k_a\left(j.\omega\right)^{\alpha}\right)} + R_{in}}} \tag{18}$$

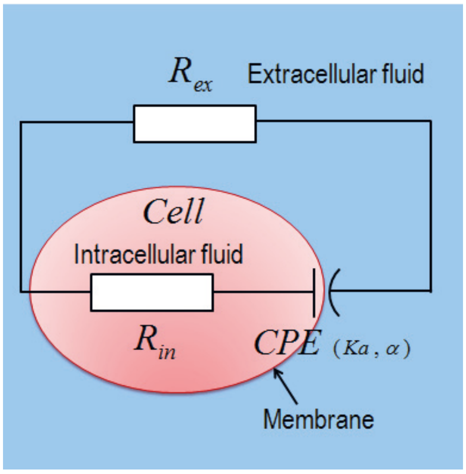

Figure 45. Fricke-Cole Cole Model

The resulting model shows good fitting performances compared to Fricke model. Fricke-Cole-Cole model yields much better results, providing more flexibility to achieve a better fit to the data and being therefore suitable for evaluation (Figure 46 and 47). Fitting results of different muscles are given in Figure 48.

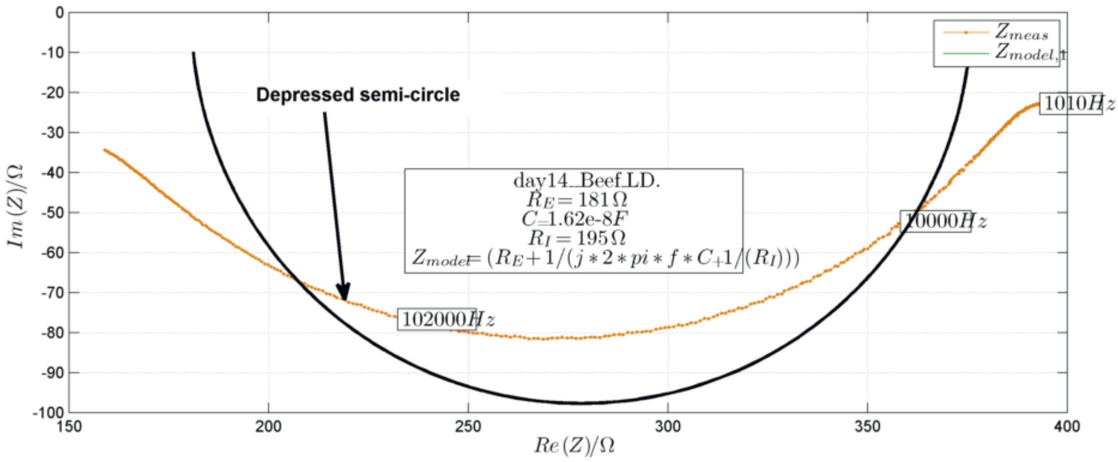

Figure 46. Fitting results day 14 / Beef /LD using Fricke model

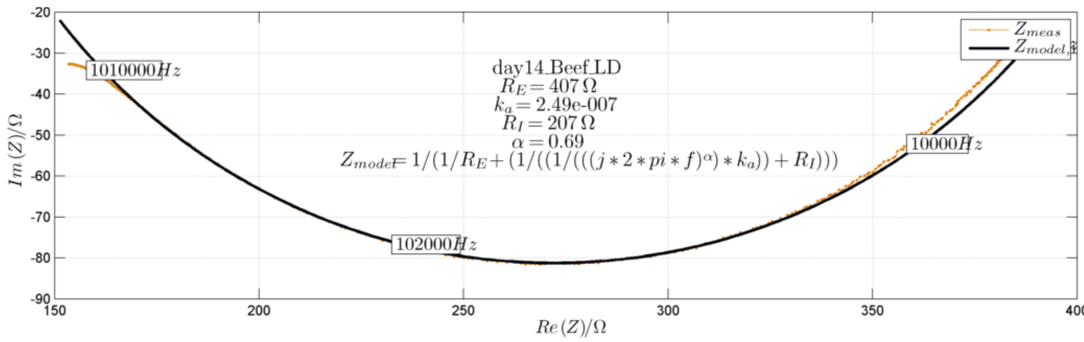

Figure 47. Fitting results day 14 / Beef /LD using Fricke-Cole-Cole model

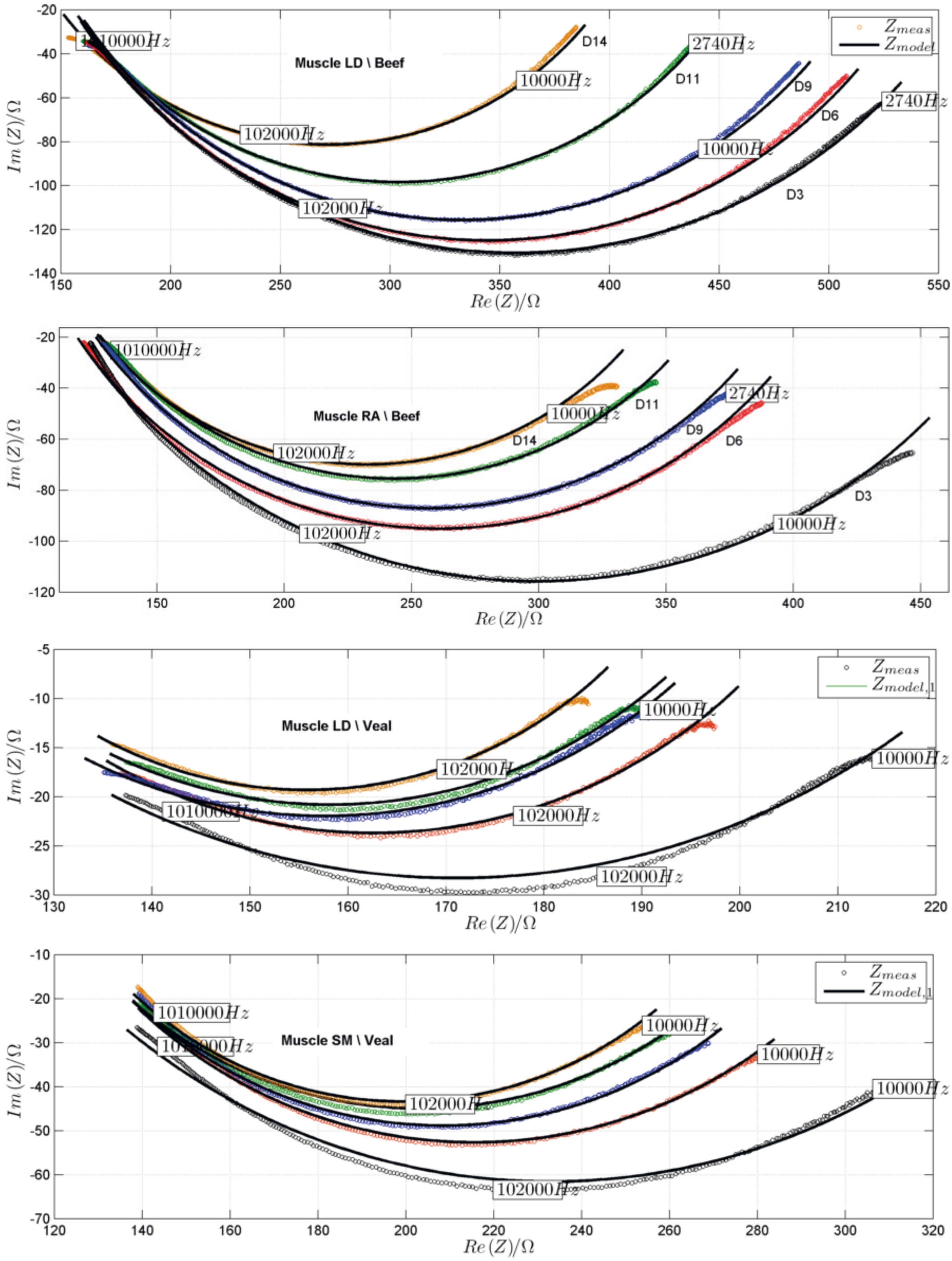

Figure 48. Fitting of beef and veal according to Fricke/Cole-Cole model

In Figure 49 we explain the consistency of the parameters values. The change of the parameters leads to a modification on the fitting performances.

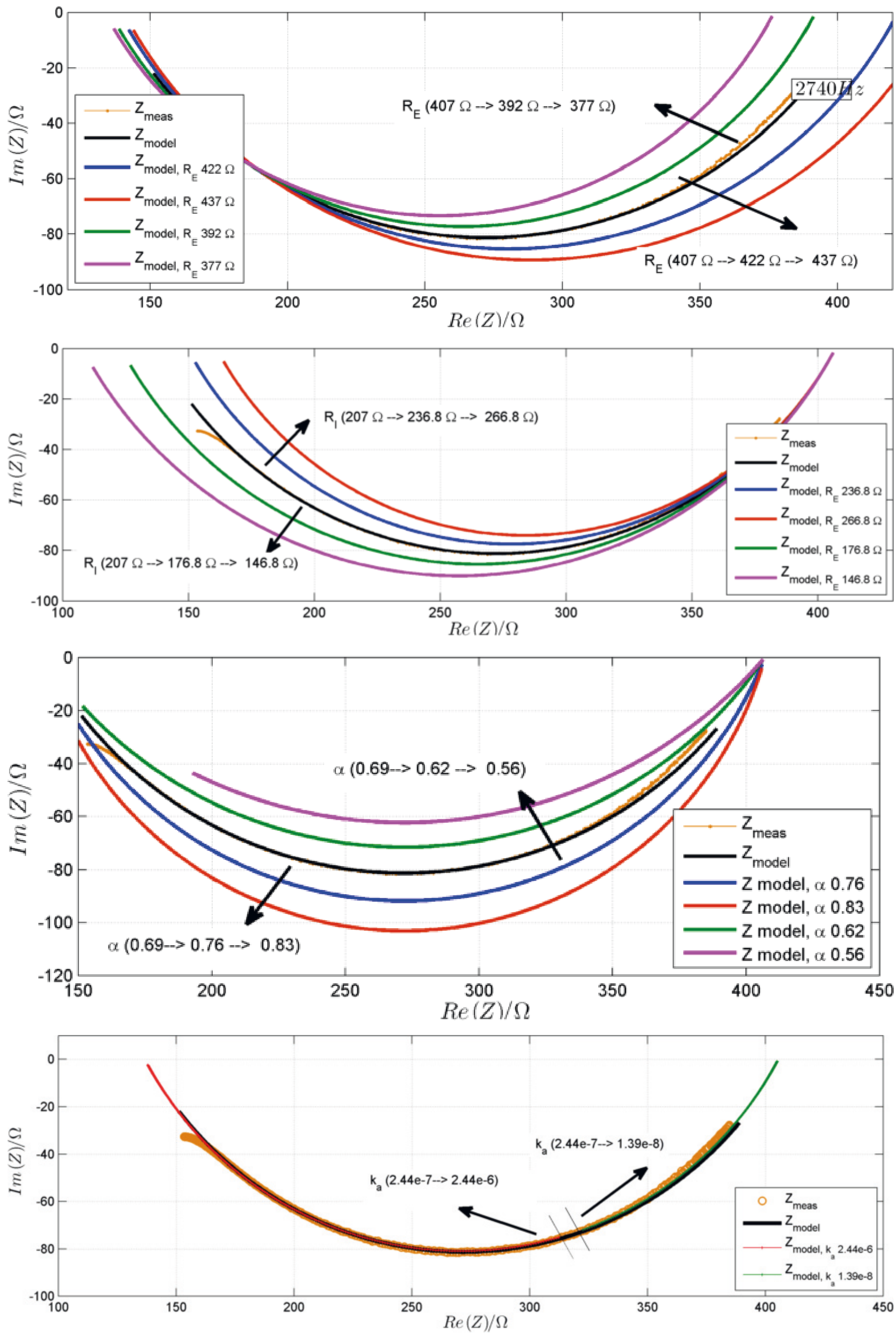

Figure 49. Fitting using Fricke-Cole-Cole model with the change of parameters

The model parameters of CPE, K_a and α are not related to the physical mechanism that occurs during meat aging (Figure 50). We transform the model parameters into a set of concentrated parameters. For this purpose the fitted k_a value are converted into a capacitance by the following equation [115].

$$C = k_a \left(\omega''_m\right)^{\alpha-1} \tag{19}$$

Where ω_m'' corresponds to the frequency corresponding to the minimum value of the imaginary part of the spectra that corresponds to the characteristic point 2.

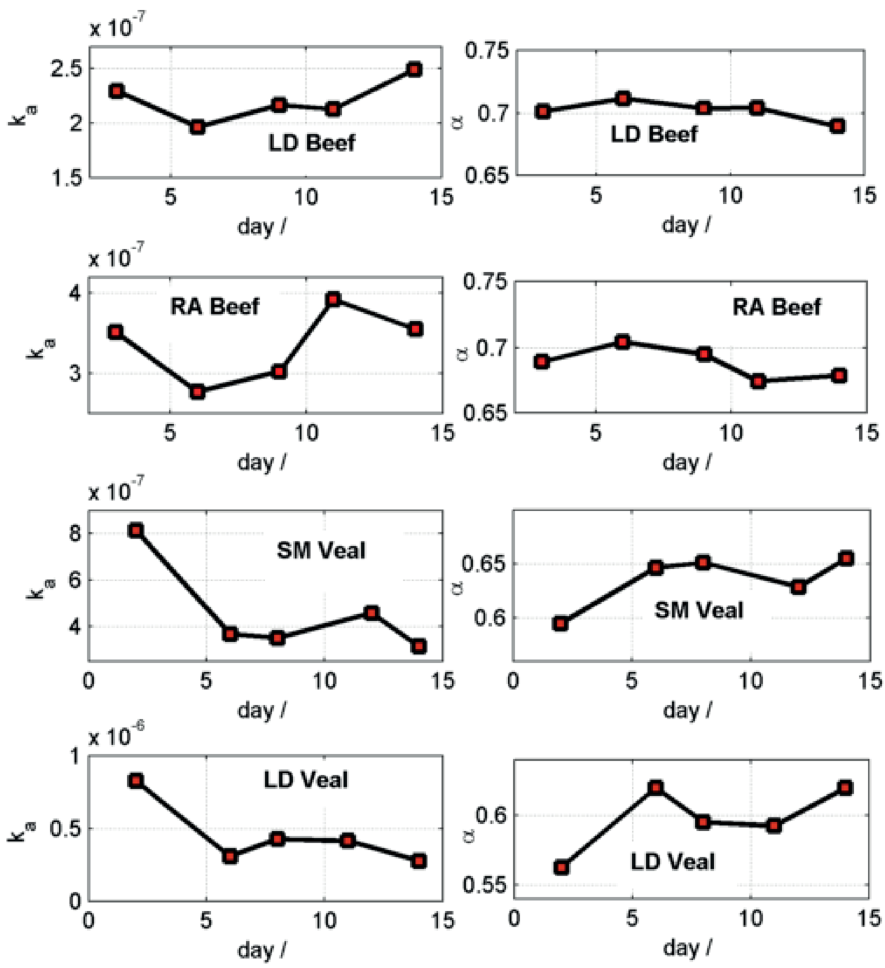

Figure 50. Parameter CPE evolution for the muscles of Beef

For the analysis of the influence of meat aging we consider the development of model parameters with respect to time (Figure 51). Frequencies and the corresponding capacitance of the local minimum imaginary part of the impedance in the semi-circle that corresponds to the dispersion β are given in Table 9.

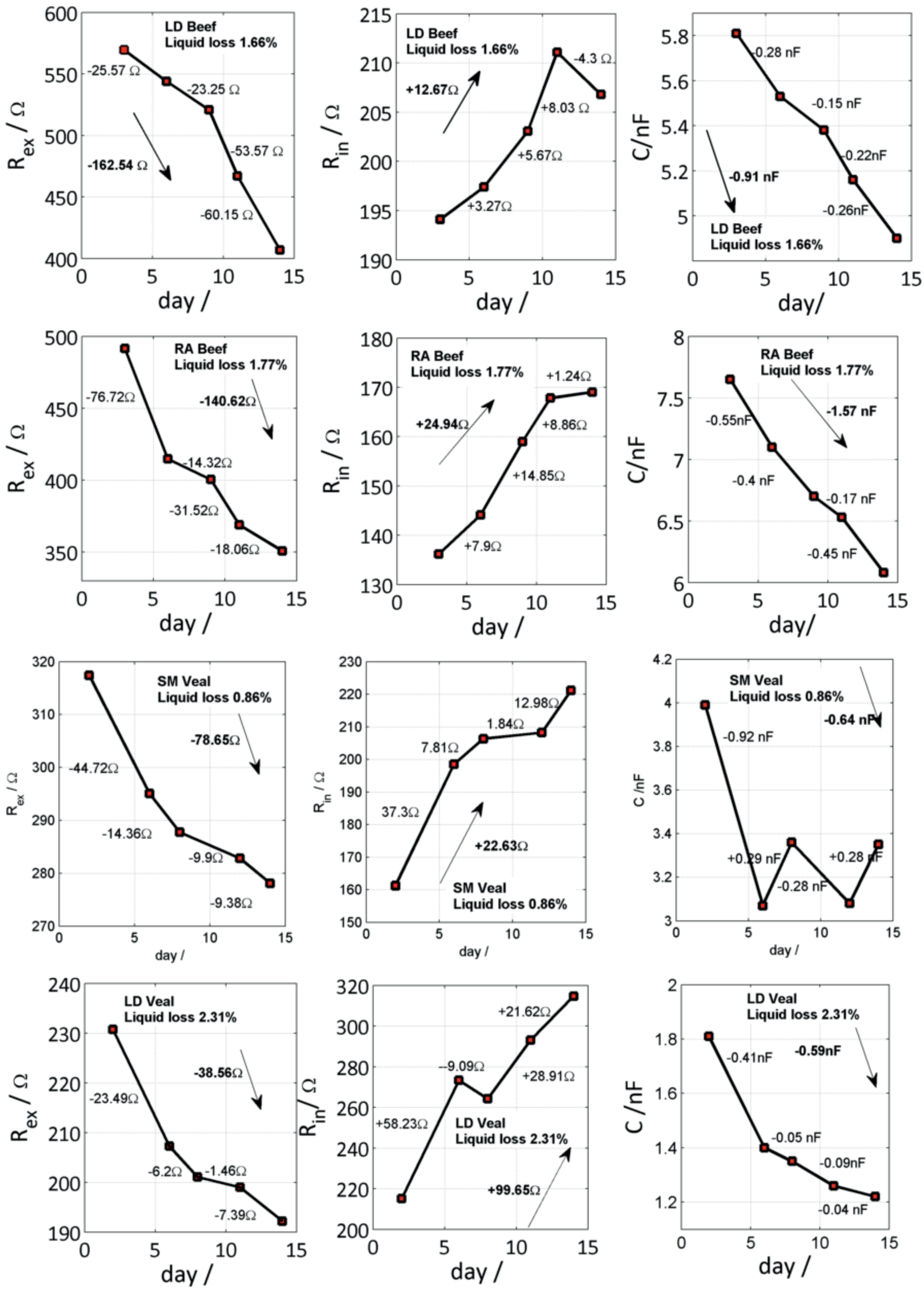

Figure 51. Parameter evolution for different muscles

Table 9. Frequencies and capacitance of CP2

Muscle	Day	Frequency (kHz)	C (nF)	Muscle	Day	Frequency (kHz)	C (nF)
	3	36.6	5.81		2	79.8	3.99
LDB	6	38.7	5.53		6	98.2	3.07
	9	39.4	5.38	SMV	8	96.1	3.36
	11	45.7	5.16		12	113.5	3.08
	14	57.2	4.90		14	109.4	3.35
	3	35.3	7.65		2	190.8	1.81
	6	38.0	7.10		6	225.4	1.40
RAB	9	41.7	6.70	LDV	8	238.3	1.35
	11	45.8	6.53		11	238.3	1.26
	14	50.0	6.08		14	238.3	1.22

At slaughter, the animal muscles are contracted due to the release of the lactic acid contained in muscle fibers. By releasing the muscle fibers, lactic acid activates the inert enzymes, already present in the muscle, which will be gradually cut muscle fibers (Figure 52). Besides the shrinkage of fibers during early postmortem period causes the release of fluids that contains electrolytes from cells to the extracellular tissue [17], according to electrical analysis, this phenomena should lead to an increase of the conductivity in the extracellular tissue, to decrease in the intracellular and proportionally the decrease of extracellular resistance and to increase of the intracellular resistance.

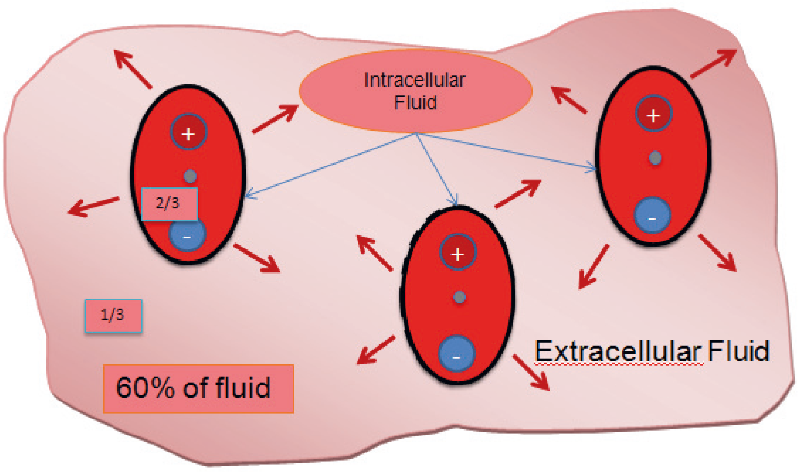

Figure 52. Meat aging mechanisms over time

Over time, an oxidation of the phospholipids membrane layers starts and makes the membrane porous. An electrical charging of lipid membranes causes electroporation. Feature analysis shows that the resistance R_i representing intracellular fluids increases over time (Table 10).

Beef muscles are less juicy and more mature than veal. The muscle fibers of beef are also thicker than the muscle fibers of veal. This corresponds to the observed behavior of the impedance in the first day of measurements. The resistivity of the extracellular tissue R_e of beef is higher than for veal (Table 11) and the capacitive effects that corresponds to the insulating cell membranes that is higher for the beef muscle because cells have a bigger surface.

Table 10. Change of parameters from day 2 to day 14

Muscle Type	ΔR_i (Ω)	ΔR_e (Ω)	ΔC (nF)
LD-B	12.67	162.54	0.91
RA-B	24.94	140.62	1.57
LD-V	22.63	78.65	0.59
SM-V	38.56	99.65	0.64

Table 11. Model parameters in day 6

	LD-B (Beef)	RA-B (Beef)	SM-V (Veal)
R_e in Ω	543.91	414.69	310.10
R_i in Ω	197.39	144.09	198.55
C in n F	5.53	7.10	3.07

The decreases of the extracellular resistance and of the capacitive element are more important in beef muscle with ΔR_e=162.54 Ω, 160.62 Ω, 78.65 Ω and 38.56 Ω and with ΔC=0.91 nF, 1.57 nF, 0.59 nF and 0.64 nF for the muscle LD-B, RA-B, SM-V and LD-V respectively. The extracellular resistance R_e shows the highest sensitivity to aging. It decreases from day 2 to day 14 about 38 Ω to 162.54 Ω depending on the muscle type. The results show that the parameters evolution of different muscles has principally the same behavior, but differs from one muscle to another in its exact value. This is mainly due to several factors, especially biologic characteristics of each muscle. For example beef muscles are more mature as veal and the muscle fibers of beef are thicker than the muscle fiber of veal according to impedance results. It has been also observed that the liquid loss during measurement, even if the probe has been well packed, such as for the beef muscles, is not uniform.

During the postmortem period, between the slaughtering times to the day 6, we can remark the big decrease of the extracellular resistance especially for the muscle RA Beef, LD Veal and SM Veal that attempt 76 Ω. An important increase of intracellular resistance is also seen for muscles of veal that attempt 58 Ω.

A second investigation is done with different conditions, circular electrodes for measurements (Figure 53) and accelerated aging during a shorter measurement time to confirm the consistency of the Fricke-Cole-Cole model [114].

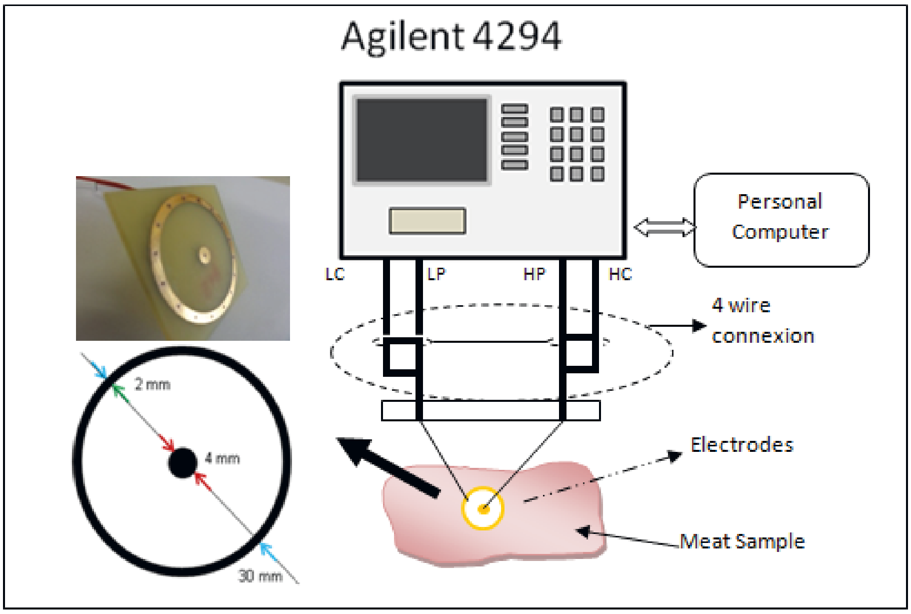

Figure 53. Measurement setup of the second investigation

Two samples of beef, Rectus abdominis (RA) and Longisimus Dorsi (LD) were investigated. The first measurement is done at the reference time, time 0 then after 2, 6 and finally 8 hours (Figure 54). It is necessary to use a high temperature, for this reason the meat has been placed in room temperature (23 °C) without vacuum packed. The fluid loss at the end of experiments for the two samples has been high with a percent of 10% after 8 hours only. Frequencies and corresponding capacitance of the local minimum imaginary part of the impedance in the semi-circle in the dispersion β are given in Table 12.

Table 12. Frequencies and capacitance of CP2

Muscle	Time	Frequency (kHz)	C (nF)	Muscle	Time	Frequency (kHz)	C (nF)
RAB	0	26.7	4.22	LDB	0	27.2	4.56
	2	41.0	3.09		2	35.9	4.26
	6	70.1	1.97		6	72.7	2.35
	8	174	0.81		8	92.6	1.68

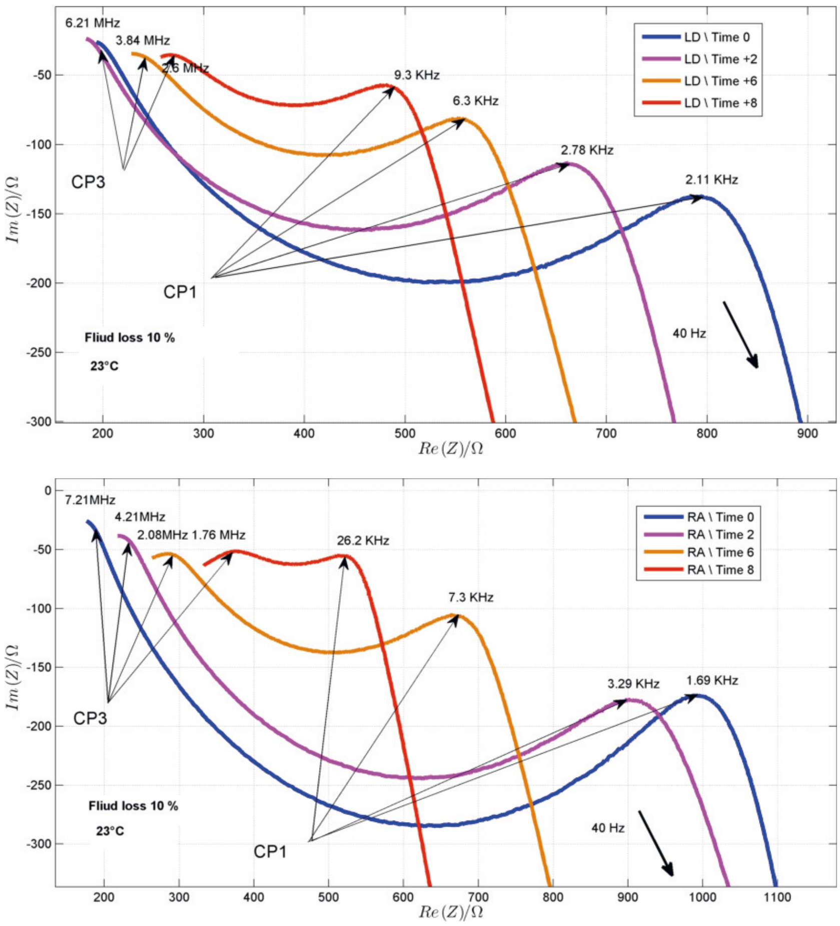

Figure 54. Parameters evolution over time for accelerated aging in a short period

Figure 55 illustrates the Fricke-Cole-Cole model parameters evolution over time the parameters results have the same behavior as the measurements during a long period. The resistive element R_i representing intracellular fluids increases over time with $\Delta_{Ri(LD)=}$202.7 Ω and $\Delta_{Ri(RA)=}$271.5 Ω. The resistive element Re that represents extracellular fluids decreases over time with $\Delta_{Re(RA)}$=331.93 Ω and $\Delta_{Rei(LD)}$= 455.45 Ω. The capacitance decreases over time with $\Delta_{C(LD)}$=5.4972e-10F and $\Delta_{C(RA)}$=8.7458e-10 F.

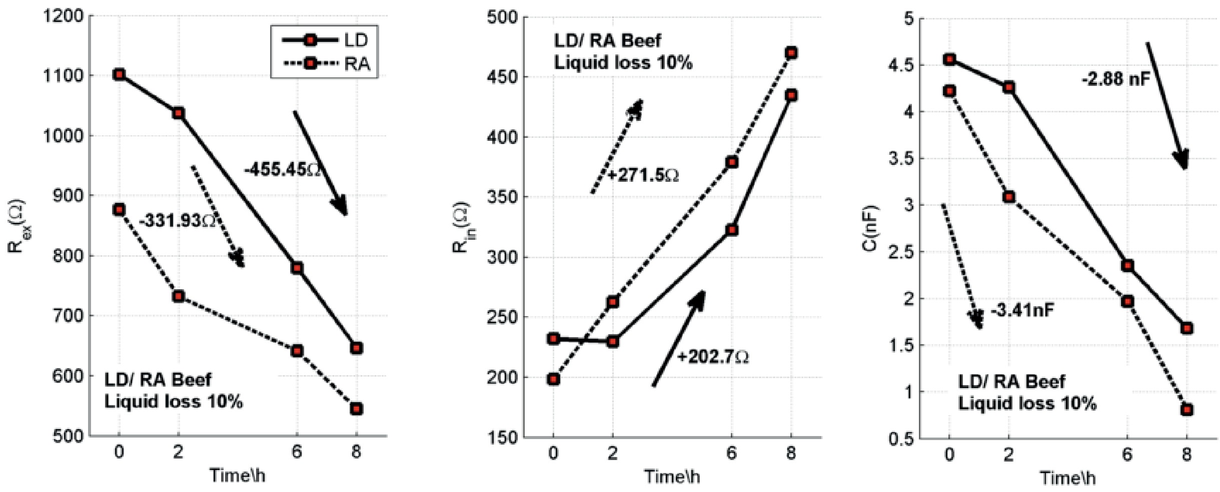

Figure 55. Parameters evolution over time for accelerated aging in a short period

4.4 Final remarks

The feature analysis shows that characteristic points and reproducible model parameters can be determined from impedance spectra, which correspond to physical changes occurring during long post-mortem period. Even if the values change depending on the muscle type, their behavior is systematic and suitable for classification.

Measured spectrum of meat have been evaluated by means of a Fricke-Cole_Cole model including a constant phase element to consider the inhomogeneity and the distributed electric parameters of the biological tissue and leads therefore to a good fitting performance. Both model parameters and characteristic points of the spectrum can be principally used for classification.

The relationship between the post-mortem state and the change of the meat impedance has been characterized in laboratory, and different results permit to have access to the information about the meat freshness. The measurement method is consistent and suitable as a basis for developing an in-vitro measurement method for the freshness of meat. The measurement results for different beef muscle of beef or veal in different periods confirm the effectiveness of the bio-impedance measurement of meat.

5. Data mining and classification of tissue type and state

5.1 Introduction

In this chapter, the aim is to propose a classification method which is able to identify the type and the freshness of the meat. Depending on the classification method, sufficient inputs should be identified using two classification methods, neural network and fuzzy logic. Noisy inputs should be evaluated in order to reach to the high index of recognition. The process of classification is composed of four blocks (Figure 56):

- Accurate feature gathered from the measured impedance
- Data preprocessing
- The classification showing the best training results
- The test validation of classification

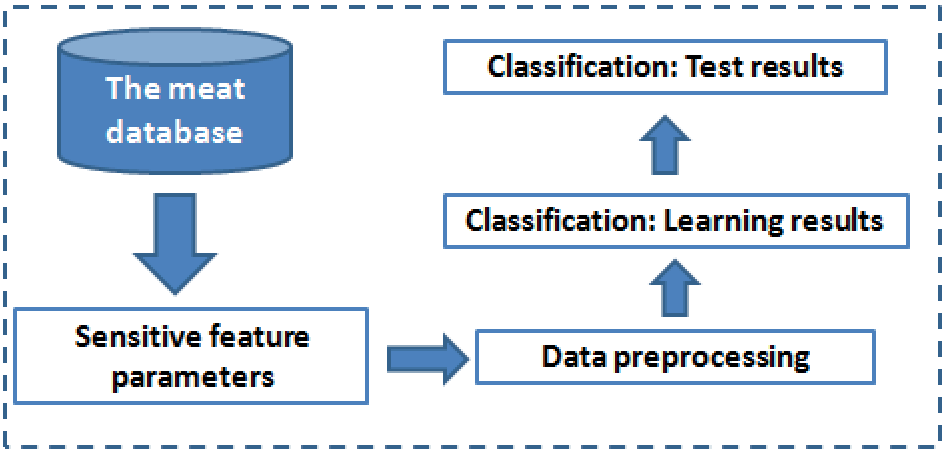

Figure 56. Process of classification

5.2 Sensitive features

Before classification, it is necessary to identify which information is important. According to our application, the most important and necessary information's for the future conception of meat monitoring sensor are the type of the muscle and the freshness of the meat. It is necessary to remove spikes in measurement due to erroneous measurements. Another important factor should be respected is the use of a reduced input in order to reduce the effort of and stability of implementation. The different possibilities of feature that can be used are model's parameters, reduced model parameters and characteristic points (Figure 57) are presented in Figures 58, 59, 60 and 61.

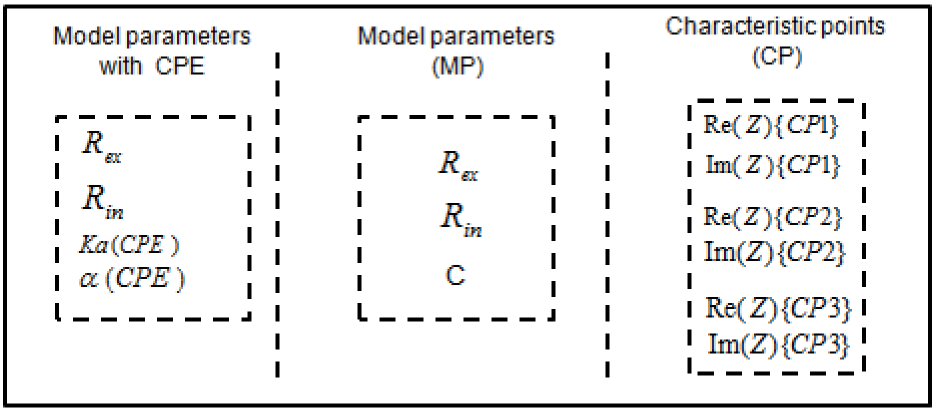

Figure 57. Different possibilities of features

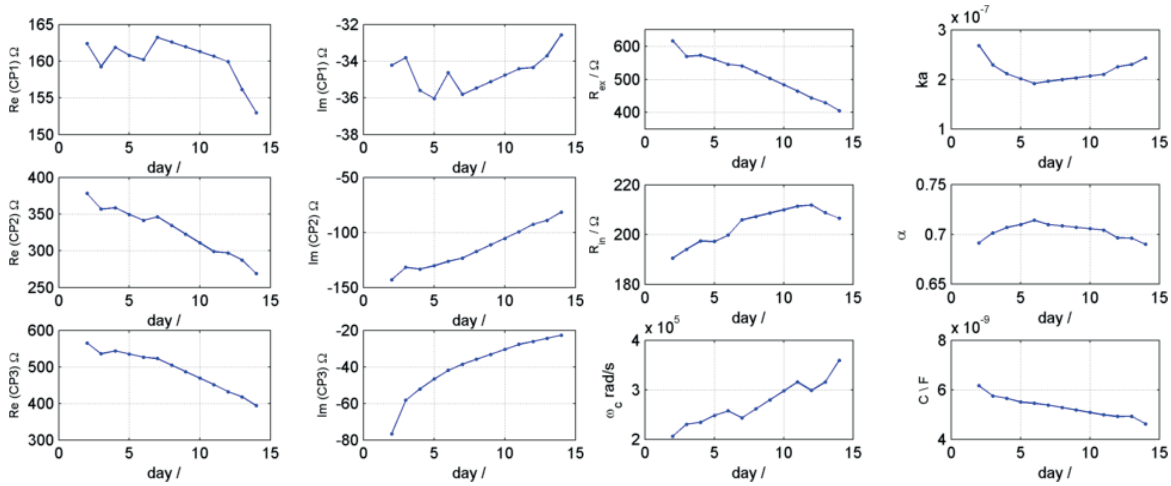

Figure 58. LD beef features

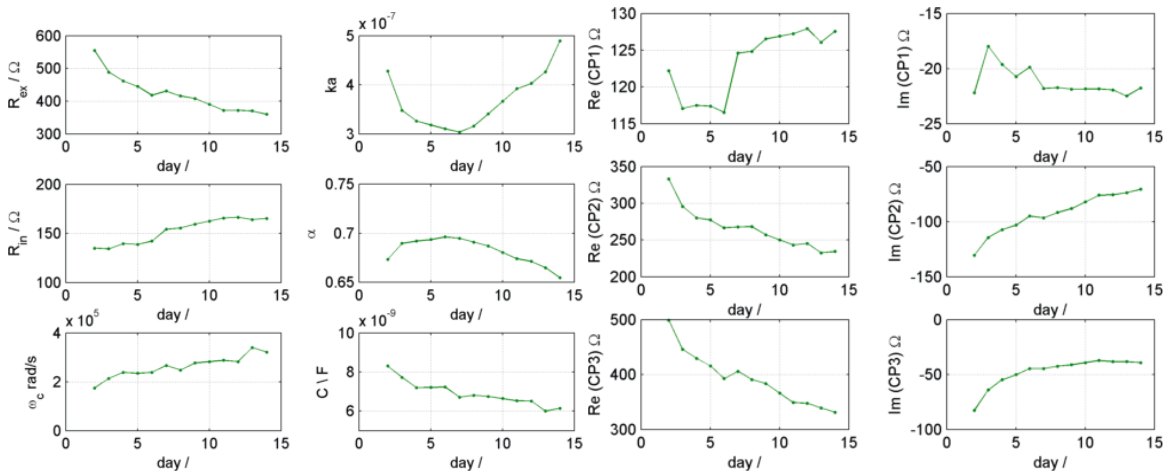

Figure 59. RA beef features

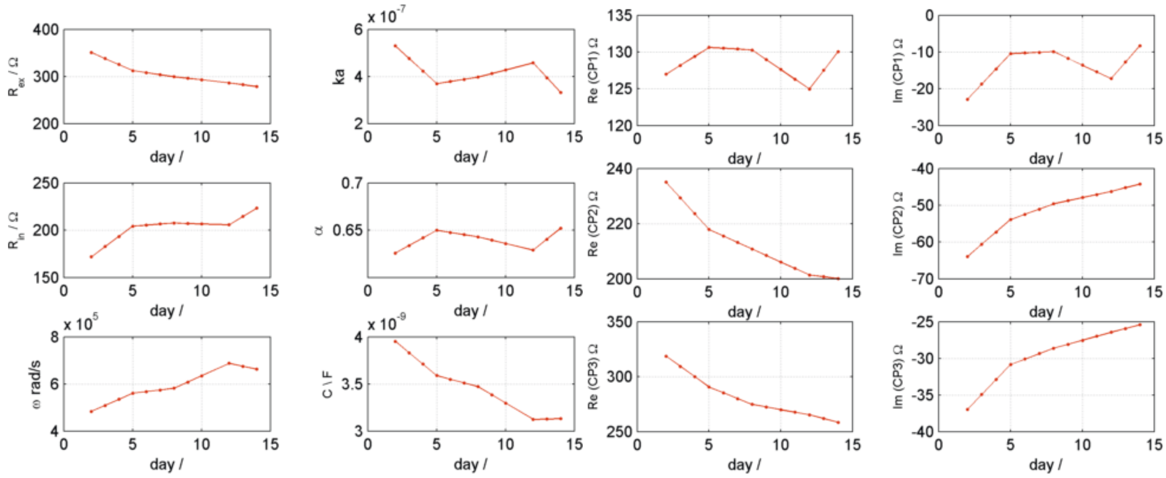

Figure 60. SM veal features

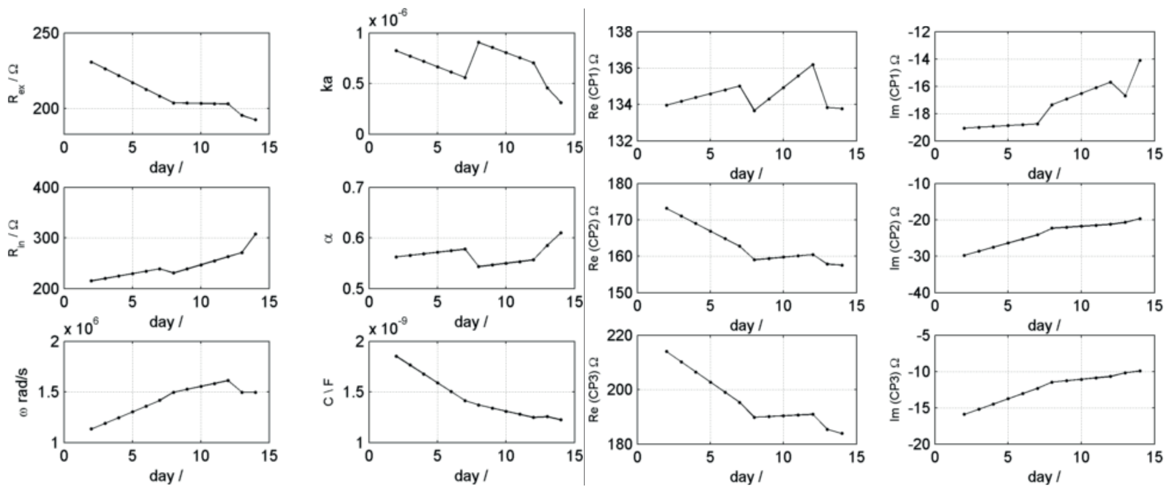

Figure 61. LD veal features

It is visible that reduced model parameters represent the better features in comparison to characteristic points and to model parameters with the constant phase element parameters (Figure 62).

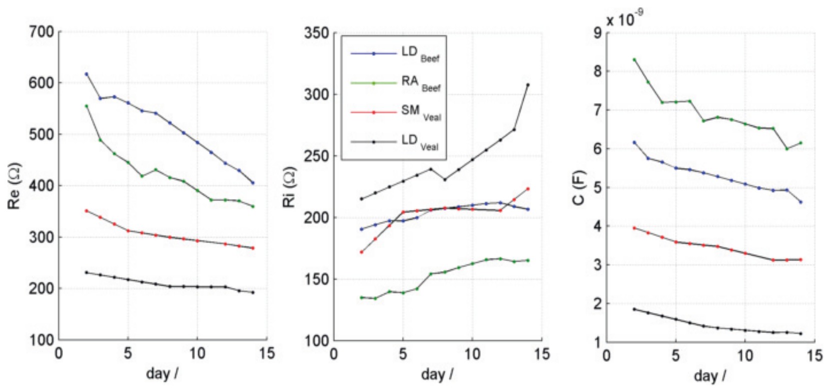

Figure 62. Model parameters as features

It is possible to distinguish between model parameters R_{ex} and the converted model parameter C for different muscles. The difficulty is obvious only for the model parameter R_{in} with the muscles LD beef and SM veal.

5.2.1 PCA computing

A second approach using the PCA method is done in order to select the suitable features (Figure 63). The main problem to solve is to get the transfer loadings (equation 20) which can be performed via the singular value decomposition (SVD), that consists of the normalization of the input matrix X to X”. Where x_j is the columns' mean value vector and $var(x_j)$ is the columns' variance vector.

$$x_{ij}^{**} = \frac{x_{ij} - x_j}{\sqrt{var(x_j)}} (i = 1,2,3,\cdots, n, j = 1,2,3,\cdots, p) \qquad (20)$$

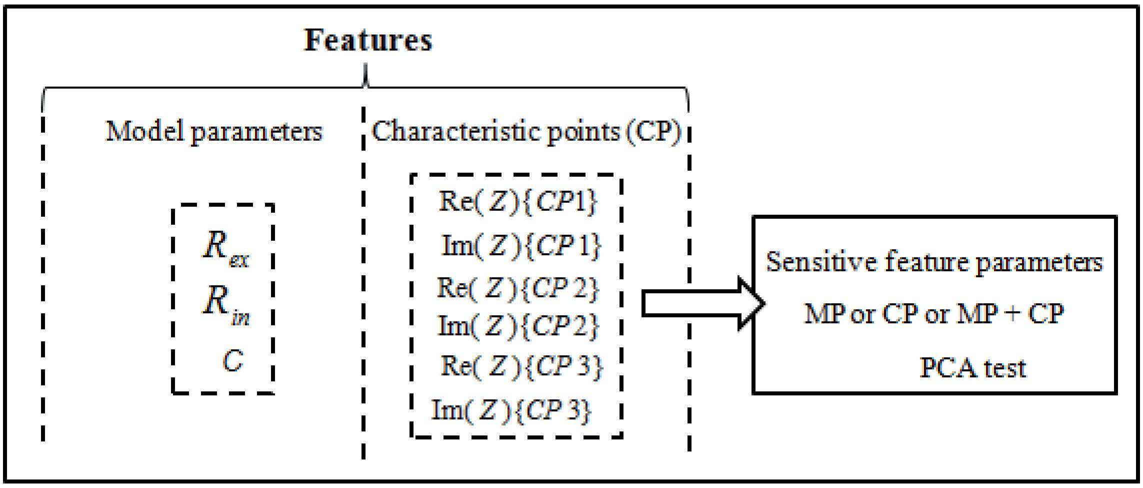

Figure 63. Feature extraction

The SVD decomposition is chosen according to the study done in [116]. The decomposition of the normalized matrix X” is done according to equation (21).

$$X'' = U \cdot S \cdot V' \qquad (21)$$

Where S is the nxp diagonal matrix with singular values σ_i of the matrix X in diagonal.

$$S_{ii} = \sigma_i \qquad (22)$$

and singular values are already sorted in a decreasing order

$$\sigma_1 > \sigma_2 > \sigma_3 > \cdots > \sigma_p \tag{23}$$

The relationship between the singular value σ_i and the eigenvalue λ is given by

$$\sigma_i = \sqrt{\lambda_i} \tag{24}$$

U is the n x n left singular valued vector matrix of X, V is the p x p right singular valued matrix of X and both are orthogonal matrices. The principal components F can be calculated by equation 25.

$$\mathrm{F} = X \cdot \mathrm{V} = U \cdot S \cdot V^{'} \cdot V = U \cdot \mathrm{S} \tag{25}$$

For the consistency of this investigation using the PCA method, we increase the number of muscles. A data base composed of 6 muscles is used in order to use well the PCA method. This data base will serve to determine the suitable feature. 3 different muscles of two animals in two periods of aging are used (Figure 64). The test data should be unknown. For that two spectra will be used for learning and two others for test in every case (Figure 64).

Before dealing with PCA computing, inputs and test data of the three cases, model parameters (MP), characteristic points (CP) and model parameters with characteristic points (MP + CP) are defined. The test data have exactly the same dimension then the inputs data:

- The input data of the model's parameters is a matrix with the dimension (12 x 3). These data are composed by the extracellular resistance, intracellular resistance and the resulting capacitance extracted from the CPE parameters.
- The input data of the characteristic points is a matrix with the dimension (12 x 6). These data are composed of the characteristics (CP1, CP2 and CP3). Every characteristic point is defined by its real and imaginary parts.
- Parameters provided from the model parameters and the characteristic points correspond to the input matrix with the dimension (12 x 9).

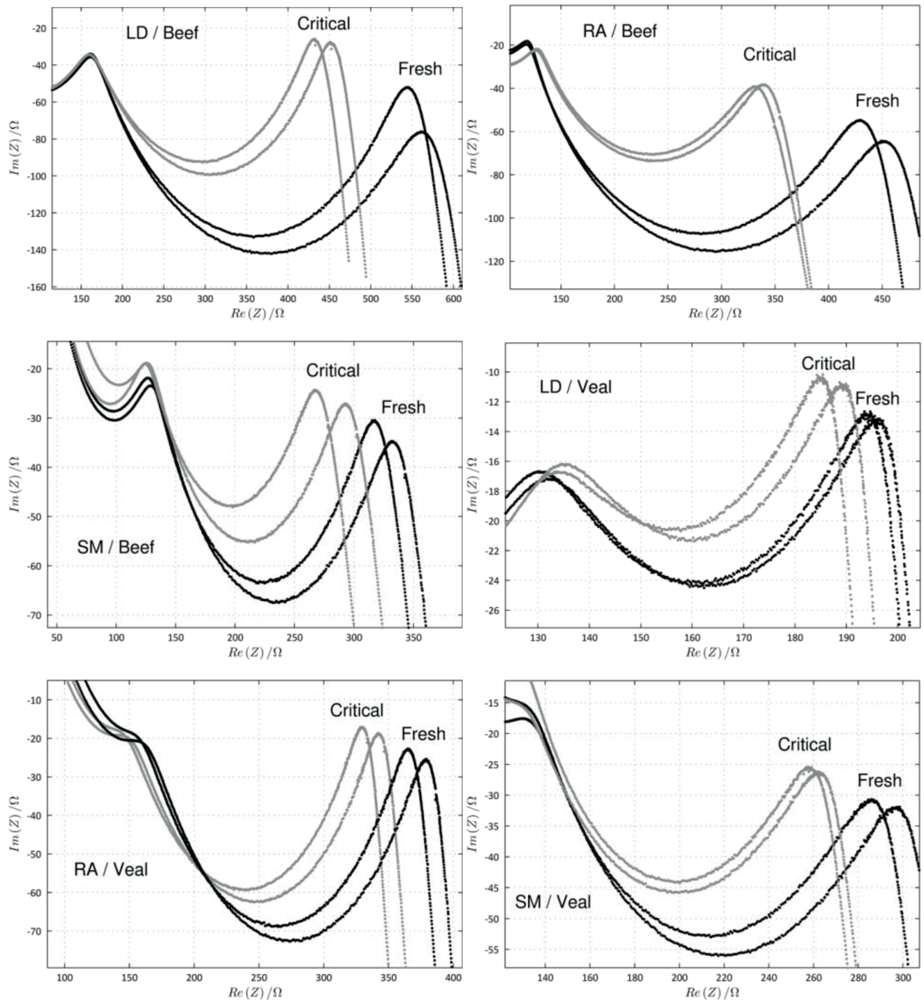

Figure 64. Impedance spectra for different muscles

The first two components for the feature composed by model parameters, for the characteristic points and for the model parameters with characteristic points explain more than 90% of the variances. Results are shown in (Figure 65).

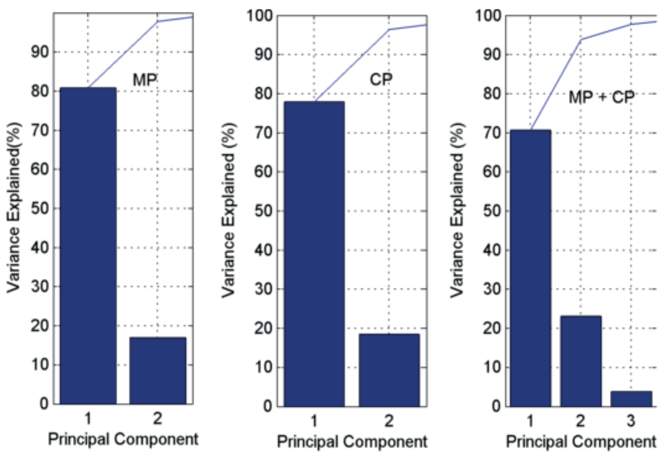

Figure 65. Variance of the principal components

The first few components (columns) of the new data set F_{new} contribute the majority of the variances and are considered to be the principal components, the first two components have been considered to be the principal components. The next step consists of the PCA computing of the input and test data (Figure 66).

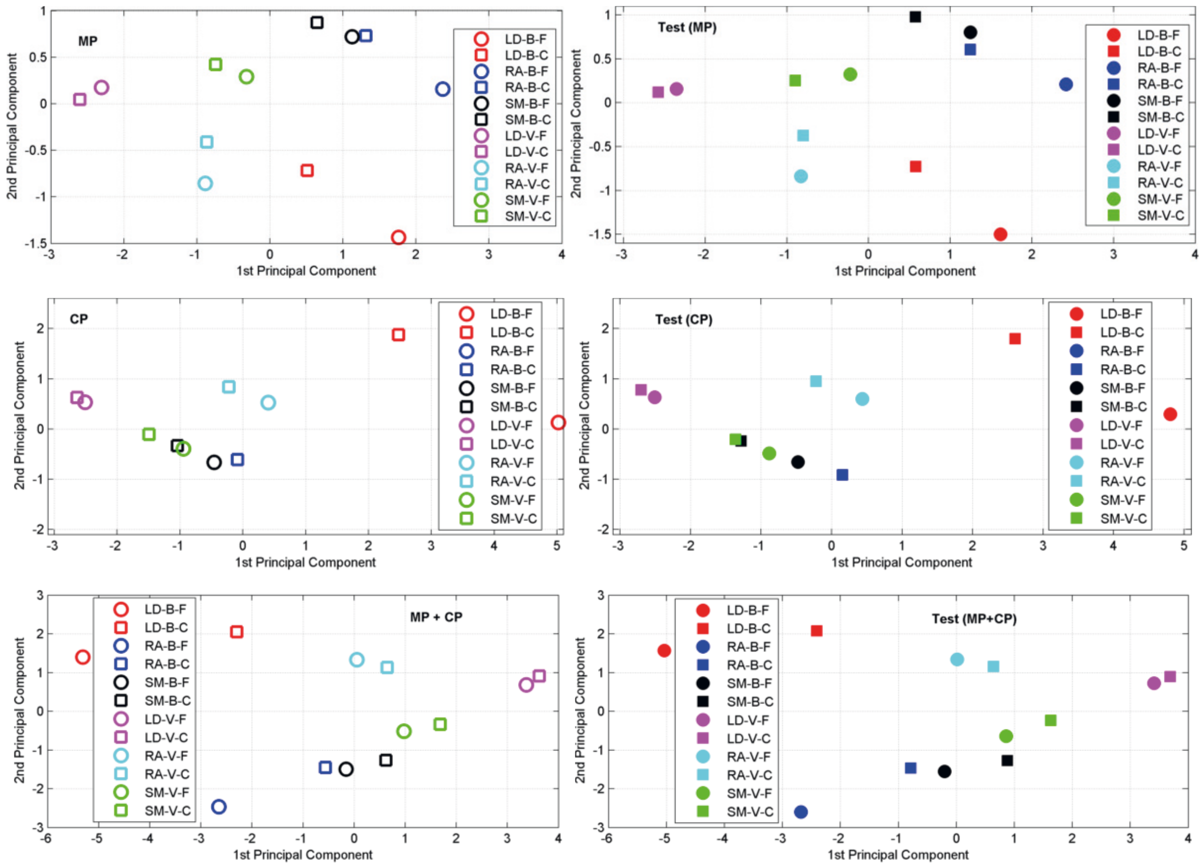

Figure 66. PCA computing inputs and test data

5.2.2 Sensitive feature results using KNN algorithm

In order to verify which feature should be uses for classification, a simple method can be used consisting of the principle of superposition of the test data in the corresponding region of inputs data after KNN calculation. The method of KNN (k-nearest neighbors algorithm) has been used to give a complete two dimensional presentations presented in a geometrical plot of the data.

The KNN algorithm requires computing distances of the test example from each of the training examples. The KNN method helps to find the nearest defined point to the input data and shows them in the plot. The test process sees for that every data should be in the corresponding muscle type, animal type and freshness. For a training vector, KNN algorithm identifies the k nearest neighbors regardless of labels. There is only one sample for each of the twelve classes and each class is presented by a region and is separated with other classes or region. In this case, k=1 gives the best classification result [117], the case is simply assigned to the class of nearest neighbor, which means the undefined points will be defined to its nearest neighbor's class. Each training vector defines a region in space, defining a Voronoi partition of the space, useful for visualization. We have used Euclidian Distance to find the nearest neighbor

$$D(\mathrm{a},\mathrm{b}) = \sqrt{\sum_k \left(a_k - b_k\right)^2} \tag{26}$$

The different test data and their corresponding superposition on the KNN Voronoi partition on the space are presented in Figures 67, 68 and 69. The result of the superposition of model parameters test data on the KNN partition is 12 correct outputs that correspond to 100% of accuracy. The same result 100% of accuracy is given by the features composed by the characteristic points and model parameters. The accuracy for the characteristic points is 66% with 4 erroneous outputs that corresponds to the muscles, SM-B-C, SM-B-F, SM-V-C and LD-V-F.

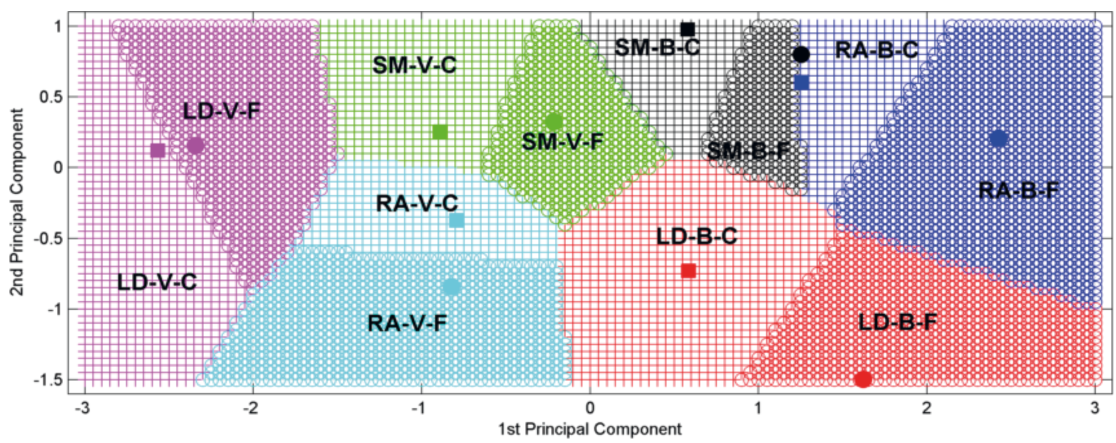

Figure 67. Superposition of MP test inputs to the KNN graph

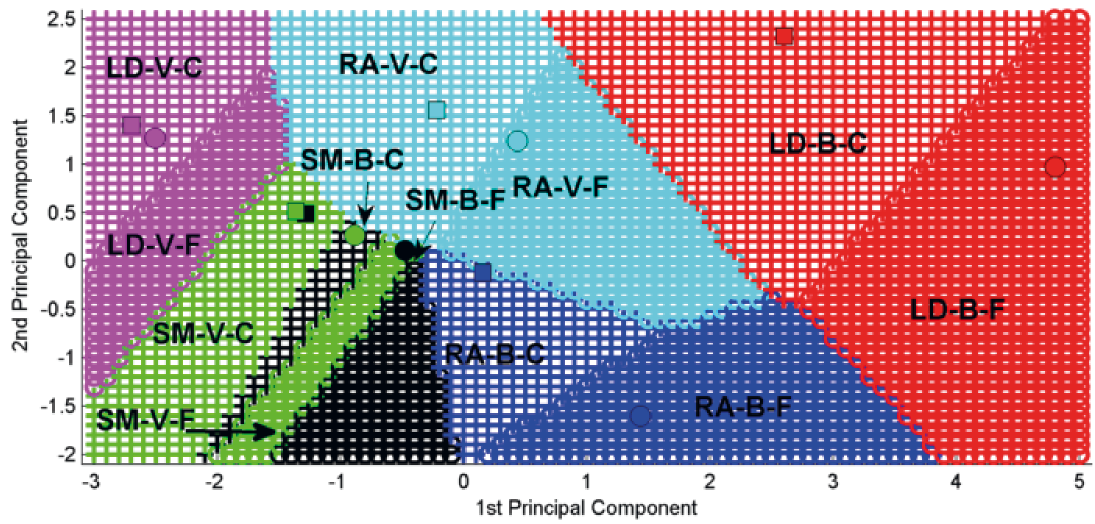

Figure 68. Superposition of CP test inputs to the KNN graph

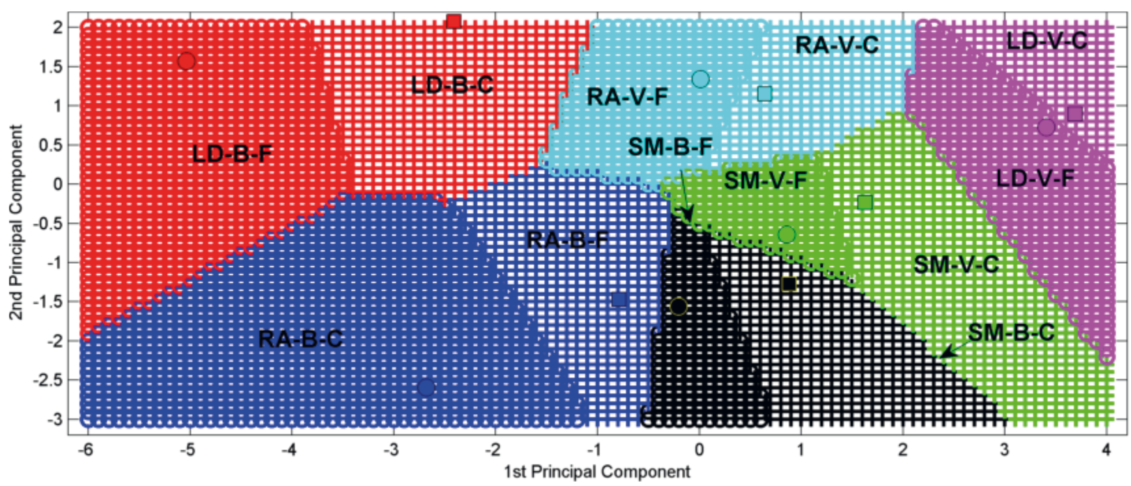

Figure 69. Superposition of MP + CP test inputs to the KNN graph

Feature extraction based on the use of model parameters and characteristic points shows good results. But with the consideration that reduced inputs increases the performance of neural network and fuzzy, selected features has been model parameters.

5.3 Neural network classification

In the following section, we will discuss and train neural networks systems previously mentioned followed each by its proper simulation via MATLAB.

Before dealing learning, data preprocessing plays a crucial role in which the first step is the normalization of the data. This step is essential when dealing with parameters of different units and scales to bring all of the variables into proportion with one another and to avoid saturation of the network when classifying with neural networks.

For that, normalizing each input is essential so they have the same effect on the weights. In this work, min-max normalization is used (equation 27). For this type of normalization, we should set firstly the minimum=‖Min‖ and the maximum=‖Max‖ of our original data. Then, we set the minimum=‖newMin‖ and the maximum=‖newMax‖ of the scaled data. In our case, normalization will fall within the uniform range [-1 1], hence ‖newMin‖=-1 and ‖newMax‖=1. Finally we calculate the normalized data for each original data as follows.

$$Nr = \frac{O - Min}{Max - Min} \cdot \left(newMax - newMin\right) + newMin \tag{27}$$

where Nr is the normalized data and O is the original data.

To reach good performances and according to the literature, we decide to use the supervised neural network Multi-Layer Perceptron (MLP) because of his efficiency reported in different studies and according to the application that needs a calculation of the exact value of day done using the back propagation of the error. Classification steps for neural network are done following the work developed in [118] and used in [119], the classification steps can be summarized as follows:

- The structure of the network is first defined. In the network, activation functions are chosen and the network parameters, weights and biases, are initialized.
- The parameters associated with the training algorithm like error goals, maximum number of epochs (iterations), etc., are defined.
- The training algorithm is executed.
- After the neural network has been determined, the result is first tested by simulating the output of the neural network with the measured input data.
- Final validation must be carried out with independent data.

5.3.1 MLP neural network

A multi-layer network perceptron (MLP) is a network which uses a supervised method of training (Figure 70).

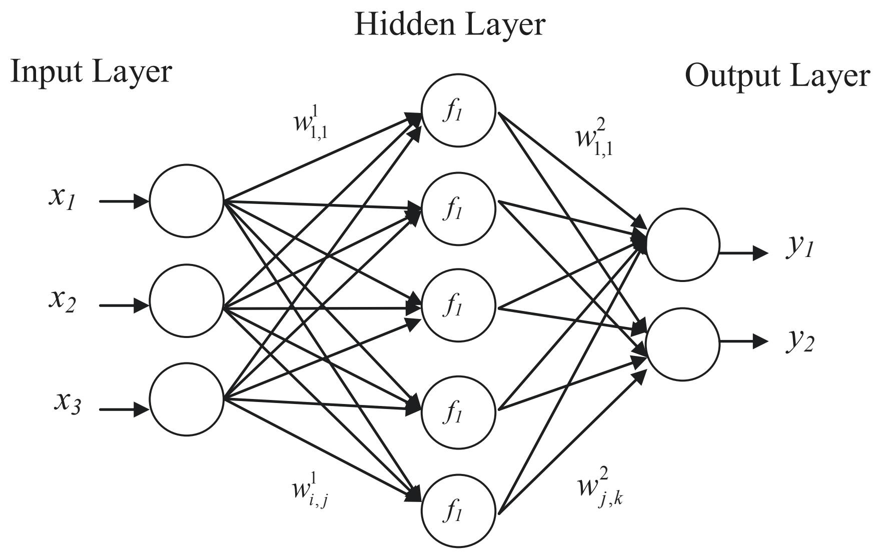

Figure 70. MLP network

The training is carried out by the algorithm of back error propagation which is based on the gradient descent. This algorithm has been published by Rumelhart et al. [120], and it is a generalization of the rule delta of Widrow-Hoff [121]. It is the first algorithm which has solved the training problem of hidden layers.

The principle of this algorithm is as follows: At each stage, an example is presented at the network, a real output is calculated by propagating the calculation between layers to another until the output layer and then the error is calculated. This is then retro propagated in the network, giving place to a modification of the weights.

This process is repeated, by repeating the presentation of each new example successively. If, for all the examples, the error is lower than a value specified in advance, the network is converged. The activation of hidden units is expressed as follows:

$$S_j = \sum_i \omega_{ji} a_i \tag{28}$$

$$a_j = f(S_j) \tag{29}$$

and for the outputs layers is

$$S_k = \sum_j \omega_{kj} a_j \tag{30}$$

$$a_k = f(S_k) \tag{31}$$

a_i designates the input of the network, s_j is the input of the hidden layer, a_j is the output of the hidden layer and a_k is the input of the layer output. The error between the desired output and obtained outputs is given by:

$$e_k = a_k - d_k \tag{32}$$

The error of the output units is calculated according to the following equation

$$\delta_k = e_k . f'(S_k) = (a_k - d_k) \cdot a_k (1 - a_k) \tag{33}$$

and of the hidden units is

$$\delta_j = \left(\sum_k \omega_{kj} . \delta_k \right) \cdot f'(S_j) = \left(\sum_k \omega_{kj} \cdot \delta_k \right) \cdot a_j \cdot (1 - a_j) \tag{34}$$

W_{ji} is the output of the network weights and W_{kj} hidden layer weights of the output layer. The learning of the hidden units is expressed by the equation (35). t denotes the number of iterations. ε(t) is the gradient step at iteration t.

$$W_{ji}(t) - W_{ji}(t-1) = \Delta W_{ji}(t) = -\varepsilon(t) \cdot \delta_j \cdot a_i \tag{35}$$

and for the output unit by the following equation:

$$W_{kj}(t) - W_{kj}(t-1) = \Delta W_{kj}(t) = -\varepsilon(t) \cdot \delta_k \cdot aj \tag{36}$$

Different tests realized in [122] denoted that the highest results are given when we use transfer functions "Tansig" or "Logsig". We use therefore only the tangent sigmoidal transfer function "Tansig" in the hidden and in the output layer:

$$\tanh(x) = \frac{e^x - e^{-x}}{e^x + e^{-x}} = 1 - \frac{2}{1 + e^{2x}} = \frac{2}{1 + e^{-2x}} - 1 \tag{37}$$

Different algorithms are used to train MLP networks which are the most important backpropagation algorithm (BP), Levenberg–Marquardt algorithm (LM), gradient ascendant algorithm and conjugate gradient (CG) algorithm. These algorithms are evaluated and tested in the literature [122]. The training algorithm functions are changed and the performance of the network is evaluated. The aim is to use the result of the network that gives best training performances with the minimum number of hidden neurons.

The same characteristics are kept and only the training algorithm is changed. BP and LM algorithms are widely known but although LM is considered to be more effective, it requires a large computer memory which justifies the use of BP algorithm in most of the practical applications.

The number of hidden layer used is started by one neuron in the hidden layer; this number will increase in order to attempt a total success learning with 100 % of accuracy. The principle consists on the use of two steps in order to determine as final result the corresponding freshness of each muscle. The first step consists on the computing of the muscle type. Once the muscle is known, the second network is used to determine the freshness of the corresponding muscle. The solution of using 2 neural networks in cascade consisting on the use of the muscle type as input for the second network of freshness produces consequent error and has showing complexity of training.

5.3.2 Learning results

The first learning is for the meat type and is realized in a first neural network. In a second neural network the meat aging computing is carried out. It corresponds to the freshness state of meat. The freshness computing is done using a specific neural network for every muscle. We present results in the case of the use of 1 neuron in the hidden layer for the 4 muscles presented in the last section. The number of neurons is increasing in order to get a successful learning (Figures 71, 72, 73, 74 and 75).

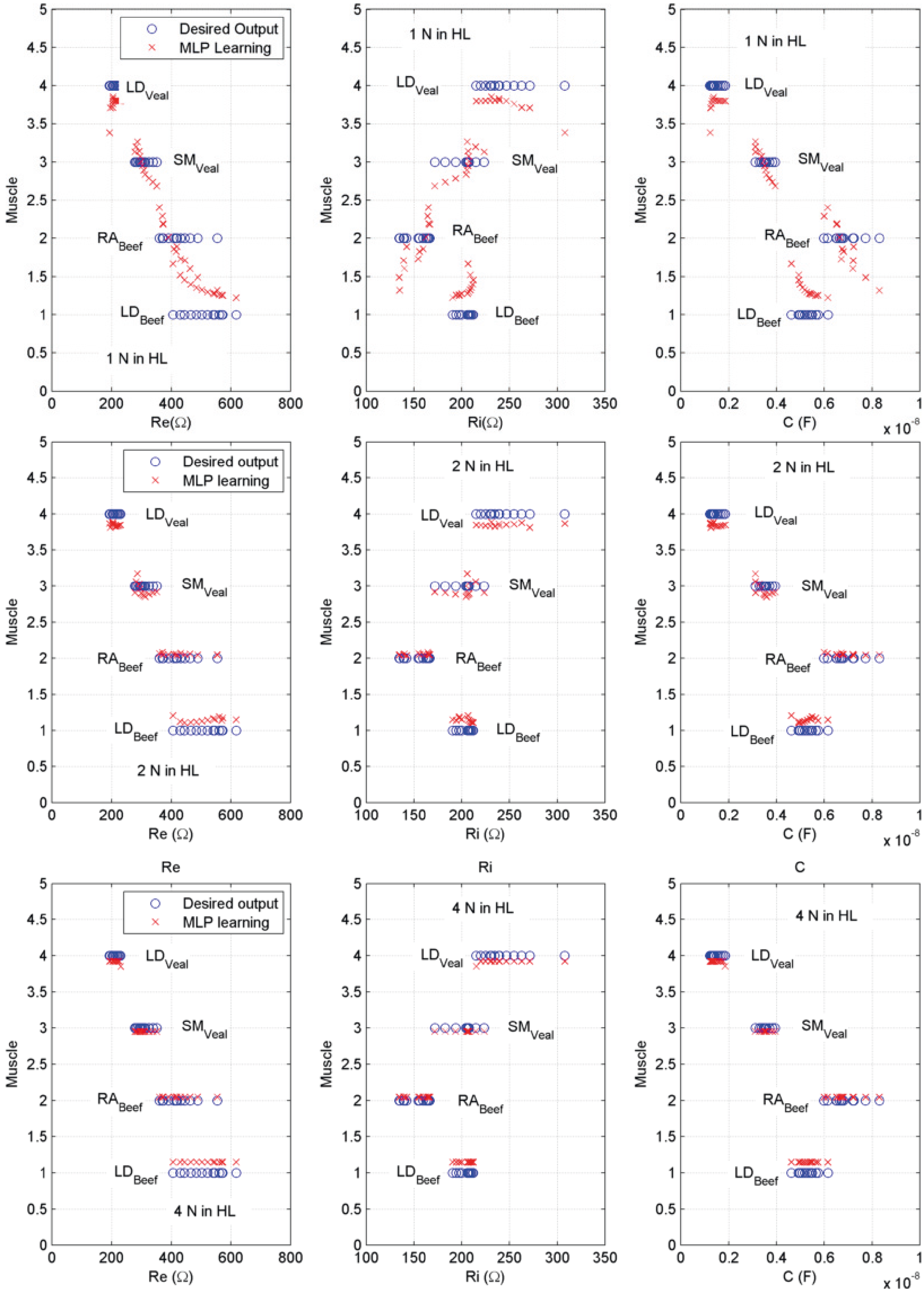

Figure 71. MLP learning results of the muscles

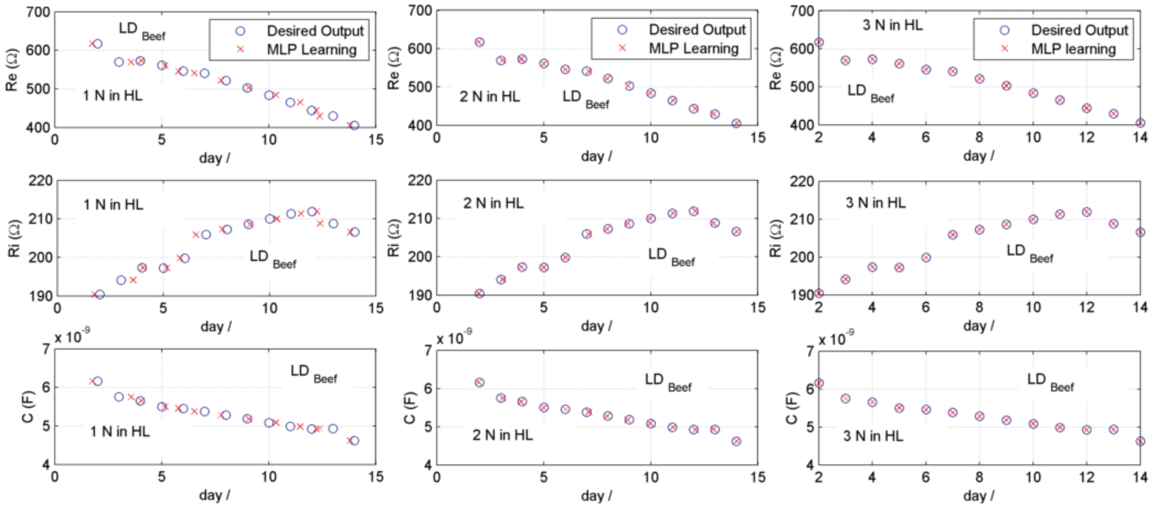

Figure 72. MLP learning results of the muscle LD beef aging

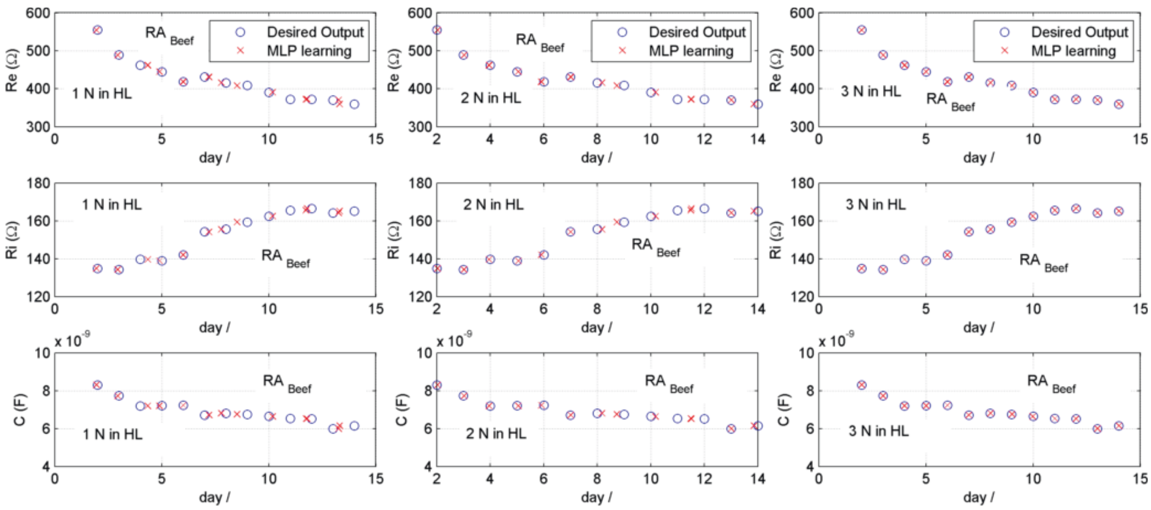

Figure 73. MLP learning results of the muscle RA beef aging

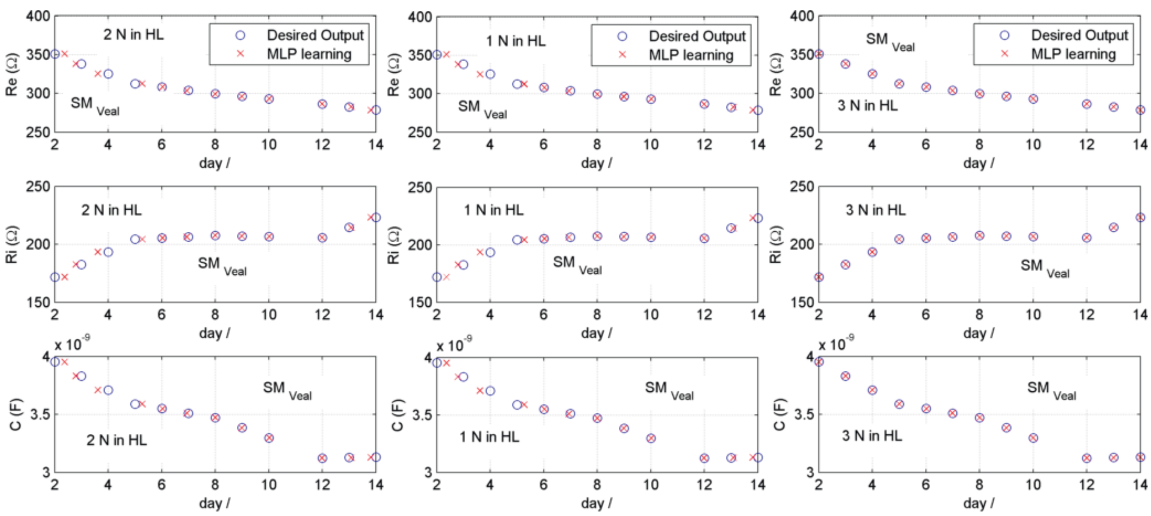

Figure 74. MLP learning results of the muscle SM veal aging

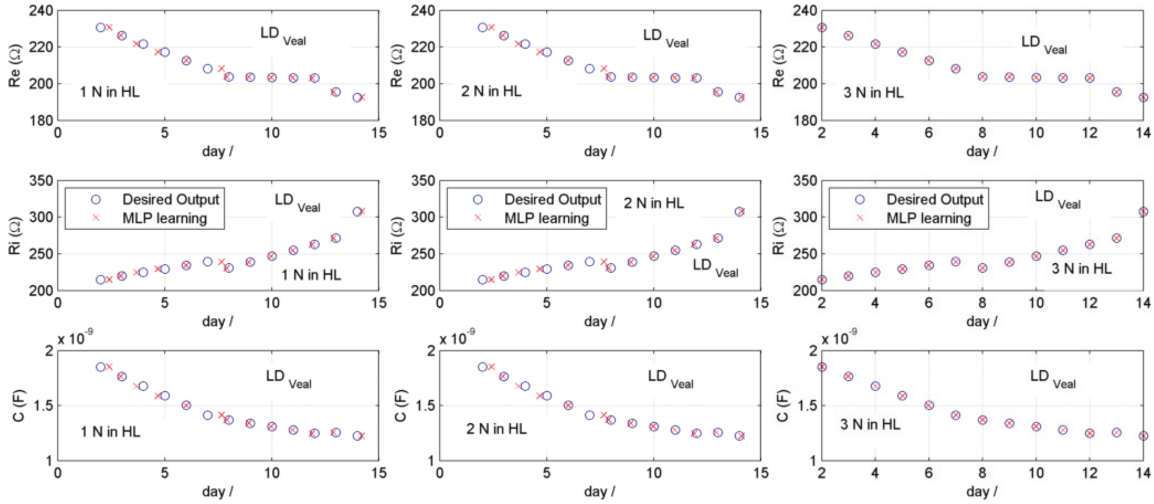

Figure 75. MLP learning results of the muscle LD veal aging

For the first network, the number of neuron in hidden layer is stopped on 4 that lead to a totally successful learning.

For the second case, freshness computing, the number of neuron in hidden layer is stopped on 3 for each neural network of the 4 measured muscles. Learning results are trained for the two networks with 100% of accuracy.

5.3.3 Test results using synthetic inputs

After the learning process, the network should be tested with a big amount of data in order to see the quality of classification it reaches. 972 synthetic inputs are created using 81 equidistant points between each two days for the test of every muscle.

This corresponds to 3888 in total for the 4 muscles. Results show that the test data are classified correctly and the results with test data reach almost 100% (Figures 76, 77 and 78).

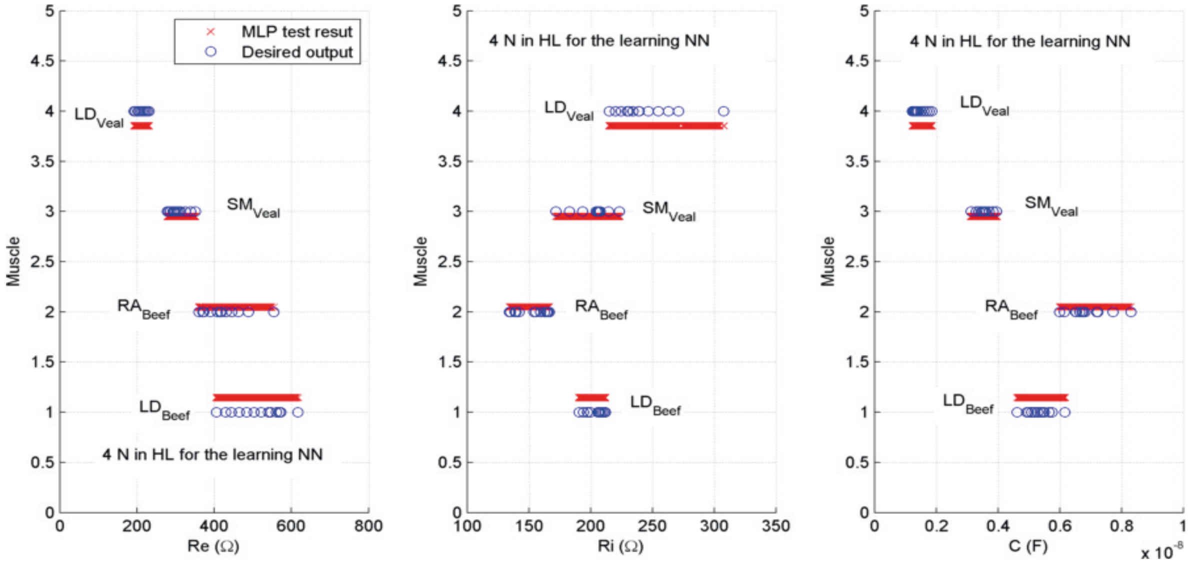

Figure 76. Test results of muscle type detection using unknown 3888 points

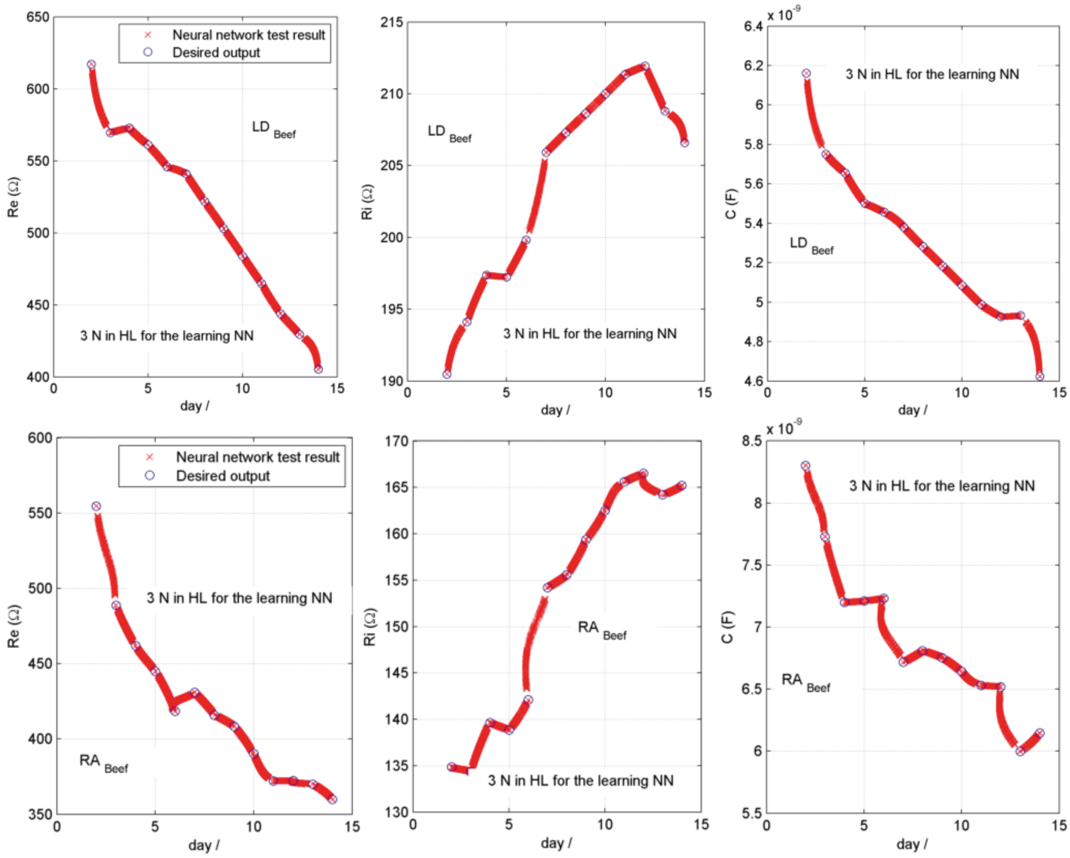

Figure 77. Test results of aging detection of beef using unknown 972 points

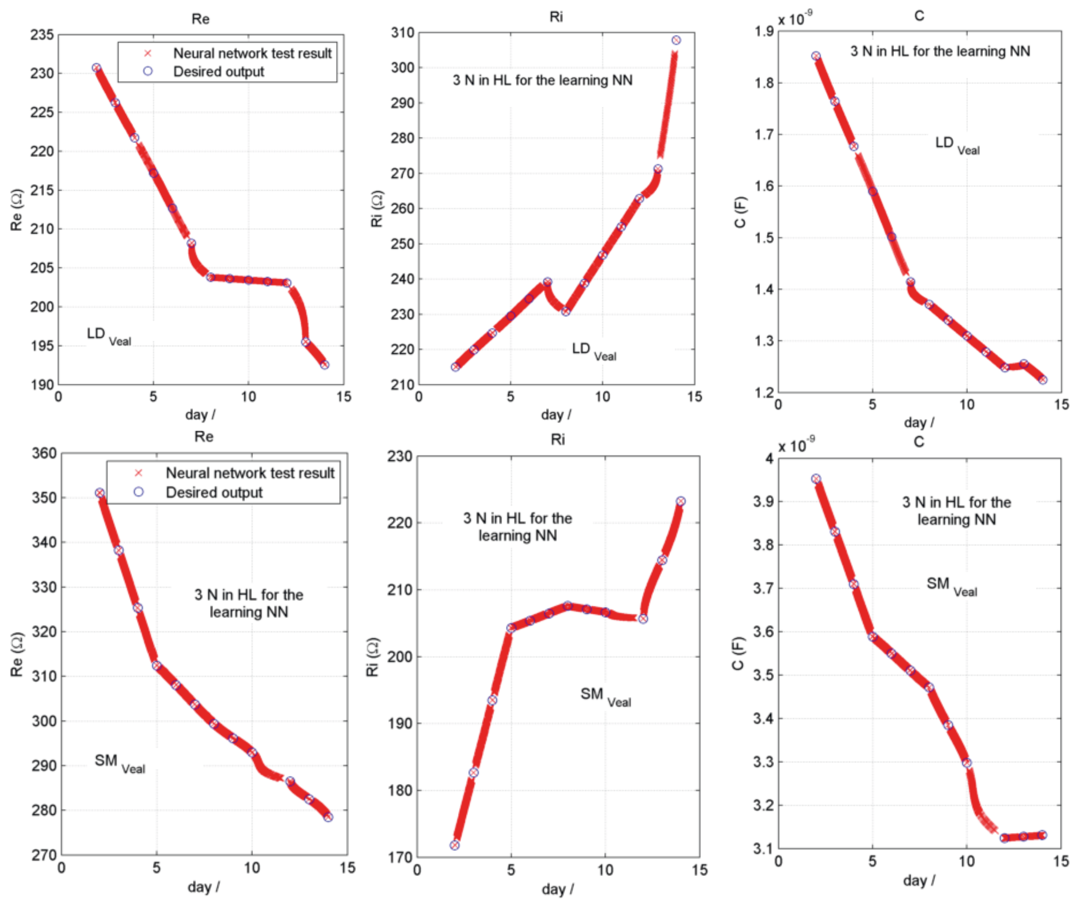

Figure 78. Test results of aging detection of veal using unknown 972 points

The MLP neural network has the ability to well and correctly classify the 972 synthetic inputs for each muscle to correctly classify the freshness of meat and muscle type.

5.3.4 Test results using noisy inputs

In order to test the neural network under more realistic conditions, we propose to use noisy inputs. The vision thereby is to have an idea about possible disturbances due to measurement noise in practice. We don't expect thereby, that its influence on the model parameters would be very high, because through the fitting process a big part of the measurement noise will be filtered out. Therefore, a perturbation for the inputs is introduced at 0.2%, 0.4%, 0.6%, 0.8% and 1%. The test results for freshness computing neural network are given in the following figures using 13 points for each muscle (Figures 79 and 80).

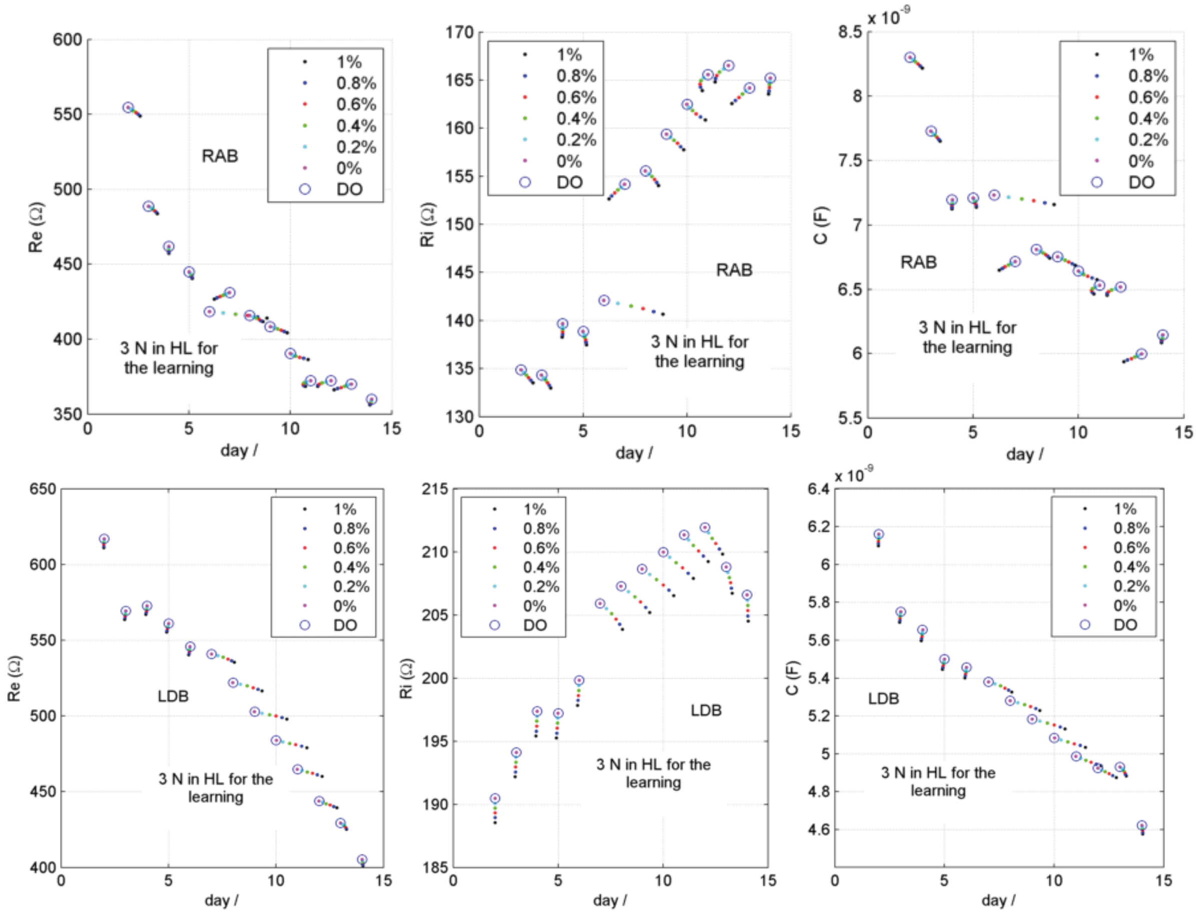

Figure 79. Model parameters for aging test of beef using noisy inputs

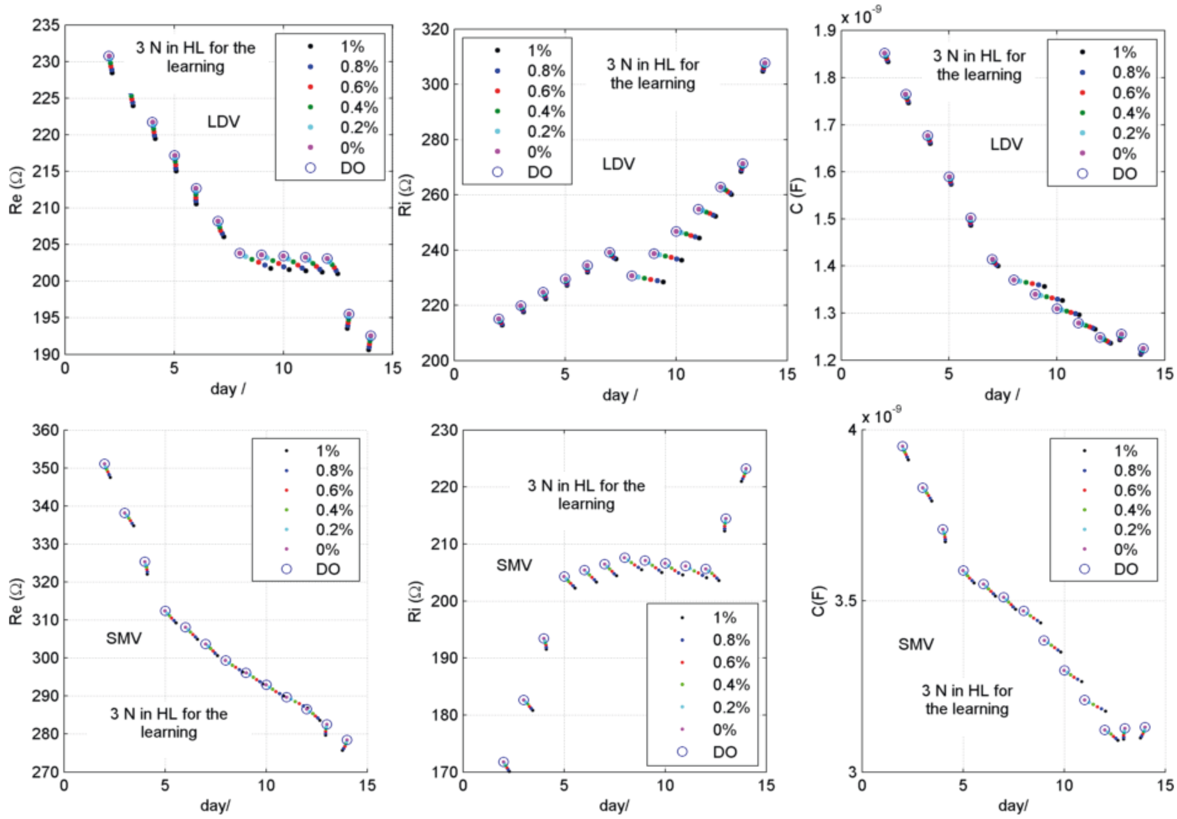

Figure 80. Model parameters for aging test of veal using noisy inputs

For muscle detection, 52 noisy inputs data sets are used with a perturbation of 1%. The confidence interval is equal to 0.5. In Figure 81, we present the results of the error between the desired output for the learning result and for the test result for noisy inputs with a noise level of 1%.

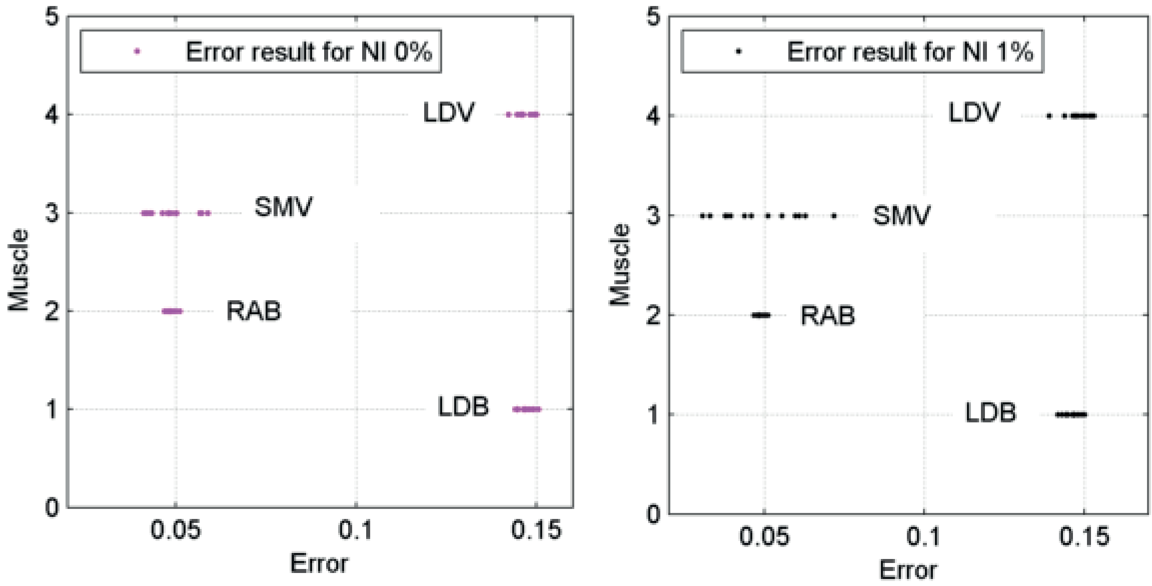

Figure 81. Error for muscle test results with noisy inputs (1%)

The error was very small in the order of 0.05 for the muscle RAB, between 0.04 and 0.06 for the muscle SMV. For the muscle LD beef and SM veal the error was more important. It was between 0.14 and 0.15 for LDB muscle and between 0.13 and 0.15 for SM veal muscle. Muscle type was classified correctly by the network in spite of the noise.

We calculate the error between the output without noise and the output for the corresponding noisy points (Figure 82). As the next figures show, the differences are not very high for noisy model parameters (inputs) and remain under one day for a noise of 0.6 % in the model parameter, which can be considered as very high and a value after impedance spectrum fitting.

One day is considered in this field as acceptable interval of time for classification of meat freshness.

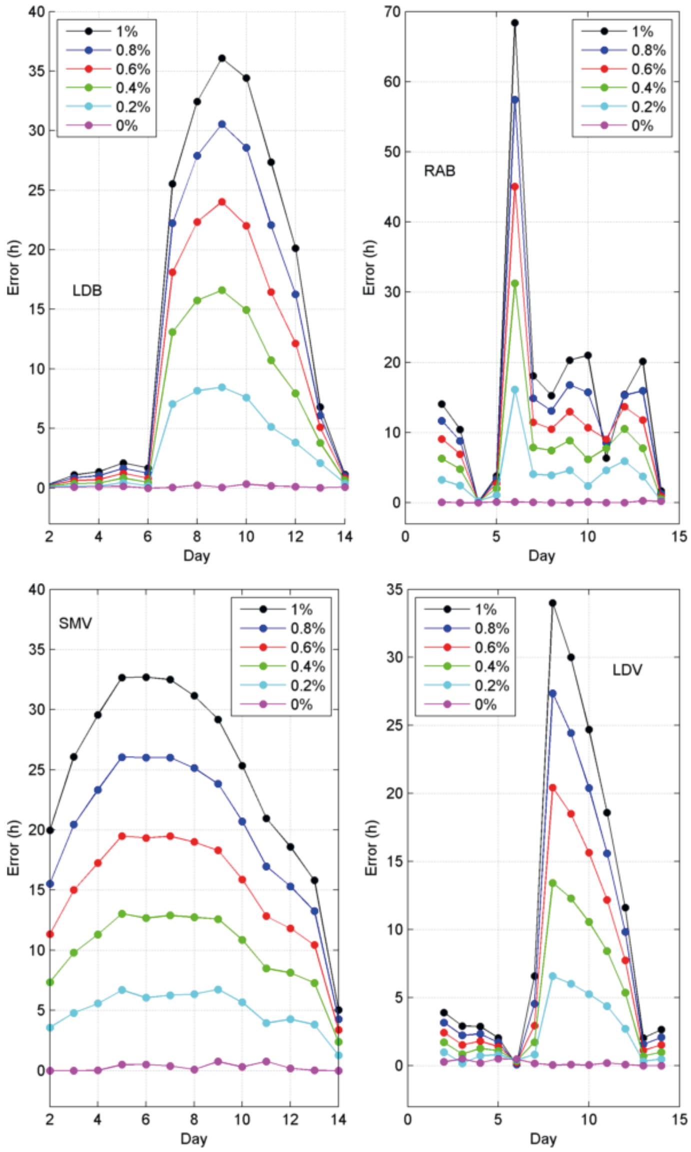

Figure 82. Error for aging test using noisy inputs

We can define different interval of confidence in order to classify and evaluate the test process. When the error is bigger than 24 hours (one day), we get a wrong result in output. For every noisy data set, we give the corresponding numerical result in the following table.

Table 13. Test results using noisy points

	0 %	0.2%	0.4%	0.6%	0.8%	1.0%
LD Beef	100 %	100 %	100 %	100%	77%	62%
RA Beef	100 %	100 %	92%	92.31%	92%	92%
SM Veal	100 %	100 %	100 %	100 %	69%	38%
LD Veal	100 %	100 %	100 %	100%	85%	77%

Considering the existing perturbation that occurs during measurement and when we add noise to the inputs, the MLP neural network has the ability to correctly classify the noisy test inputs when the noise was less than 0.6% that corresponds to the right decision with 100% for the muscles LD beef, SM beef and LD veal and with 92.31% for the muscle RA.

5.4 Fuzzy logic classification

Classification with fuzzy logic was developed with the GUI fuzzy logic toolbox. We have chosen the type of fuzzification, the number of membership functions, the functional forms of the membership functions, the parameters of the membership functions, the implication and aggregation methods and the type of defuzzification.

5.4.1 Muscle type classification using Sugeno-Takagi method

The classification is carried out using Sugeno-Takagi method that it is close to Mamdani model in fuzzifying the inputs and applying the fuzzy operator. The major difference between the two types is that Sugeno-Takagi method output membership can be either constant or linear. In this application we use Sugeno-Takagi method with constant output memberships and MF inputs as usual. The first step consists in the choice of the input and output variables and selecting carefully their intervals' ranges. By this step, we try to collect the data which generate the same output in one interval range. This process is treated for all the inputs. In one side, we define the three model's parameters R_e, R_i and C as our inputs, the output corresponds to the muscles LD Beef, RA Beef, SM Veal and LD Veal.

The output membership function or more precisely the rule consequent is only linear or constant. If the rule consequent is constant we call the model a zero-order Sugeno model which has the following form already defined in the state of the art:

$R_0 : IF \;\; L(x_1 \; is \; A_1, ..., x_k \; is \; A_k) \;\; THEN \;\; y = k$

where k is a crisply constant defined by the operator.

For each muscle we affect a corresponding constant number:

- 1 for the muscle LD beef
- 2 for the muscle RA beef
- 3 for the muscle SM veal
- 4 for the muscle LD veal

An explanatory architecture of the fuzzy inference process of muscle type classification developed with the GUI fuzzy logic toolbox is shown in Figure 83.

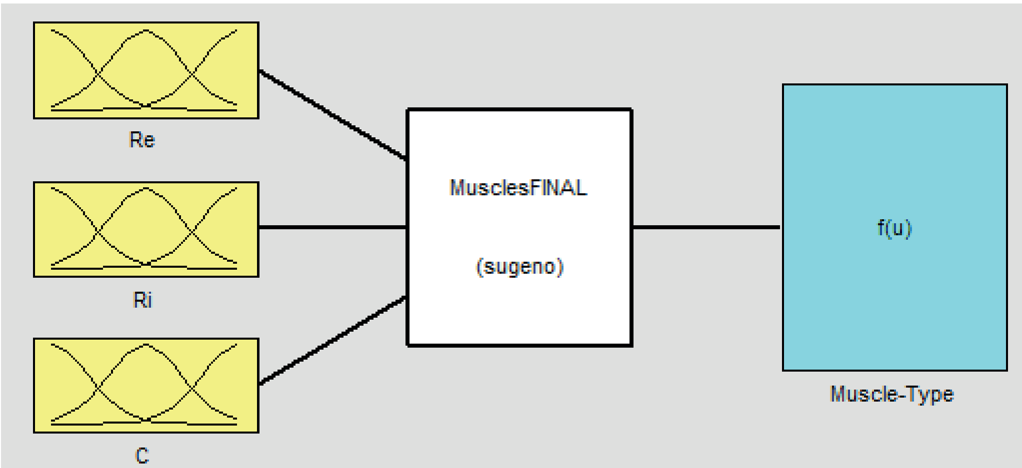

Figure 83. Fuzzy Logic system

Zadeh defines linguistic functions [100] which every element is associated with a membership degree. Fuzzy sets deal with vagueness via membership functions (MF) since they are characterized by a certain flexibility and smoothness. Hence, a membership function can be defined as:

$\mu_A : X \rightarrow [0,1]$

A membership function is determined depending on a subjective view of the problem and an individual's perception of the situation [123]. Depending on the desired outputs and performances, simple functions are used to build the membership functions (MF). The most important membership functions are triangular, trapezoidal, Gaussian. After several trials for the muscle type classification, we select the Gaussian MF defined by a central value c and a standard deviation σ > 0.

$$\mu_A(x) = f(x;\sigma,c) = e^{\frac{-(x-c)^2}{2\sigma^2}} \tag{38}$$

For each of the three inputs R_e, R_i and C, we attribute the Gaussian membership functions associated with the intervals' ranges extracted from the database. Necessity to use different zones for each input is related to the performance of the learning (Figure 84).

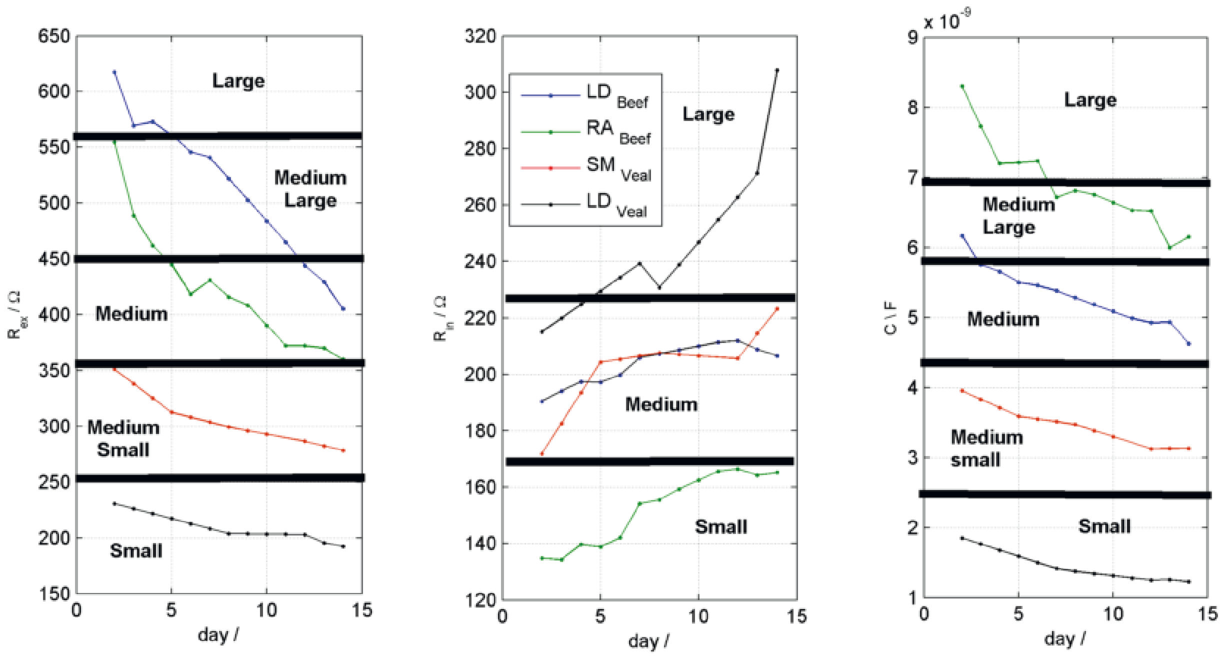

Figure 84. Muscles feature zones

For the inputs R_e and C, we attribute 5 membership degrees and 3 for the input R_i. for Each input the corresponding number of membership functions (MF) that leads to a high accuracy for the hole data base representing the type of the meat (table 14 and Figure 85).

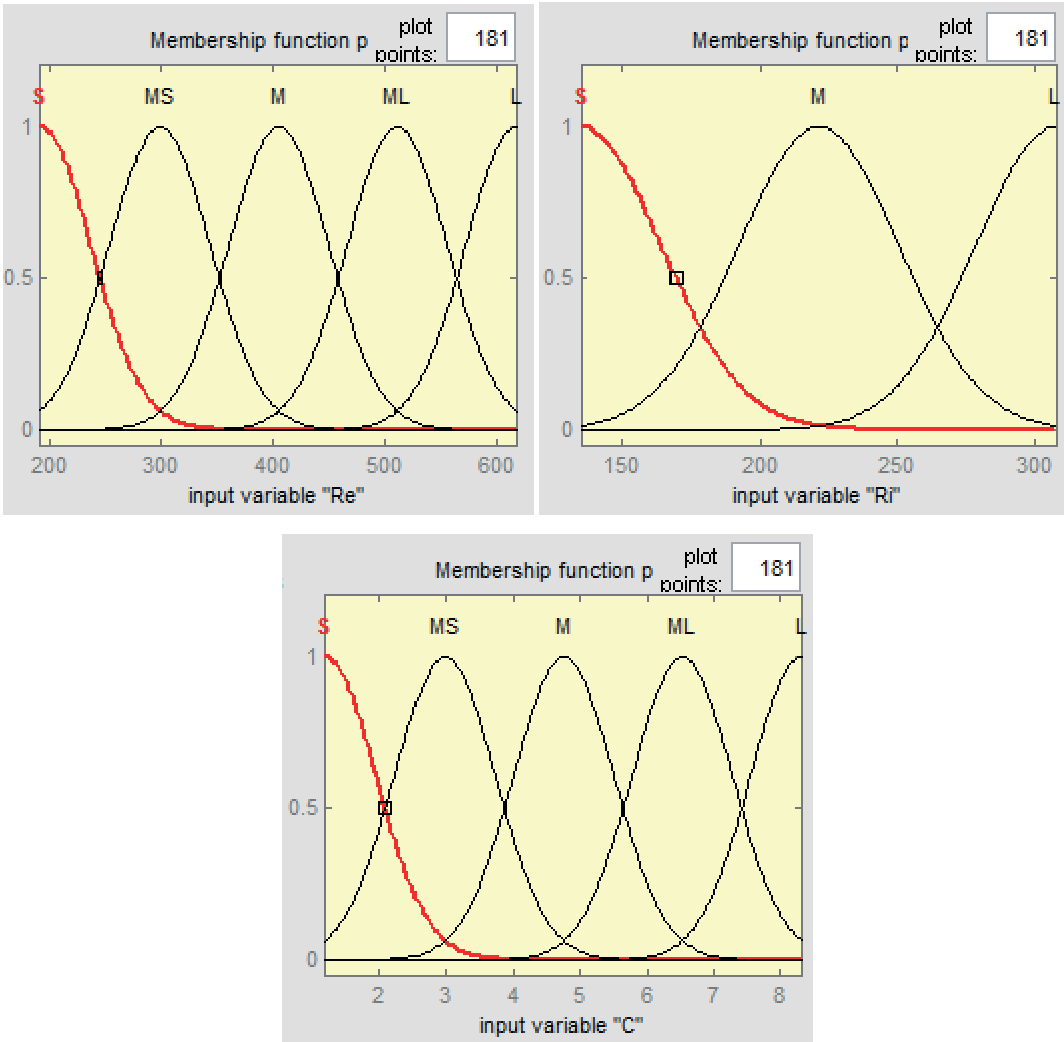

Figure 85. Membership function of the inputs muscle type classification

Table 14. Linguistic function for 3 fuzzy sets

Feature	linguistic function	Designation
Re	Small	S
	Medium Small	MS
	Medium	M
	Medium Large	ML
	Large	L
Ri	Small	S
	Medium	M
	Large	L
C	Small	S
	Medium Small	MS
	Medium	M
	Medium Large	ML
	Large	L

5.4.1.1 Fuzzy rules

Fuzzy rules have the general form of "IF X is A THEN Y is B". They are destined to map the fuzzy input X to the fuzzy output Y. In a logical context, X is referred to be a linguistic variable and A is a linguistic value. The 'IF' part of the rule is called antecedent; the 'THEN' part is called consequent. In the used MATLAB toolbox, five logical operators are supported: two forms of AND operator, two forms of OR operator and the negation form NOT.

$$AND(A,B)\begin{cases}\min(A,B)\\ prod(A,B)=A.B\end{cases}$$

$$OR(A,B)\begin{cases}\max(A,B)\\ probor(A,B)=A+B-A.B\end{cases}$$

$$NOT(A)=\overline{A}$$

We use the logical operator probor for OR and prod for AND. According to the data base and in order to have learning for the muscle with a complete independency to its freshness. 14 rules should be used and defined (Table 15). The corresponding interference matrix is given in table 16.

Table 15. Rules of the muscle detection

Rule			
1	If R_e is L and R_i is M and C is ML then Output is	Muscle 1	or
2	If R_e is L and R_i is M and C is M then Output is	Muscle 1	or
3	If R_e is ML and R_i is M and C is ML then Output is	Muscle 1	or
4	If R_e is ML and R_i is M and C is M then Output is	Muscle 1	or
5	If R_e is M and R_i is M and C is ML then Output is	Muscle1	or
6	If R_e is M and R_i is M and C is M then Output is	Muscle 1	or
7	If R_e is ML and R_i is S and C is L then Output is	Muscle 2	or
8	If R_e is ML and R_i is S and C is ML then Output is	Muscle 2	or
9	If R_e is M and R_i is S and C is L then Output is	Muscle 2	or
10	If R_e is M and R_i is S and C is ML then Output is	Muscle 2	or
11	If R_e is MS and R_i is M and C is MS then Output is	Muscle 3	or
12	If R_e is M and R_i is M and C is MS then Output is	Muscle 3	or
13	If R_e is S and R_i is M and C is S then Output is	Muscle 4	or
14	If R_e is S and R_i is L and C is S then Output is	Muscle 4	

Table 16. Interference matrix for the three inputs

X_R		R_i														
		S					M					L				
		R_e														
C		S	MS	M	ML	L	S	MS	M	ML	L	S	MS	M	ML	L
	S						M4					M4				
	MS							M3	M3							
	M								M1	M1	M1					
	ML			M2	M2				M1	M1	M1					
	L			M2	M2											

5.4.1.2 Decision making

Decision making is the most important part in a fuzzy logic system. In any decision process, we consider the information about the outcome and choose among two or more alternatives for subsequent action. If good decisions are made, then a good output is realized. The decision is made based on the given rules following certain reasoning. This stage is accomplished when applying what we call an "implication function", which is responsible for the second part of the IF-THEN rule: the consequent. The symbol of an implication is $A \rightarrow B$. An implication method specifies how a fuzzy logic system scales the membership functions of an output linguistic variable based on the rule weight of the corresponding rule. However, before applying any implication method we should know that every rule has its own weight value between 0 and 1.

Generally, the rule's weight of 1 implies that it has no effect on the implication process. Once the weights are attributed to each rule, implication method could be applied. There are 40 types of implication functions but only the minimum and product methods are the most used in fuzzy domain especially in MATLAB interface. Minimum method is used in this case. This implication method is proposed by Mamdani as a simplified version of Zadeh implication operator. It consists in truncating the output membership functions at the value of the corresponding rule weights. To make decisions in fuzzy logic, rules must be combined in some manner to have simpler and clearer output architecture which is the role of aggregation. In fact, aggregation is the process by which fuzzy sets that represent the outputs of each rule are combined into a single fuzzy set. It is the stage where outputs of all rules are unified. This step is indispensable for the next part of fuzzy logic process: “defuzzification”.

The input of the aggregation process is the list of truncated output functions returned by the implication process for each rule. The output of the aggregation process is one fuzzy set for each output variable. The curve presenting the fuzzy output can be the result of different methods of aggregation which the most known are the max (maximum) chosen in our work, probor (probabilistic or), and sum (simply the sum of each rule’s output set). Function probor [124] returns the probabilistic OR (also known as the algebraic sum) of the columns of x. if x has two rows such that x = [a; b], then y = a + b - ab. If x has only one row, then y = x (Figure 86).

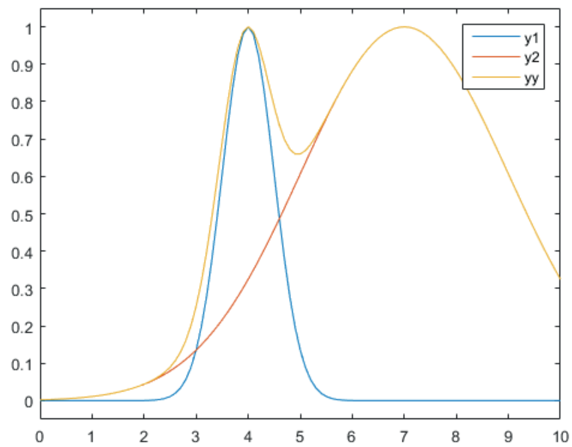

Figure 86. Example of the function Probor [123]

After the aggregation process, we should go through a defuzzification process to get finite numbers that best represent the fuzzy results. Indeed, defuzzification is the conversion of a fuzzy set quantity to a precise and deterministic set quantity. This step is necessary because in several applications, where implementation is required, machines could only work with crisp or binary values and not with linguistic variables. Several methods could be used for defuzzification.

The most important used for Sugeno fuzzy logic and recommended by Matlab toolbox are between weighted average or weighted sum. Therefore, we choose weighted average that returns the mean value of the elements of the membership function outputs for the defuzzification process.

All the learning result are given in table 17 and table 18. The use of noisy inputs reaches also to the same results. The fuzzy logic classification results show a high accuracy of 100 %.

The result of each muscle is in the close interval of the corresponding value, for example for the muscle SM veal, the accepted result that correspond to this muscle should be in the range [2.5, 3.5].

Table 17. Fuzzy logic classification result for beef muscle classification

	LD Beef				RA Beef			
	R_e (Ω)	R_i (Ω)	C (nF)	R	R_e (Ω)	R_i (Ω)	C (nF)	R
2	617.12	190.46	6.16	1.01	554.54	134.85	8.30	2.00
3	569.48	194.12	5.75	1.05	488.80	134.31	7.72	2.00
4	572.85	197.37	5.65	1.03	461.93	139.66	7.19	1.99
5	561.02	197.22	5.50	1.03	444.96	138.85	7.21	1.99
6	545.87	199.82	5.45	1.03	418.35	142.09	7.23	1.98
7	540.91	205.91	5.38	1.01	430.95	154.19	6.71	1.92
8	521.91	207.27	5.28	1.01	415.82	155.58	6.81	1.84
9	502.91	208.63	5.18	1.01	408.46	159.37	6.75	1.92
10	483.91	209.99	5.08	1.01	390.35	162.48	6.64	1.88
11	464.91	211.35	4.98	1.00	372.23	165.59	6.53	1.78
12	443.87	211.93	4.92	1.00	372.32	166.50	6.51	1.79
13	429.47	208.80	4.93	1.01	370.05	164.19	5.99	1.76
14	405.26	206.58	4.62	1.01	359.86	165.21	6.14	1.75

Table 18. Fuzzy logic classification result for veal muscle classification

	SM Veal				LD Veal			
	R_e (Ω)	R_i (Ω)	C (nF)	R	R_e (Ω)	R_i (Ω)	C (nF)	R
2	351.07	171.82	3.95	2.72	230.75	215.03	1.85	3.97
3	338.19	182.65	3.83	2.80	226.23	219.86	1.76	3.98
4	325.32	193.48	3.71	2.94	221.72	224.70	1.67	3.98
5	312.44	204.31	3.58	2.98	217.21	229.53	1.59	3.99
6	308.08	205.40	3.54	2.99	212.69	234.37	1.50	3.99
7	303.72	206.48	3.51	2.99	208.18	239.2	1.41	3.99
8	299.37	207.57	3.47	2.99	203.81	230.74	1.37	3.99
9	296.16	207.10	3.38	3.00	203.63	238.77	1.34	3.99
10	292.95	206.62	3.29	3.01	203.44	246.79	1.31	3.99
11	289.74	206.15	3.20	3.01	203.26	254.81	1.27	4.00
12	286.53	205.67	3.12	3.02	203.08	262.84	1.24	4.00
13	282.52	214.45	3.12	3.03	195.50	271.25	1.25	4.00
14	278.50	223.24	3.13	3.04	192.57	307.79	1.22	4.00

5.4.2 Freshness classification using Sugeno-Takagi method

Classification of the freshness classification is also done using the Sugeno-Takagi method. The major difference to the section before is that we make the learning for each muscle alone in order to determine the aging that corresponds to its freshness. Similar to the fuzzy logic learning for muscle classification, the three model's parameters R_e, R_i and C are defined as inputs and affected after several trials for the freshness classification to the Trapezoidal MF defined by:

$$\mu_A(x) = \begin{cases} 0 & if \quad x \le a \\ \dfrac{x-a}{b-a} & if \quad a \le x \le b \\ 1 & if \quad b \le x \le c \\ \dfrac{d-x}{d-c} & if \quad c \le x \le b \\ 0 & if \quad x \ge d \end{cases} \tag{39}$$

$$\Rightarrow f(x;a,b,c,d) = \max(\min(\frac{x-a}{b-a},1,\frac{d-x}{d-c}),0)$$

Trapezoidal MF corresponds to the membership given the highest performances, is defined by a lower limit a, an upper limit d, a lower support limit b, and an upper support c where a < b < c < d. Membership functions of the beef LD, beef RA and veal SM are presented in Figure 87. It is the same membership but with the corresponding input interval for each muscle. Membership of the veal LD is shown in Figure 88.

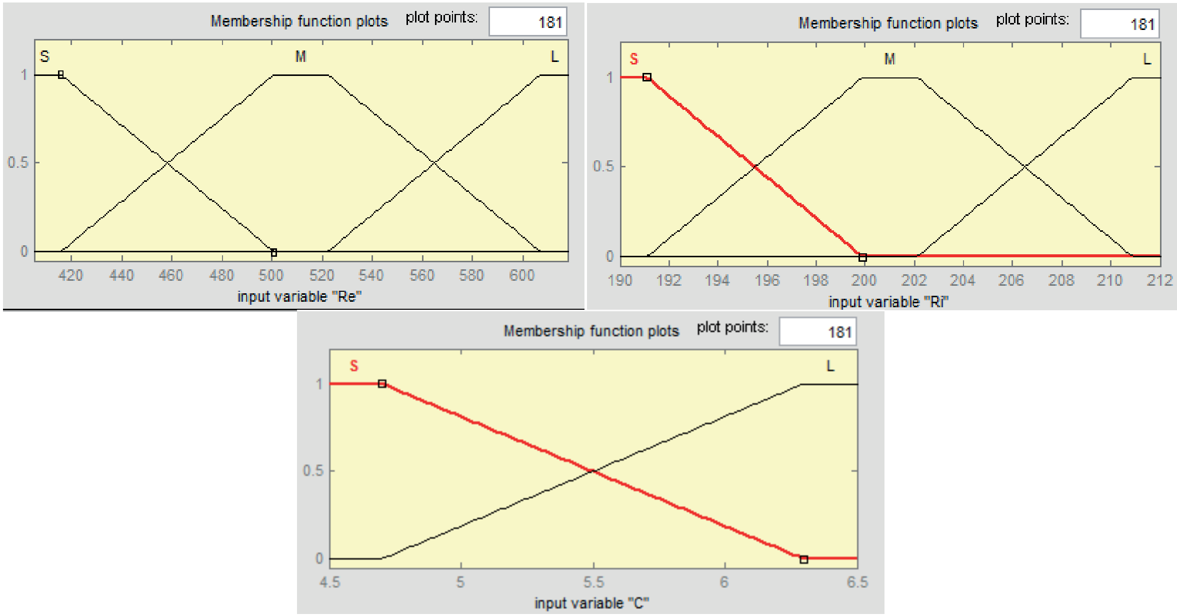

Figure 87. LD, RA beef and SM veal membership function

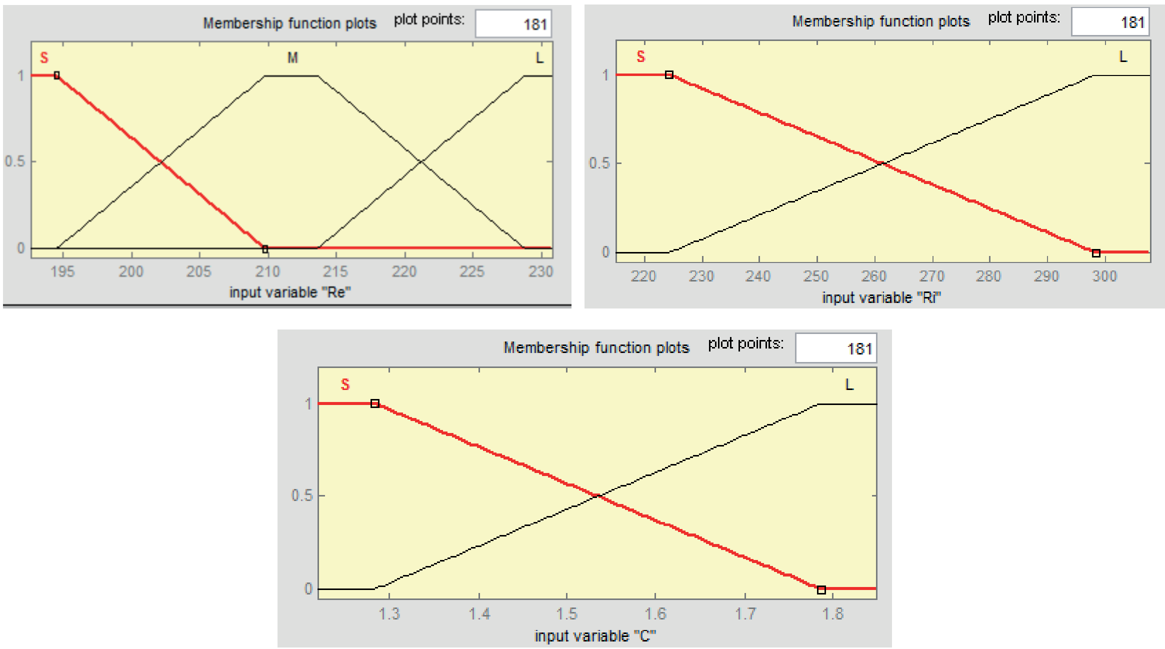

Figure 88. Membership function of the inputs freshness classification of LDV

For each muscle we affect a corresponding constant number as output:

- 1 for fresh meat
- 2 for edible meat
- 3 for critical meat
- 4 for dangerous meat

As fuzzy rules, we use the logical operator probor for OR and prod for AND. The minimum method for implication, the maximum for the aggregation process and the weighted average for the defuzzification. Rules of the fuzzy logic of freshness classification of the muscle LD beef and LD veal are given in table 19. The rules used for the muscles RA beef and SM veal are shown in table 20.

Table 19. Rules of the freshness computing of the muscles LD beef and LD veal

Rule		
1	If R_e is L and R_i is S and C is L then Output is	Fresh or
2	If R_e is L and R_i is M and C is L then Output is	Edible or
3	If R_e is M and R_i is M and C is L then Output is	Edible or
4	If R_e is M and R_i is L and C is S then Output is	Critical or
5	If R_e is S and R_i is L and C is S then Output is	Dangerous or

Table 20. Rules of the freshness computing of the muscles RA beef and SM veal

Rule		
1	If R_e is L and R_i is S and C is L then Output is	Fresh or
2	If R_e is L and R_i is M and C is L then Output is	Fresh or
3	If R_e is M and R_i is M and C is L then Output is	Edible or
4	If R_e is M and R_i is L and C is S then Output is	Critical or
5	If R_e is S and Ri is L and C is S then Output is	Dangerous

The fuzzy logic classification results in Table 21 show a high accuracy. The results of the muscles correspond to the exact freshness class and to the corresponding period of time (table 21).

The fuzzy logic classification considers the noisy inputs and reaches to the same results then the used inputs. In the diagnosis process achievement, the choice of confidences areas is decisive in order to assess the learning.

Table 21. LD and RA beef fuzzy logic classification results

	LD Beef		RA Beef		SM Veal		LD Veal	
Day	Result	Freshness	Result	Freshness	Result	Freshness	Result	Freshness
2	1.00	Fresh	1.00	Fresh	1.00	Fresh	1.00	Fresh
3	1.49	Fresh	1.00	Fresh	1.18	Fresh	1.00	Fresh
4	1.67	Edible	2.00	Edible	1.74	Edible	1.00	Fresh
5	1.80	Edible	2.00	Edible	2.21	Edible	1.43	Fresh
6	2.00	Edible	2.00	Edible	2.30	Edible	2.57	Critical
7	2.41	Edible	2.73	Critical	2.55	Critical	2.85	Critical
8	2.71	Critical	3.01	Critical	2.81	Critical	3.23	Critical
9	2.87	Critical	3.40	Critical	3.18	Critical	3.33	Critical
10	3.17	Critical	3.72	Dangerous	3.47	Critical	3.38	Critical
11	3.42	Critical	3.97	Dangerous	3.70	Dangerous	3.43	Critical
12	3.67	Dangerous	3.97	Dangerous	3.83	Dangerous	3.43	Critical
13	3.82	Dangerous	3.99	Dangerous	4.00	Dangerous	4.00	Dangerous
14	4.00	Dangerous	4.00	Dangerous	4.00	Dangerous	4.00	Dangerous

If we select and define the period of time such as:

- Fresh, between day 2 and day 3.
- Edible, between day 4 and day 6.
- Critical, between day 7 and day 10.
- Dangerous, more then day 11.

Different errors exist in fuzzy logic results according to the defined periods. The accuracy is 84.62% for the muscle LD beef, 92.31 % for the muscle RA beef, 100 % for the muscle SM veal and 61.54% for the muscle LD veal.
Results show that fuzzy logic classify correctly the inputs to the corresponding classes and we reach successful results related to the choice of tolerance interval during the conception of the diagnosis system.

5.5 Final remarks

Model parameters including the converted capacitance are used as inputs in the classification process. Using PCA method and the method of KNN (k nearest neighbor) makes sure, that model parameters are sufficient as features and have enough information content to accurately realize the classification process.

For meat classification, learning has been successful using multi-layer network perceptron (MLP) neural network together with a supervised training method carried out by the algorithm of back error propagation, which is based on the gradient descent.

A successful learning is attempt using 4 neurons in the hidden layer for the first step that consists on the computing of muscle type. Once the muscle is known, the second network is used to determine the freshness of the corresponding muscle. A successful learning is attempt using 3 neurons in the hidden layer for the four used muscles. Data used of test follow correctly the corresponding classes and we attempt successful results of test equal to 100%.

The MLP neural network has the ability to well generalize and correctly classify the 972 created inputs used for test for each muscle to reach to the freshness of the meat and correctly classify the 3888 inputs for the muscle type computing. Considering the existing perturbation that occurs during measurement and when we add a noise for the inputs, the MLP neural network has the ability to well and correctly classify the noisy testing inputs especially when the noise was less than 0.6% that corresponds to the real situation with 100% for the muscles LD beef, SM beef and LD veal and with 92.31% for the muscle RA. Neural network represents an important tool of classification that offer an important percent of accuracy and precision. The use of neural network in the final design of the diagnosis system is an excellent choice especially with the ability of implementation in a digital signal processor.

Using the Gaussian membership functions for the first learning related to muscle classification and trapezoidal member function for the classifiers related to the freshness classification, fuzzy logic permit to leads to an easy method of classification. Zero-order Sugeno fuzzy logic classify correctly the inputs to the corresponding classes for the first step of meat type classification with a high index of recognition equal to 100%. For the second step, related to the freshness computing, Zero-order Sugeno fuzzy logic reach to a high index of recognition equal to the accuracy 84.62% for the muscle LD beef, 92.31 % for the muscle RA beef, 100 % for the muscle SM veal and 61.54% for the muscle LD veal.

Fuzzy logic has many advantages that can be beneficial in the final design of the diagnosis system, this advantages are especially the consideration of noisy inputs, the simplicity of the classification process, the tolerance that leads to a compact program according to the conception procedure and finally the possibility to combine different sensors and evaluate the output with high accuracy.

6. Conclusion

The objective of this thesis is to develop a method for in-vitro beef and veal muscles tissue measurement, monitoring and diagnosis based on impedance spectroscopy. The investigation should a. o. permit a future realization of a meat monitoring sensor, in order to get information about the state of the packed meat in meat selling sector.

It has been proved, that the impedance spectroscopy builds a suitable basis for development of in-vitro measurement system for assessing the freshness of meat. The maturation state of meat leads to observable changes of its complex impedance that infer to a it's post-mortem state. Different challenges should be considered for the development of this novel method, which are the bio-impedance measurement of meat as anisotropic material and the meat diagnosis as a classification procedure.

The first challenge faced in bio-impedance measurement is the definition of the working frequency range that permits to have sensitive information. For meat monitoring, we have shown by measurements that the dispersion β is more suitable than α and γ dispersion because it includes information referring to the behavior of the cell membranes integrity, which changes with aging. The frequency range denoted is between few kHz to few MHz.

Another challenge is the development of an accurate electrode design that can guarantee reproducible and consistent measurements. An experimental setup is build up to avoid appearance of bacteria and to reduce water losses during experiments. For this, an electrode configuration is developed to avoid several disadvantages produced by needle electrodes and cylindrical non-penetrating electrodes. Finite Element Method modeling show that the electric field propagates in the whole volume of the meat and less in the surrounding. The developed electrode reduces especially the 2-D-anisotropy and the electrode contact faults. Experimental measurements have been carried out for a long period of time of 14 days with cylindrical penetrating multi electrodes on beef and veal muscles.

A further challenge in bio-impedance spectroscopy is the development of appropriate methods for the analysis of the measured spectra. For this, we propose to use the Fricke-Cole-Cole model, which considers distributed electric parameters in the biological tissue and leads therefore to a good fitting performance in the β dispersion frequency range. The evolution of model parameters corresponds to the expected behavior with aging. Results show that evolution of model parameters evolution shows principally the same behavior, but differs strongly from one muscle to another.

Features consisting of the model parameters are used as inputs in the classification procedure. Thereby, the constant phase element was converted to an equivalent capacitance. After PCA calculation, the method of KNN (k nearest neighbor) has been used to find out the accurate features to be used for the classification process. Results show that model parameters as features lead to high accuracy and permit the use of reduced number of inputs in the classification process.

In order to define a classification method for meat diagnosis we propose a procedure composed of three principle blocks: Data preprocessing, classification allowing selection of the parameters showing the best training results and test validation to select the best network to finally evaluate it.

Data used of test follow correctly the corresponding classes and we attempt successful results of test equal to 100%. The MLP neural network shows the ability to well generalize and correctly classify the 972 created inputs for each muscle leading to the right meat freshness level. It correctly classifies the 3888 inputs for the muscle type computing. MLP neural network has also the ability to well and correctly classify the noisy test inputs with a high index of recognition, especially when the noise was less than 0.6%, that corresponds to the real situation with 100% for the muscles LD beef, SM beef and LD veal and with 92.31% for the muscle RA.

Using the Gaussian membership functions for the first learning related to muscle classification and trapezoidal member function for the classifiers related to the freshness classification, fuzzy logic permits to realize an easy classification. Zero-order Sugeno fuzzy logic classifies correctly the inputs to the corresponding classes for the first step of meat type classification with a high level of recognition equal to 100%. For the second step, related to the freshness computing, fuzzy logic reaches a high level of recognition equal to 84.62% for the muscle LD beef, 92.31 % for the muscle RA beef, 100 % for the muscle SM veal and 61.54% for the muscle LD veal.

In this thesis all requirements for a diagnosis system for meat monitoring were fulfilled. As outlook we propose to design of a portable device for muscle tissue's monitoring using an online electronic device able to implement MLP neural network, or the fuzzy logic. Such a device can be used for generalization of the results for more than veal and beef meat. It can be also easily configured after corresponding experimental investigation for food quality monitoring in general, e. g. for fruits and cheese.

7. Annex

Basics of Impedance spectroscopy

The voltage has the following form

$$U(t) = U \cdot \sin(2\pi ft + \varphi_u) \quad (40)$$

U is the amplitude of the signal, and ω is the radial frequency. The relationship between radial frequency ω (expressed in radians/second) and frequency f (expressed in hertz) is

$$\omega = 2 \cdot \pi \cdot f \quad (41)$$

The current, is shifted in phase (φ) and has different amplitude.

$$I(t) = I \cdot \sin(2\pi ft + \varphi_i) \quad (42)$$

The electrochemical impedance is defined as

$$Z = \frac{U}{I} \;\; and \;\; \varphi = \varphi_u - \varphi_i \quad (43)$$

The complex number Z (ω) measured in Ohms as.

$$\underline{Z} = Z \cdot e^{j\varphi} \quad (44)$$

$$Z(\omega) = Z\cos\varphi + jZ\sin\varphi \quad (45)$$

$$\underline{Z} = Z' + jZ'' \quad (46)$$

The resistive part causes power losses. An expression analogous to Ohm's Law allows us to calculate the impedance of the system as the following equation

$$\underline{Z} = \frac{\underline{U}}{\underline{I}} = R + j \cdot X \quad (47)$$

The real part and the imaginary part (reactance) of impedance are defined as:

$$R = Z \cdot \cos(\varphi) \;\; and \;\; X = Z \cdot \sin(\varphi) \tag{48}$$

The complex admittance is defined as

$$Y(\omega) = Y\cos(\varphi_Y) + jY\sin(\varphi_Y) \tag{49}$$

$$\underline{Y} = \frac{1}{\underline{Z}} = \frac{1}{Z}e^{-j\varphi} = Ye^{j\varphi_Y} \tag{50}$$

The real part, called conductance and the imaginary part, called susceptance are defined as:

$$G = Y\cos\varphi_Y \;\text{ and }\; B = Y\sin\varphi_Y \tag{51}$$

The admittance can be written using the conductance and the susceptance as

$$\underline{Y} = G + jB \tag{52}$$

The impedance magnitude and the phase angle are defined according to the following equations

$$|Z| = \sqrt{R^2 + X_c^2} \tag{53}$$

$$\theta = \tan^{-1}\left(\frac{X_c}{R}\right) \tag{54}$$

The common model of equivalent circuits that will be shown and explained in this section considered in the Nyquist and bode plot serve to interpret simple impedance spectra. The simplest element is the impedance of a resistor without reactance term:

$$R = \mathrm{Re}\;\{Z\} \tag{55}$$

The impedance of a capacitance depends on the frequency. The current through a capacitor is phase shifted -90 degrees relative to the voltage. The impedance of a capacitance is:

$$\underline{Z} = -j\frac{1}{\omega c} \tag{56}$$

The impedance of an inductor increases as frequency increases. Inductors have only an imaginary impedance component. As a result, an inductor's current is phase shifted 90 degrees relative to the voltage.

$$\underline{Z} = j\omega L \tag{57}$$

The Nyquist plot of the parallel RC element (Figure 89) is a semicircle in the impedance plane and has a single time constant τ. ω_c is the pulsation which gives the maximum imaginary part of the Nyquist plot of impedance.

$$\tau = R_P C_P \tag{58}$$

$$\omega_c = \frac{1}{R_p C_p} \tag{59}$$

Admittance of a parallel RC element is shown in the following equation.

$$\underline{Y} = \frac{1}{R_P} + j \cdot \omega \cdot C_P \tag{60}$$

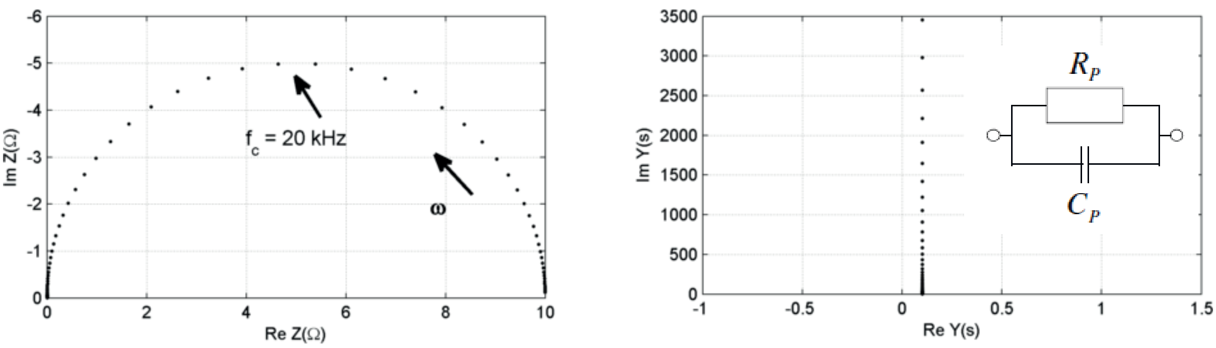

Figure 89. Nyquist plot of parallel RC element, R=10 Ω, C=5μF and f ϵ [40 Hz 110 MHz]

- For low frequencies, the capacitance is open, the current flows through the resistance.
- For middle frequencies, the current flows over resistance and capacitance.
- For high frequencies, the capacitance is a short circuit and current flows it.

The Nyquist plot of a serial RC element (Figure 90) is a semicircle in the admittance plane having a single time constant. ω_c is the pulsation which gives the maximum imaginary part of the Nyquist plot of impedance.

$$\tau = R_s C_s \tag{61}$$

$$\omega_c = \frac{1}{R_s \cdot C_s} \tag{62}$$

The impedance of the serial RC element is shown by the following equation.

$$\underline{Z} = R_s + \frac{1}{j\omega C_s} \tag{63}$$

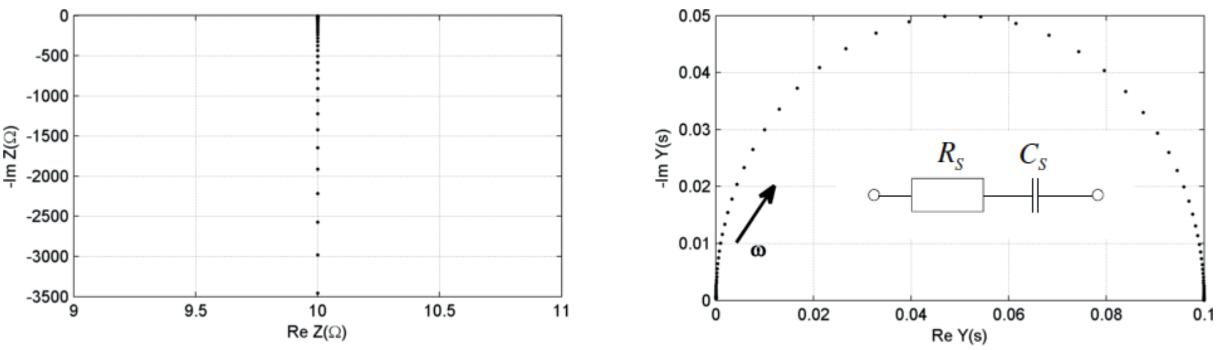

Figure 90. Nyquist plot of the serial RC element, R=10Ω, C=5μF and f= [40 Hz-100 MHz]

- For low frequencies, the capacitive behavior dominates
- For high frequencies, the resistive behavior dominates

Literature

[1] S. Grimnes, O. Martinsen: "Bio-impedance and biolectricity basics", Second Edition, ISBN: 978-0-12-374004-5, pp. 7, 2008.

[2] J. Damez, S. Clerjon: "Meat quality assessment using biophysical methods related to meat structure", Meat Science, Vol. 80, Issue 1, pp. 132-149, 2008.

[3] S. Goyal: "Artificial neural networks (ANNs) in food science - A review", International Journal of Scientific World, Vol 1, Issue 2, pp. 19-28, 2013.

[4] M. Prevolnik, D. Skorjanc, M.Candek-Potokar, M. Novic: " Application of Artificial Neural Networks in Meat Production and Technology", Artificial Neural Networks - Industrial and Control Engineering Applications, ISBN 978-953-307-220-3, edited by Prof. K. Suzuki, pp. 224-238, 2011.

[5] E. Funes, Y. Allouche, G. Beltrán, A. Jiménez: "A Review: Artificial Neural Networks as Tool for Control Food Industry", Process Journal of Sensor Technology, Vol. 5, pp. 28-43, 2015.

[6] H. Tränkler, O. Kanoun, M. Min, M. Rist: "Smart sensor systems using impedance spectroscopy", Proc. Estonian Acad. Sci. Eng, 13, 4, pp. 455-478, 2007.

[7] A. Tetyuev, O. Kanoun: "Method of soil moisture measurement by impedance spectroscopy with soil type recognition for in-situ applications", Technisches Messen, Vol. 73, pp. 404-412, 2006.

[8] U. Tröltzsch, O. Kanoun: "Miniaturized impedance measurement system for battery diagnosis", Proceedings SENSOR, Vol. 1, ISBN: 978-3-9810993-4-8, pp. 251-256, Nürnberg, 2009.

[9] D. Wulf, J. Page: "Using measurements of muscle color, PH, and electrical impedance to augment the current USDA beef quality grading standards and improve the accuracy and precision of sorting carcasses into palatability groups", Journal of Animal Science, Vol. 78, pp. 2595-2607, 2000.

[10] U. Pliquett: "Bio-impedance: A review for food processing", Food Eng. Rev., Vol. 2, Issue 2, pp. 74-94, 2010.

[11] S. Grimnes, O. Martinsen: "Bio-impedance and biolectricity basics", ISBN 0-12-303260-1. pp. 201, 2000.

[12] J. Ross Macdonald, E. Barsoukov: "Impedance spectroscopy theory, experiment, and applications", ISBN: 0-471-64749-7, Second Edition, 2005.

[13] M. Orazem, B. Tribollet: "Electrochemical impedance spectroscopy", ISBN: 978-0-470-04140-6, 2008.

[14] E.H. Callow: "The electrical resistance of muscular tissue and its relation to curing", Annual Report of Food Investigations Board, pp. 57, HMSO, London, 1936.

[15] E.H. Callow: Report Food Invest. Board, HMSO, London, 1937.

[16] E.H. Callow: Report Food Invest. Board, HMSO, London, 1938.

[17] J.L. Damez, S. Clerjon, S. Abouelkaram, J. Lepetit: "Beef meat electrical impedance spectroscopy and anisotropy sensing for non-invasive early assessment of meat ageing", Journal of Food Engineering, Vol. 85, Issue 1, pp. 116-22, 2008.

[18] J.L. Damez, S. Clerjon, S. Abouelkaram, J. Lepetit: "Electrical impedance probing of the muscle food anisotropy for meat ageing control", Journal Food Control, Vol. 19, Issue 10, pp. 931-39, 2008.

[19] J.L. Damez, S. Clerjon, S. Abouelkaram, J. Lepetit: "Dielectric behavior of beef meat in the 1–1500 KHz range, simulation with the Fricke/Cole–Cole model", Meat Science, Vol. 77, Issue 4, pp. 512-519, 2007.

[20] M. Altmann, U. Pliquett, R. Suess E. Von Borell: "Prediction of lamb carcass composition by impedance spectroscopy", J. Anim. Sci., Vol. 82, Issue 3, pp. 816-825, 2004.

[21] M. Altmann, U. Pliquett, R. Suess, Ev. Borell: "Prediction of carcass composition by impedance spectroscopy in lambs of similar weight", Meat Science, Vol. 70, Issue 2, pp. 319-327, 2005.

[22] Z. Ghatass, M. Soliman, M. Mohamed: "Dielectric technique for quality control of beef meat in the range 10 kHz - 1 MHz", American-Eurasian Journal of Scientific Research, Vol. 3, Issue 1, pp. 62-69, 2008.

[23] D. Padmaraja, J. H. Miller Jr., J. Wosika, W. Zagozdzon-Wosika: "Reduction of electrode polarization capacitance in low-frequency impedance spectroscopy by using mesh electrodes", Biosensors and Bioelectronics, Vol. 29, pp. 13-17, 2011.

[24] O. T. Ogunnika, S. B. Rutkove, H. Ma, P. M. Fogerson, M. Scharfstein, C. Cooper, J. L. Dawson: "A portable system for the assessment of neuromuscular diseases with electrical impedance myography", J. medical engineering & technology, pp. 1-9, 2010.

[25] M. Oliver, I. Gobantes, J. Arnau, J. Elvira, P. Riu, N. Grebol, J. Monfort: "Evaluation of the electrical impedance spectroscopy equipment for ham meat quality", Meat Science, Vol. 58, Issue 3, pp. 305-312, 2001.

[26] L. H. Negri, P. Bertemes-Filho, A. S. Paterno: "Computational intelligence algorithms for bio-impedance-based classification of biological material", 5^{th} European Conference of the IFMBE, IFMBE Proceedings, Vol. 37, pp. 1229-1232, 2011.

[27] J. Lepetit, P. Salé, R. Favier, R. Dalle: "Electrical impedance and tenderisation in bovine meat", Meat Science, Vol. 60, Issue 1, pp. 51-62, 2002.

[28] M. Altmann, U. Pliquett: "Prediction of intramuscular fat by impedance spectroscopy", Meat Science, Vol. 72, Issue 4, pp. 666-671, 2006.

[29] H. J. Swatland: "Post-mortem changes in pork using parallel needles for both light scattering and low frequency electrical properties", Food Research International, Vol. 30, Issue 3-4, pp. 293-298, 1991.

[30] B. Bodakian, F. Hart: "The dielectric properties of meat", IEEE Transactions on Dielectrics and Electrical Insulation, Vol. 1, Issue 2, pp. 181-187, 1994.

[31] E. García-Breijo, J. M. Barat, O.L. Torres, R. Grau, L. Gil, J. Ibáneza, M. Alcaniz, R. Masot, R. Fraile: "Development of a puncture electronic device for electrical conductivity measurements throughout meat salting", Sensors and Actuators A: Physical, Vol. 148, Issue 1, pp. 63-67, 2008.

[32] D. Chevalier, F. Ossart, C. Ghommidh: "Development of a non-destructive salt and moisture measurement method in salmon (Salmo salar) fillets using impedance technology", Food Control, Vol. 17, Issue 5, pp. 342-347, 2006.

[33] A. Mohiri, A. Burhanudin, I. Ismail, L. Ismail: "Blood volume dependence of meat permittivity using dielectric mixing rules", IEEE National Postgraduate Conference (NPC), ISBN: 978-1-4577-1882-3, pp. 1-5, 2011.

[34] A. Rabih, M. Rawther, T. Ibrahim: "Capacitive variations study of fish, cow and pig meat", IEEE International Conference on Intelligent and Advanced Systems (ICIAS), ISBN: 978-1-4244-6623-8, pp. 1-4, 2010.

[35] M. Giráldez, P. Botella, F. Toldrá, P. Fito: "Low-frequency dielectric spectrum to determine pork meat quality", Innovative Food Science and Emerging Technologies, Vol. 11, Issue 2, pp. 376-386, 2010.

[36] H. J. Swatland: "Anisotropy and postmortem changes in the electrical resistivity and capacitance of skeletal-muscle, Journal of animal science, Vol 50, pp. 67-74, 1980.

[37] M. Guermazi, O. Kanoun, N. Derbel: "Investigation of long time beef and veal meat behaviour by bio-impedance spectroscopy for meat monitoring", IEEE Sensors Journal, Vol. 14, Issue 10, pp. 3624-3630, 2014.

[38] H. P. Schwan: "Electrical properties of tissue and cell suspensions", Advances in Biological and Medical Physics, Vol. 5, pp. 147-209, 1957.

[39] K. Foster, H.P. Schwan: "Dielectric properties of tissues and biological materials: a critical review", Critical Reviews in Biomedical Engineering, Vol. 17, Issue 1, pp. 25-104, 1989.

[40] M. Guermazi, O. Kanoun, N. Derbel: "Reduction of anisotropy influence and contacting effects in in-vitro bio-impedance measurements", Journal of Physics: Conference Series, Vol. 434 pp. 1-4, 2013.

[41] O. Martinsen, S. Grimnes, H.P. Schwan: "Interface phenomena and dielectric properties of biological tissue", Encyclopedia of Surface and Colloid Science, Vol. 20, pp. 2643-2652, 2002.

[42] H. P. Schwan: "Electrical properties of tissues and cell suspensions: mechanisms and models", Proceedings of 16th Annual International Conference of IEEE Engineering in Medicine and Biology Society, pp. 70a-71a, Baltimore, MD, USA, 1994.

[43] G. Schwartz: "A theory of the low frequency dispersion of colloid particles in electrolyte solution", J. Phys. Chem, Vol. 66, Issue 12, pp. 2636-2642, 1962.

[44] J. Damez, S. Clerjon, S. Abouelkaram, J. Lepetit: "Beef meat electrical impedance spectroscopy and anisotropy sensing for non-invasive early assessment of meat ageing", Journal of Food Engineering, Vol. 85, pp. 116–122, 2008.

[45] N. Demmiere: "Continuous-flow separation of cells in a lab-on-a- chip using “liquid electrodes” and multiple-frequency dielectrophoresis", Ph.D Thesis, Ecole Polytechnique Fédéral de Lausanne, Suisse, pp. 35-43, 2008.

[46] N. M. Barlea, S.I. Barlea, E. Cuela: "Maxwell-Wagner effect on the human skin", Romanian J. Biophis, Vol. 18, Issue 1, pp. 87-98, Bucharest, 2008.

[47] J. P. Pérez, R. Carles, R. Fleckinger: "Électromagnétisme: vide et milieux matériels: avec exercices et problèmes résolus", Paris, Masson, 1990.

[48] J. C. Maxwell: "A treatise on electricity and magnetism", Vol. 2, 1873.

[49] H. Morgan, N.G. Green: "AC electrokinetics: colloids and nanoparticles", ISBN: 0863802559, 2003.

[50] P. Debye: "Polar molecules", Chemical Catalog Company, New York, 1929.

[51] K. R. Foster, H.P. Schwan: "Dielectric properties of tissues", Handbook of Biological Effects of Electromagnetic Fields, pp. 25-102, 1996.

[52] H. Fricke, S. Morse: "The electric resistance and capacity of blood for frequencies between 800 and 44 million cycles", J. Gen. Physiol., Vol. 9, Issue 2, pp. 153-167, 1925.

[53] H. Fricke: "The theory of electrolytic polarization", Philosophical Magazine and Journal of Science, Taylor and Francis, Vol. 14, Issue 90, pp. 310-318, 1932.

[54] K. Cole, H. Cole: "Dispersion and absorption in dielectrics alternating current characteristics", J. Chem. Phys., Vol. 9, Issue 4, pp. 341-351, 1941.

[55] K. S. Cole: "Membranes, ions, and impulses: a chapter of classical biophysics", University of California Press., ISBN: 0-520-00251-2, 1972.

[56] E. T. Adams, J. Jossinet: "Tissue impedance: a historical overview", Physiol. Meas. Vol. 16, pp. A1-A13, 1995.

[57] K. S. Cole: " Permeability and impermeability of cell membranes for ions". Quantitative biology, Vol. 8, pp. 110-122, 1940.

[58] E T McAdams, J Jossinet: "Tissue impedance: a historical overview", Physiol. Meas. 16, ALA13, 1995.

[59] J. R. Macdonald: "Note on the paramerization of the constant phase admittance element", Solid State Ionics Vol 13, pp. 147-149, 1984.

[60] R. E Dodde: "Bio-impedance of soft tissue under compression and applications to electrosurgery", dissertation in Biomedical Engineering, University of Michigan, 2011.

[61] F. Gómez, J. Bernal, J. Rosales, T. Cordova: Modeling and simulation of equivalent circuits in description of biological systems - A Fractional Calculus Approach", Journal of electrical bio-impedance, Vol. 3, pp. 2-11, 2012.

[62] R. Bragos, X. Gamez, J. Cairo, P. J. Riu, F Godia: "Biomas monitoring using impedance spectroscopy" Anals, New York academy of sciences, pp. 299-305, 1999.

[63] D. Haemmerich, R. Ozkan, S. Tungjitkusolmun, J.Z. Tsai, D.M. Mahvi, S.T. Staelin, J.G. Webster: "Changes in electrical resistivity of swine liver after occlusion and postmortem", Med. Biol. Eng. Comput., Vol. 40, Issue 1, pp. 29-33, 2002.

[64] Y. Konishi, T. Morimoto, Y. Kinouchi, T. Iritani, Y. Monden: "Electrical properties of extracted rat liver tissue", Res. Exp. Med., Vol. 195, Issue 4, pp. 183-92, 1995.

[65] W. Kuang, S. O. Nelson: " Low-frequency dielectric properties of biological tissues: a review with some new insights", Transactions of ASAE, Vol. 41(1), pp. 173-184, 1998.

[66] A. Ivorra, M. Genesc, A. Sola, L. Palacios, R. Villa, G. Hotter, J. Aguil: "Bio-impedance dispersion width as a parameter to monitor living tissues", Physiological measurement, Vol. 26, Issue 2, 2005.

[67] V. Yu. Musatov, V. V. Sysoev, M. Sommer, I. Kiselev: "Assessment of meat freshness with metal oxide sensor microarray electronic nose: A practical approach", Sensors and Actuators B: Chemical, Vol. 144, Issue 1, pp. 99-103, 2010.

[68] T. Eklöv, G. Johansson, F. Winquist, I. Lundström: "Monitoring sausage fermentation using an electronic nose", Journal of the Science of Food and Agriculture, Vol. 76, Issue 4, pp. 525-532, 1998.

[69] J. A. Balejko, N. Zbigniew, B. Edyta: "Artificial neural network as the tool in prediction rheological features of raw minced meat" Acta Sci. Pol., Technol. Aliment, Vol. 11, Issue. 3, pp. 273-281. 2012.

[70] C. E. Jr. Floyd , J. Y. Lo, A. J. Yun, D. C. Sullivan, P. J. Kornguth: "Prediction of Breast Cancer Malignancy Using an Artificial Neural Network", Journal Cancer, Vol. 74, Issue 11. pp. 2944-2948,1994.

[71] B. Kim, S. Park: "An optimal neural network plasma mo el: a case study", Chemometrics and Intelligent Laboratory Systems, Vol. 56, pp. 39–50, 2001.

[72] L. Guerrero, I. Gobantes, M.A Oliver, J. Arnau, M.D. Guardia, J. Elvira, P. Riu, N. Grebol, J.M. Monfort: "Green hams electrical impedance spectroscopy (EIS) measures and pastiness prediction of dry cured hams", Meat Science, Vol. 66, Issue 2, pp. 289-294, 2004.

[73] P. Bertemes-Filho, L.H. Negri, A.S. Paterno: "Detection of bovine milk adulterants using bio-impedance measurements and artificial neural network", 5th European Conference of the IFMBE, IFMBE Proceedings, Vol. 37, pp. 1275-1278, 2011.

[74] M. O'Farrell, E. Lewis, C. Flanagan, W.B. Lyons, N. Jackman: "Combining principal component analysis with an artificial neural network to perform online quality assessment of food as it cooks in a large-scale industrial oven", Sensors and Actuators B: Chemical, Vol. 107, Issue 1, pp. 104-112, 2005.

[75] J. Qiao, M. O. Ngadi, N. Wang, C. Gariepy, S. O. Prasher: "Pork quality and marbling level assessment using a hyperspectral imaging system", Journal of Food Engineering, Vol. 83, Issue 1, pp.10-16, 2007.

[76] F. Winquist, E.G. Hörnsten, H. Sundgren, I. Lundström: "Performance of an electronic nose for quality estimation of ground meat", Measurement Science & Technology, Vol. 4, Issue 12, pp.1493-1500, 1993.

[77] M. R. Chandraratne, S. Samarasinghe, D. Kulasiri, C. Frampton,, R. Bickerstaffe: "Determination of lamb grades using texture analysis and neural net works", Proceedings of the 3rd IASTED International Conference visualization, imaging and image processing,, pp. 656-661, Benalmadena, Spain September 8-10, 2003.

[78] R. R. Janghel, A. Shukla, R. Tiwari, R. Kala: "Breast cancer diagnosis using artificial neural network models", 3rd IEEE International Conference on Information Sciences and Interaction Sciences (ICIS), pp. 89-94, 2010.

[79] X. Xing-Chuang, F. Xiang, O. Yang-Zheng, J. You, H. Ze-Jian, Z. Yu-Kui: "Artificial neural networks for classification and identification of data of biological tissue obtained by mass-spectrometry imaging", Chinese Journal of Analytical Chemistry, Vol. 40, Issue 1, pp. 43-49, 2012.

[80] M. Prevolnik, M. Candek-Potokar, M. Novic, D. Skorjanc: "An attempt to predict pork drip loss from pH and colour measurements or near infrared spectra using artificial neural networks", Meat Science, Vol. 83, Issue 3, pp. 405-411, 2009.

[81] S. Balasubramanian, S. Panigrahi, C. M. Logue, H. Gu, M. Marchello: "Neural networks-integrated metal oxide-based artificial olfactory system for meat spoilage identification", Journal of Food Engineering, Vol. 91, Issue 1, pp. 91-98, 2009.

[82] V. Prasath, N. Lakshmi, M. Nathiya, N. Bharathan, N. P. Neetha: "A Survey on the applications of fuzzy logic in medical diagnosis", International Journal of Scientific & Engineering Research, Vol. 4, Issue 4, pp. 1199-1203, 2013.

[83] A. A. E. Saleh, S. E. Barakat, A. A. E Awad: "A fuzzy decision support system for management of breast cancer", International Journal of Advanced Computer Science and Applications, Vol. 2, Issue 3, pp. 34-40, 2011.

[84] K. C. Latha, B. Madhu, S. Ayesha, R. Ramya, R. Sridhar, S. Balasubramanian: "Visualization of risk in breast cancer using fuzzy logic in Matlab environment", International Journal of Computational Intelligence Techniques, Vol. 4, Issue 1, pp. 114-117, 2013.

[85] V. Balancia, I. Dumitrache, M. Carmihai, W. Rae, C. Herbst: "Evaluation of breast cancer risk by using fuzzy logic", U.P.B. Sci, Bull., Series C, Vol. 73, Issue 1, pp. 53-64, 2011.

[86] A. Yilmaz, K. Ayan, E. Adak: "Risk analysis in cancer disease by using fuzzy logic", Annual Meeting North American Fuzzy Information Processing Society, pp. 1-5, 2011.

[87] L. Fernando, C. Nascimentoa, N. Regina, S. Ortega: "Fuzzy linguistic model for evaluating the risk of neonatal death", Rev Saúde Pública, Vol. 36, Issue 6, pp. 686-692, 2002.

[88] M. Jampour, M. Jampour, M. Ashourzadeh, M. Yaghoobi: "A fuzzy expert system to diagnose diseases with neurological signs in domestic animal", 8th International Conference on Information Technology, pp. 1021-1024, 2011.

[89] M. Neshat, M. Yaghobi, M. B. Naghibi, A. Esmaelzadeh: "Fuzzy expert system design for diagnosis of liver disorders", International Symposium on Knowledge Acquisition and Modeling, pp. 252-256, Wuhan, 2008.

[90] I. T. Jolliffe: "Principal component analysis, second edition", Springers Series in Statistics, Springer, 2002.

[91] W. S. McCulloch, W. Pitts: "A logical calculus of ideas immanent in nervous activity", Bulletin of Mathematical Biophysics, Vol. 5, pp. 115-133, 1943.

[92] D.O. Hebb: "The organization of behavior: a neurophysiological theory", New York Wiley, 1949.

[93] F. Rosenblatt: "Principles of neurodynamics: perceptrons and the theory of brain mechanisms", Washington D.C, 1961.

[94] B. Widrow, M. E. Hoff: "Adaptive switching circuits", IRE WESCON Convention Record, New York IRE, pp. 96-104, 1960.

[95] M. Minsky, S. Papert: "Perceptrons", Cambrige, MA, MIT press, pp. 1-20, 1969.

[96] T. Kohonen: "Self-organization and associative memory", Springer-Series in information sciences, Vol. 8, 1989.

[97] J. J. Hopfield: "Neural networks and physicals systems with emergent collective computational abilities", Proceedings of the national academy of sciences, Vol. 79, pp. 2554-2558, 1982.

[98] S. Haykin: "Neural networks A comprehensive foundation", ISBN:0132733501.1999.

[99] A. K. Jain, J. Mao, K. M. Mohiuddin: "Artificial neural networks: a tutorial", IEEE Computer, Vol. 29, Issue 3, pp. 31-44, 1996.

[100] L. A. Zadeh: "Fuzzy sets", Information and Control, Vol. 8, Issue 3, pp. 383-353, 1965.

[101] H. J. Zimmermann: "Fuzzy set theory and its applications", ISBN 978-94-015-7951-3, London, 1991.

[102] A. M. Aziz: "Effects of fuzzy membership function shapes on clustering performance in multisensor-multitarget data fusion systems", IEEE International Conference on Fuzzy Systems, pp. 1839-1844, Korea, 2009.

[103] E. H. Mamdani and S. Assilian: “An experiment in Linguistic Synthesis with a Fuzzy Logic Controller”. Int. J. Man Machine Studies, vol. 7, no. 1, pp. 1-13, 1975.

[104] E. H. Mamdani: "Advances in the linguistic synthesis of fuzzy controllers", International Journal of Man-machine Studies, Vol. 8, Issue 6, pp. 669-678, 1976.

[105] T. Takagi, M. Sugeno: "Fuzzy identification of systems and its applications to modeling and control", IEEE Transaction on System, Man and Cybernetics, Vol. SMC-15, Issue 1, pp. 116-132, 1985.

[106] V. Palade, R. J. Howlett, L. C. Jain: "Knowledge-Based Intelligent Information and Engineering Systems 1", ISBN 978-3-540-30132-5, 2004.

[107] Agilent Technologies: "Agilent 4294A precision impedance analyzer, programming manual". Part N° 04294-90061, 8th Edition, 2012.

[108] P. Büschel, U. Tröltzsch, O. Kanoun: "Use of stochastic methods for robust parameter extraction from impedance spectra", Electrochimica Acta, Vol. 56, Issue 23, pp. 8069-8077, 2011.

[109] O. Kanoun, U. Tröltzsch, H. Tränkler: "Benefits of evolutionary strategy in modeling of impedance spectra", Electrochimica Acta, Vol. 51, Issue 8-9, pp. 1453-1461, 2006.

[110] M. Guermazi, U. Tröltzsch, O. Kanoun, N. Derbel: "Assessment of Beef Meat Aging using Impedance Spectroscopy", 8th IEEE International Multi-Conference on Systems, Signals & Devices, Sousse Tunisia, 22-25 Mars, 2011.

[111] J. P. Andretzko: "Contribution à l’optimisation et à la modélisation d’un banc de mesure CEM", PhD instrumentation and microelectronic, Université Nancy-I27, 2007.

[112] C. Gabriel, S. Gabriel and, E. Corthout: "The dielectric properties of biological tissues I. Literature survey". Phys Med Biol, Vol. 41, pp 2231-2349, 1996.

[113] S. Gabriel, R.W. Lau, C. Gabriel: "The dielectric properties of biological tissues: II. Measurements in the frequency range 10 Hz to 20 GHz", Phys. Med. Biol., Vol. 41, Issue 11, pp. 2251-2269, 1996.

[114] M. Guermazi, O. Kanoun, U. Tröltzsch, N. Derbel: "Influence of meat aging on modified Fricke models parameter", Lecture Notes on Impedance Spectroscopy, CRC-Press, Taylor and Francis, ISBN: 978-0-415-64430-3, Vol. 3, pp. 157-166, 2012.

[115] C. S. Hsu, F. Mansfeld: "Concerning the conversion of the constant phase element parameter Yo into a capacitance", Corrosion, Vol. 57, pp. 747-755, 2001.

[116] F. Zhang: "Feature extraction for the meat's freshness characterization using the method of Principal Component Analysis", Master of Science, TU Chemnitz, 2014.

[117] M. O'Farrell, E. Lewis, C. Flanagan, W. Lyons, N. Jackman: "Comparison of k-NN and neural network methods in the classification of spectra data from an optical fiber-based sensor system used for quality control in the food industry", Sensors and Actuators B: Chemical, Vol. 111-112, pp. 354-362, 2005.

[118] M. Guermazi: "Systeme d'irrigation automatique utilisant le capteur spectrometre d'impedance et classifiant les données par réseaux neuronaux", Master of Science, National Engineering School of Sfax, 2008.

[119] M. Guermazi, O. Kanoun, N. Derbel, F. Derbel: "Method of model's parameters classification using neural network for meat characterization", 10th IEEE International Multi-Conference on Systems, Signals & Devices, pp.1-5, Hammamet, 2013.

[120] D. E. Rumelhart, G.E. Hinton, R.J. Williams: "Learning internal representations by error propagation", in Parallel Distributed Processing: Explorations in the Microstructure of Cognition, Cambridge, MA: M.I.T. Press, Vol. 1, pp. 318-362, 1986.

[121] B. Widrow, M.E. Hoff: "Adaptive switching circuits", IRE WESCON Convention Record, part 4, pp. 96-104, 1960.

[122] H. Mkaouar: "Use of mathematical tools for classification of meat muscles", Master of Science in Robotics, National Engineering School of Sfax, 2014.

[123] L. X. Wang, J.M. Mendel: "Generating fuzzy rules from numerical data, with applications", IEEE Trans. Systems Man and Cybernetics, Vol. 22, Issue 6, pp. 1414-1427, 1992.

[124] The Mathworks, Inc. User guide, Fuzzy Logic Toolbox, Fuzzy inference System Modeling, "Probor".

Scientific Reports on Measurement and Sensor Technology

(1) Bouchaala, Dhouha (2016)
Investigation of Current Excitation for Personal Health and Biological Tissues Monitoring
ISBN 978-3-941003-96-9
Volltext: http://nbn-resolving.de/urn:nbn:de:bsz:ch1-qucosa-204801

(2) Heidary Dastjerdi, Maral (2016)
Ein Beitrag zur Verbesserung der Eigenschaften magnetisch-induktiver Tastspulen
ISBN 978-3-944640-98-3
Volltext: http://nbn-resolving.de/urn:nbn:de:bsz:ch1-qucosa-207628

(3) Guermazi, Mahdi (2016)
In-Vitro Biological Tissue State Monitoring based on Impedance Spectroscopy
ISBN 978-3-96100-003-6
Volltext: http://nbn-resolving.de/urn:nbn:de:bsz:ch1-qucosa-206710